

CHALMERS



Voltage Stability and Distance Protection Zone3

Master of Science Thesis in the Programme of Electric Power Engineering

Shehu Abba-Aliyu

Division of Electric Power Engineering
Department of Environment and Energy
CHALMERS UNIVERSITY OF TECHNOLOGY
Göteborg, Sweden, May 2009

Voltage Stability and Distance Protection Zone3

Shehu Abba-Aliyu

In partial fulfilment for the award of Master of Science degree in Electric Power Engineering, in the Department of Environment and Energy, Division of Electric Power Engineering, Chalmers University of Technology, Göteborg, Sweden

© Shehu Abba-Aliyu, May 2009.

Examiner: Daniel Karlsson

Division of Electric Power Engineering

Chalmers University of Technology

SE-412 96 Göteborg

Sweden

Telephone + 46 (0)732 498923

Abstract

In this work, an investigation of the role played by line distance protection zone3 towards voltage instability resulting into a major system blackout of large power network was carried out. This is with a view of finding out the scenarios that can lead to voltage collapse with all the three zones of the distance protection relays activated.

The motivation for doing so is that; recent large power blackouts generated lots of controversial debates in Europe and in the United States and the concept of voltage collapse is still a subject of research under investigation. In addition, there is a disagreement over the exact nature of the negative forces that triggered the big blackouts. This raised several questions as “who to be blamed”. Among several others distance protection zone3 has been blamed for the majority of voltage collapse incidence that took place in 2003.

The study begins with developing and solving the load flow of the simple IEEE14-bus test system. To create a scenario similar to the actual blackout in 2003 Sweden/Denmark a detailed dynamic simulation of standard CIGRE Nordic32-bus network which closely resembles Swedish network is carried out and the critical lines that led to cascaded tripping were identified using PSS/E software. As a short term solution to voltage collapse, a mitigation scheme incorporating underfrequency relays and undervoltage relays is implemented.

According to the findings of this work, within 2.52 seconds with respect to the triggering event all the critical lines tripped in cascade and 370 milliseconds is the time lag observed between the commencements of the cascaded trippings to the last event. As an additional example from the simulation result, the reactive power losses increases for the same loading condition by 47% during the pre-fault condition when tap changers are blocked and raised to 52% when tap changers are in operation.

It was observed that zone3 distance relay operation should not be entirely blamed for the cascaded trippings because even when zone3 and zone1 were blocked, the voltage collapse still occurred in zone2, since at that critical condition the apparent impedance seen by the distance relay traverse through all the three zones.

Moreover, it is shown that switching out of major transmission lines is associated with large increase in power losses and if these losses are determined using simulation software prior to granting a planned outage and adequate reactive compensation is provided, then the need for load shedding and risk of voltage collapse could be reduced.

Key words: cascaded tripping, distance protection zone3, load dynamics, mitigation scheme, on-load tap changer, underfrequency relay, undervoltage relay, voltage collapse.

Acknowledgments

My profound gratitude goes to Almighty God for giving me the health, means and ability to scale through the rigour of all the years of my studies.

This study wouldn't have been possible without the financial support of His Excellency Malam Ibrahim Shekarau the Governor of Kano State, Nigeria for shouldering one year expenses of my studies. The follow-up made by my cousins Alhaji Aminu Shariff and Malam Ujudud Shariff in this regard is highly appreciated. Also, the financial support of Honourable Alhaji Aminu Umar, the Chairman of Dawakin-Kudu Local Government Area is highly appreciated.

My gratitude goes towards my adept supervisor Dr. Daniel Karlsson for guiding me not only through this thesis work but also for his understanding and encouragement during the difficult period of this work.

Many special thanks are extended to Dr. Ola Carlson for giving me the opportunity by admitting me to study Electric power engineering at Chalmers. The helpful discussion with Prof. Torbjörn Thiringer, Drs Tuan Anh Le, Abram Perdana and Nayeem Rahmat Ulla is highly appreciated.

Many thanks to my lecturers at the Division of Electric Power Engineering as well as all my classmates; Andreas Bergqvist, Didi Istardi, Emir Isabegovic, Anders Eliasson to mention but a few.

The support and interest shown by my senior colleagues Engrs Isa Musa, Olusola Akinniranye and Sylvester Enemuoh from the start to the end of the studies is highly and respectfully acknowledged. In the same fashion I wish to extend special thanks to my colleagues numerous to mention at 330/132/33kV Kano transmission sub-region for constantly keeping in touch and particularly to Engrs A. A.D Ismail, M. K. Bello and A.G. Adamu for numerous logistic support to my family.

Special thanks are extended to all my friends and siblings for their support and encouragement. Last but not the least my warm and affectionate appreciation goes towards my family; Amina Idris, Hauwa, Habiba and Mukhtar for their continuous prayer, encouragement and patience throughout out the period of the study.

To my mother Amina Abba-Aliyu

Table of Contents

Abstract.....	iii
Acknowledgments.....	iv
Dedication.....	v
Chapter One: Introduction	1
1.1. Aim and Objectives	2
1.2. Scope and Limitations.....	2
1.3. Thesis Layout.....	3
Chapter Two: Voltage Stability and Protective relay Concepts.....	4
2.1 Recent Major Blackouts in Europe and the US.....	4
2.1.1 Sequence of Events.....	5
2.1.2 System security requirements.....	6
2.1.3 Contingency Criterion: N-1 and N-2.....	7
2.1.4 Who to Blame?.....	7
2.2 Voltage stability overview.....	8
2.2.1 Basic definitions and classifications.....	8
2.2.1.1 Voltage stability	9
2.2.1.2 Voltage collapse	9
2.2.2 Causes of Voltage instability	9
2.2.3 Power Electronics-based solutions to system stability.....	10
2.3 Unit Protection scheme concept	10
2.3.1 Fundamental Objectives of unit protection schemes.....	11
2.3.2 Performance Assessment of Protective Relay	11
2.3.3 Protection Zones.....	11
2.4 Basics of System Protection Scheme	12
2.4.1 Load shedding scheme.....	13
2.4.2 Tap changer operation and blocking scheme.....	13
2.4.3 Distance protection zones and settings.....	14
Chapter Three: System Modelling.....	17
3.1 System Modelling overview.....	17
3.2 Generator model.....	17
3.2.1 Synchronous generators	17
3.2.2 Induction generators.....	20

3.2.2.1	Detailed induction generator model.....	20
3.2.3	Dynamic generator modelling.....	21
3.3	Transmission line protection model	24
3.3.1	Distance relay model and setting calculations	24
3.3.2	Protective relay fault-clearing times.....	24
3.3.3	System backup protection	25
3.4	The On-load tap-changer model.....	25
3.5	Load Models.....	26
3.5.1	Static load models.....	27
3.5.1.1	Exponential load	27
3.5.1.2	Polynomial load.....	28
3.5.2	Dynamic load model	29
3.5.3	Induction motor load model.....	30
3.5.3.1	CLODBL MODEL	31
3.5.3.2	CIM5BL MODEL	31
Chapter Four:	Standard Test system and network Modelling descriptions.....	33
4.1	IEEE14-bus Test System	33
4.2	CIGRE Nordic32-bus power system	34
Chapter Five:	Dynamic Simulation in PSS/E.....	36
5.1	Basic procedure:	36
5.2	Dynamic Stability studies of IEEE14-bus test case.....	36
5.2.1	IEEE14-bus base case stability run	37
5.2.2	Pre-fault condition	38
5.3	The IEEE14-bus Voltage collapse scenario.....	40
5.3.1	Distance relay operation.....	40
5.3.2	Voltage profile and OLTC action	42
5.3.3	Dynamic load behaviour	43
Chapter Six:	Case study of Nordic32-bus system	45
6.1	Base case and pre-fault condition of Nordic32-bus system-static analysis approach.....	45
6.2	Dynamic simulation of the Nordic32-bus system	49
6.3	Pre-fault and voltage collapse scenario.....	49
6.3.1	Time frame for the simulation	50
6.4	Simulation results for the voltage collapse scenario	50
6.4.1	Distance relay operations	50

6.4.2	Generator active, reactive power and terminal voltage output.....	51
6.4.3	Voltage profile, system frequency and OLTC action.....	52
6.4.4	Branch flows and losses.....	53
6.4.5	Dynamic load profile.....	55
6.5	Mitigation scenario of voltage collapse.....	56
6.6	Simulation results for the mitigation of voltage collapse.....	57
6.6.1	Distance relay operations.....	58
6.6.2	Generator active, reactive power and terminal voltage output.....	58
6.6.3	Voltage profile, system frequency and OLTC action.....	59
6.6.4	Branch flows and losses.....	61
6.6.5	Load shedding actions.....	63
6.7	Effects of zone3 distance relay operation.....	65
Chapter Seven: Conclusion and Recommendation.....		67
7.1	Conclusion.....	67
7.2	Recommendation.....	68
7.3	Future work.....	68
REFERENCES.....		69
APPENDIX A: Block diagram of Generators, stabilizers, exciters and governors models.....		71
APPENDIX B: Distance relay data used in IEEE14-bus and Nordic32-bus test systems.....		74
APPENDIX C: Load characteristics models.....		75
APPENDIX D: Load Shedding Scheme and OLTC.....		78

Chapter One: Introduction

Power system network unreliability vis-à-vis insecurity, sudden and catastrophic failures of large plants, natural disasters, system faults, genuine protective relay operation, distance protection zone3 relay unwanted operation, generator current limiters, transformer tap changer operation, load dynamics such as abrupt huge electricity demand, deregulation policy, lack of investments in transmission line reinforcement and human errors are all linked to the causes of large scale blackouts. However, large power blackouts are rare events that are difficult to predict and hard to control. It has been argued that these kinds of blackouts are inevitable events that are bound to happen, irrespective of the investment and regulation policy put in place, in the future [9].

A significant number of the large power blackouts the world witnessed in 2003 and the shifting of power system operation from the monopolistic regulation to the deregulation era have raised a lot of questions, debates and opened up yet another wide area of research [6][7][8].

Classical transient stability studies are not enough in terms of long term system reliability and security considerations [5][22][23][24]. This results in making voltage stability a major issue and of great concern worldwide. It attracts large technical paper publications and it continues to attract more papers [10][21][27][29] due to the fact that the voltage collapse phenomenon is still not fully understood. There are many publications on power system blackouts with the objectives of early identification, quantification and mitigation. Other publications [15][17][19] on the role played by zone3 protection towards aiding system blackout reported in the literature are few . Hence, the main aim in this work is to critically look at whether or not zone3 distance protection is to be blamed for the recent major blackouts in Europe and the US.

It is appropriate at this juncture to note that the role of power engineers and system operators changed within the last decade due to deregulation. Before deregulation engineers have the sole responsibility of planning and reinforcing power grid, while the system operators ensures the electricity is kept always on.

The modern electric power industry now is deregulated and relies heavily on powerful software packages for simulation, analysis, design tools and even economic transactions. The power system operators in addition to running the system with high security were also charged with the responsibility of ensuring buying and selling of electric commodity to consumers at lowest possible cost. This opened a new opportunity for power system operators but at the same time put them under considerable pressure to strike a balance between more profit on one hand and fear of possible voltage collapse on the other hand.

The deregulation witnesses a huge increase in electricity demand with economic consideration playing a leading role. These economic aspects invariably put more stress on the transmission network subjecting the power system to be operated with transmission lines near their thermal limits and possible occurrence of voltage collapse. In order to minimize the probability of blackout occurrence more emphasis should be given to power system protection.

A protection system based on a number of protection terminals connected via a system wide data communication network and synchronized by GPS technology known interchangeably as wide area protection system (WAPS) or system protection scheme (SPS) to mitigate voltage collapse, loss of synchronism, power oscillations etc, have been proposed and discussed extensively in a number of publications [1][2][3][4].

System protection schemes address situations where; the power system is severely stressed, no particular equipment is faulted or overloaded but approaching towards voltage instability which may result in a wide spread blackout, if no remedial actions are taken. Defence plans using SPS implemented in Canada, France and Romania are illustrated in [2].

As transmission systems become more heavily loaded, the risk of voltage instability increases. Correct but unwanted operation of zone3 distance protection relays need to be fully understood due to its significant role in system voltage collapse.

Recent blackouts have shown that power swings have a strong influence on the operation of protective relays. The common method of investigating system swings and their effect on relays is to use a stability program and determine the effective apparent impedance seen by the relay. Unfortunately it is difficult to test a relay scheme with the resulting impedance trajectory. The inputs to relays are vectors -voltage and current waveforms- not phasors or impedances.

Power oscillations have a great impact in the operation of protective relays. Modern modelling tools such as; PSCAD a general-purpose time domain simulation tool for studying transient behaviour of electric networks, Alternative Transient Program (ATP-EMTP) a universal program system for digital simulation of transient phenomena of electromagnetic as well as electromechanical nature are available for performing stability studies. However, the most widely used by power utilities is the Power System Simulator for Engineers (PSS/E). It is a phasor-domain industry standard software for performing both transient and dynamic stability studies of large power networks. In view of its wide acceptability, PSS/E would be the main tool to be applied for the study of voltage stability and zone3 distance protection in this thesis work.

1.1 Aim and Objectives

The main aim in this thesis work is to carry out further investigations on zone3 distance protection operation during voltage instability which led to the 2003 major blackout in Europe and the US, by achieving the following objectives:

- Carrying out a comprehensive literature survey on the sequence of events that led to a number of recent voltage collapses.
- To see and document the triggering effect of the distance protection zone3.
- Set up a small power system in PSS/E, such as the IEEE14-bus and the Nordic32 bus test systems.
- Set up a distance protection scheme with zone1, 2 and 3 settings for major critical transmission corridors.
- Simulate voltage collapse scenarios and evaluate the simulation results and see the net effect of zone3.
- Propose some recommendations on how to handle zone3 and critical controls to mitigate system breakdown after a voltage instability incident.

1.2 Scope and Limitations

The objective of this study is to test the behaviour of distance relay protection zone3 operation during long term voltage instability using the existing models available in the model library of PSS/E software.

The effects of current and potential transformer errors are not considered. Line impedance variation due to frequency variation is neglected. The generator, exciter and governor models are based on the available data and in consistence with the built-in models in the PSS/E 29 software version.

1.3 Thesis Layout

The layout of this thesis is organized as follows: a literature review of some major power blackouts that took place in 2003 in Europe and the US. The triggering and sequence of events that leads to voltage instability as documented in the literature are presented in Chapter 2. Essential concepts of voltage stability, transmission line protection and load shedding schemes are also presented in the chapter.

The power system modelling and its various components are presented in Chapter 3. This includes performance and modelling of generators, transmission lines, tap changer and load models based on the available data required for dynamic simulation.

Standard test systems comprising the IEEE14-bus and the Nordic32-bus test system are set up in Chapter 4. This is to initially carry out normal load flow studies to satisfy the N-1 & N-2 stability criteria in preparation for the detailed dynamic simulation of a voltage collapse scenario.

In Chapter 5 the tools for carrying out dynamic simulation in PSS/E is presented, followed by simulation results with on-load tap changer in operation and distance protection zones enabled for the IEEE14-bus network. This is in order to see the net effect of zone3 operation on the system behaviour during a typical voltage collapse incident.

Similar simulation of voltage collapse scenario is repeated with Nordic32-bus system used as a case study in Chapter 6. This is to resemble the 2003 blackout incidence in the Swedish network with all the distance relay zones activated having their standard time settings. Similarly, additional simulations following the same sequence of events are made according to three different strategies such that; zone1 is blocked while zone2 and zone3 are in operation, zone1 and zone2 blocked while zone3 in operation and lastly with zone1 and zone3 blocked while only zone2 in operation.

Finally, in Chapter 7 conclusion and recommendations on the findings are made and suggestions for future studies on the work are proposed.

Chapter Two: Voltage Stability and Protective relay Concepts

Voltage stability issues have gained prominent attention in the world since in the nineties due to the occurrences of blackouts. When voltage collapse occurred it is often accompanied with large sequence of events such as protective relay operations. In the light of this, the phenomenon of voltage stability and protective relay operation need to be fully understood. This chapter begins with a short review of major power blackouts with associated sequence of events and then presents the basic concept of voltage stability, transmission line protection and load shedding schemes.

2.1 Recent Major Blackouts in Europe and the US

The world has witnessed several voltage collapse incidence in the last decades, prominent incidents that attract much attention happened at; Belgium (Aug 1982), Sweden (Dec. 1983), Tokyo (July 1987), Tennessee (Aug. 1987), and Hydro Quebec (March 1989). A comprehensive list comprising the time frame is summarised in [5].

However, recent major blackout incidence happened in 2003, during the era of electricity deregulation. Opening up electricity sector to competition helps at improving the efficiency of power generation with the competition been facilitated by an independent transmission network. But at the same time these attractive economic considerations invariably subject the transmission system into more stress, because power flows over long distances due to the buy and sell to meet the customers demand at the lowest possible cost. The challenge is in the balancing of gaining more profit with the fear of losing system reliability and high probability of the occurrence of voltage collapse [6].

After the 2003 major blackouts, a panel session to look into the subject matter was sponsored by the Power System Dynamic Performance Committee (PSDPC) of the IEEE Power Engineering Society and a high-level policy-oriented paper on the 2003 blackouts was prepared by the administrative committee of the PSDPC. This led to the formation of IEEE Task Force on Blackout Experience, Mitigation and role of New Technology [7]. Among these incidents are those at; US and Canada (Aug 14, 2003), Sweden/ Denmark (Sept 23, 2003) and Italy (Sept 28, 2003).

Two main problems were identified to have contributed significantly to the size and extent of the blackout. First, the transmission corridors (lines) are over fifty years old and the power consumption continues to grow up to a point where small disturbances can easily exceed the Available Transfer Capability (ATC) of the transmission corridor. With nearly every transmission corridor operated near its thermal capacity during winter (or a hot day as the case may be), failure of one transmission line can cause a cascading effect, as huge increase in demand would exceed the ATC of the remaining healthy lines to which the power from the failed line was rerouted and secondly transmission system upgrades were not forthcoming for many years due to several factors such as lack of investments, environmental and legal issues [8].

In power systems it is impractical to achieve 100% reliability and uneconomical to design power systems to be stable for every possible disturbance. The design contingencies are selected on the basis that they have a reasonably high probability of occurrence. However some professionals believed that the occurrence of large power blackouts could be significantly minimized if not completely avoided by good operating practice and use of: ancillary services for more reactive power support; the wide area protection in conjunction with wide area monitoring system. However, other groups of professionals suggest, using advanced mathematical modelling, that big blackouts are inevitable [9]. The major voltage instability events that occurred in 2003 are described in Table1.

Table 1.1 Recent voltage collapse

Date	Location	Time Frame	Prior System condition	Sequence of Events	Triggering Events
14th August 2003	US/Canada	5 minutes	Operated in compliance with NERC operating policy	Apparent reactive power supply problems. State Estimator and real time contingency analysis (RTCA) software problem	Tripping of Unit 5 generator at Eastlake due to control and protection problems. High reactive power generated by unit 5 causes its voltage regulator on over excitation to toggle from auto to manual. An attempt to return the control to auto resulted in tripping Unit 5. Line tripped at 3:05pm due to tree contact. Another line tripped at 3:32 due to tree contact. Heavily overloaded 345kV SS line tripped at 4:05:57 on zone3 relay operating on real and reactive current overload and depressed voltage. This triggered the cascading event. Tripping of many additional lines on zone3 relays followed. At 4:10pm, the voltage collapse , due to cascading loss of major tie lines in Ohio and Michigan and the reverse power flow subjecting hundreds lines to heavy overload.
23th August 2003	Swedish / Danish System	7 minutes (2.30-2.37pm)	Moderately loaded with Two 400kV lines and Three HVDC link were out on schedule maintenance	Loss of 1200MW Nuclear unit in the Southern Sweden, due to problems with steam valve. Occurrence of a double bus bar fault leading to the loss of 400kV lines and two 900MW nuclear units. A high power transfer on 400kV lines from North to South	The system experienced voltage collapse leading to the islanding separation of region of the southern Swedish and Eastern Denmark system. The islanded system collapse both in voltage and frequency in a matter of seconds which resulted in a large blackout.
28th September 2003	Italy	4 minutes (3.24-3.28pm)	Heavy power import into Italy	The automatic breaker controls did not reclose the previously tripped line. The phase angle difference across the line was too large due to the heavy power import. Frequency started to fall rapidly in the Italian system.	Tree flashover caused the tripping of a major tie-line between Italy and Switzerland. Overload on parallel transmission paths. A second 380kV line also tripped at the same boarder (Italy-Switzerland) due to tree contact. Cascaded tripping commenced and continued for a few seconds. Italy started to loose synchronism with the rest of Europe. The lines on the interface between France and Italy tripped due to distance relays. 220kV interconnection between Italy and Austria tripped on distance relays. The final 380kV corridor between Italy and Slovenia became overloaded and tripped as well. Many generators tripped on under frequency and within minutes the system collapse.

2.1.1 Sequence of Events

The majority of the blackout events were initiated by a single or multiple triggering events such as transmission line faults cleared by relay operation. Unwanted but correct relay operation can gradually developed into cascading outages and eventually system collapse may occur. A pictorial chart showing generically the sequence of events leading to a voltage collapse is shown below in Fig. 1.1. A typical voltage collapse scenario is associated with the following events; high power flows close to limit, serious system faults, and significant decrease in voltage, protective relay operation, cascade tripping before eventual system breakdown.

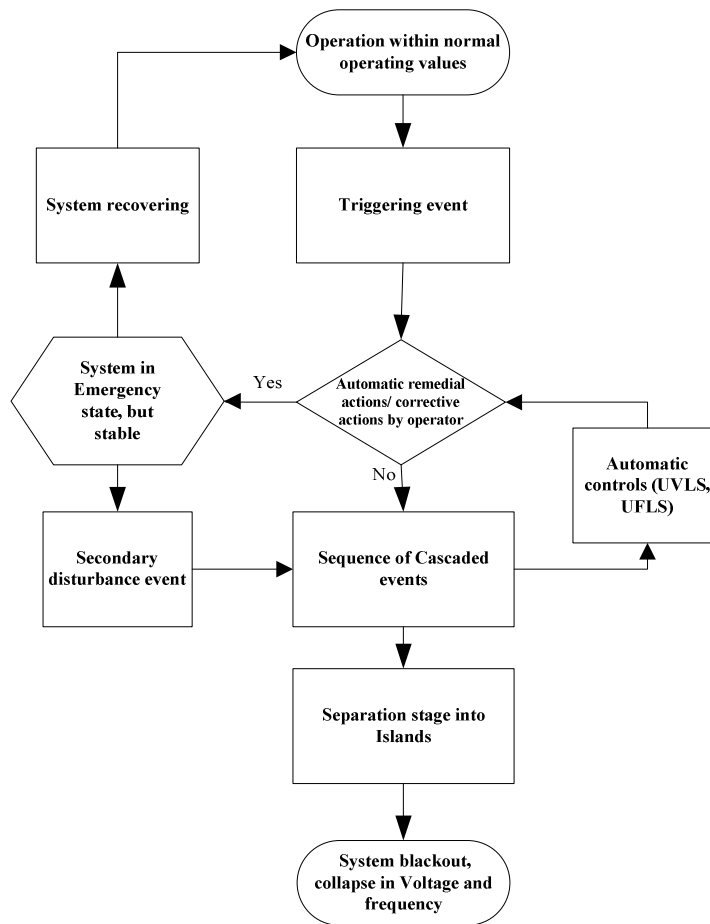


Figure 1.1: Sequence of events leading to a blackout

2.1.2 System security requirements

Reliability councils such as NERC (North American Energy Regulatory Commission) have developed certain guidelines for transmission utilities and system operators to follow, such that power systems should always be operated in a manner that no credible contingency could trigger cascading outages or any other form of instability. However, all power systems have a certain degree of uncertainty in the form of unpredictable faults, failure of major generating plant, lightning strikes on transmission lines, etc. Some of these events are unavoidable and relatively frequent; as such power system should be able to endure without causing blackouts or wide scale consumer disconnection.

Most modern power systems are designed to operate normally for single or multiple common outages. However, following a disturbance and depending on its severity, the system may transit from a stable state into an emergency state particularly during peak demand periods or high power transfer as shown in Fig. 1.1. If quick remedial actions are not initiated by system operators or taken by automatic control action the system may face further cascaded tripping.

To achieve the desired stability, a sufficient security margin must be available in the form of spinning reserve to make up for possible loss of a generating unit and enough transmission capacity to counterbalance the change in the direction of power flow due to outage of a line. Since securing the system against all possible contingencies is not economically feasible and impractical, the rules specifically limit the system security criteria to withstand all credible contingencies. The requirement for most utilities is for the power system to withstand N-1, and sometimes N-2 credible contingencies [4][19].

2.1.3 Contingency Criterion: N-1 and N-2

The security of a network as discussed in [10] is determined by the rule that governs its operation. Increasing the capacity of the transmission network without adjusting the contingency rules does not enhance the security of the power system or reduce the probability of blackouts.

In addition, the security rule that applies during regulated power is the same rule that is used in the present deregulated power market. In particular, the transmission network would be subjected to increase level and duration of stress due to bigger, longer and more frequent economic power transactions which cumulatively would lead to an increase in the probability of blackouts.

N-1 contingency event is referred to as any single event that cause single or multiple common outages. Example of N-1 event may be; a tree touching a transmission corridor that results in the operation of distance protection relay and subsequent isolation of the corridor or, a bus bar fault causing bus bar differential protection relay to operate thereby isolating one or more transmission lines connected to it. Before deregulation, N-1 contingency criteria worked well because blackouts occurred not frequently and were tolerable. The system was simpler to monitor and implement and did not require complex probabilistic calculations.

After deregulation, competition significantly increases the magnitude and duration of the stress in the transmission networks thereby rendering the system- using N-1 contingency rule- susceptible to frequent blackouts. It is very rare but equally likely to have another uncorrelated tripping event happening under this emergency state following an N-1 event, prior to system adjustment. This is referred to as N-2 contingency event. For the system to withstand independently two mutually exclusive events, the rules need to be tightened such that, the system can be operated with N-2 security.

The security criteria guiding the operation of power systems have not changed significantly since the introduction of deregulation. It was argued that the level of security has not been affected by deregulation and strict adherence to N-1 security criteria does not guarantee complete elimination of blackouts. There is always a possibility that a critical event that is not considered credible will happen. The risk associated with such non credible events is much higher when the system is operating close to its maximum limit because the power system is less stable. A transmission network that is operated at its limit is thus “secure” but much more at risk than a system that is not under stress [6].

Improving security is not cost free and results in a huge rise in hourly cost and low power transfer of transmission corridors. As such the design and operation of the power system should involve not only the cost of building and running the system but also the cost of the unavoidable blackouts to the society [6][7][8].

2.1.4 Who to Blame?

It must be acknowledged that blackouts will occasionally happen. While the exact causes of the blackout vary from one power network to another, we should be cautious in assigning blame.

It has been discussed that deregulation has resulted in a much more intensive use of transmission system [6]. Most of the time more power is being transmitted over longer distances and most likely the transmission network is operated at its limits for longer periods of time. The probability of a blackout therefore increases. When the rule such as N-1 security is adopted, the assumption made is that abiding by the rule is enough to prevent blackouts and major incidents.

Deregulation is not the only reason for recent large scale power blackouts but also lack of modernized protection system such as the wide area protection, automatic load shedding schemes, enhanced communication, control and computational tools for the system operators.

Recent regulatory developments, environmental constraints, limited power system growth, increased demands on the electricity supply, and the need for system economic optimization have a significant impact on power system reliability.

Typically, in the 2003 blackouts, the unscheduled power outages occurred because lines were overloaded and sagged into trees causing faults in the power system that were cleared by relay systems and/or because of inadequate reactive power support that caused extremely low voltages, line overloads, and subsequent operation of distance or other types of protective relays.

Over the last six years the role played by protective relay systems during emergency or extreme power system operating conditions have been an important subject of discussion. Protective relays are designed to quickly detect faults and other abnormal conditions in the power system, take quick action to isolate only the faulted area, and allow continuity of service to electric utility customers. Protective relays are often involved during major system disturbances, and in most cases, they prevent further propagation of the disturbance. Sometimes, however, older distance protection relays caused unwanted operations due to unexpected system loading and emergency operating conditions during major power system disturbances and have been among those that carry the blame which contributed to cascading blackouts that affected millions of people. To the relay protection engineers, the protective relays are doing the job they are meant to do, considering the stochastic nature of power system and probability of multiple credible contingencies – though very rare, circuit breaker and/or dc failures of a remote substation, it would be catastrophic to block any of the distance protection zones, rather automatic undervoltage and underfrequency load shedding should be allowed to act as the first defence mechanism to be adopted.

Advances in modern relays can, however, be integrated into the new concept of system protection scheme (SPS) to mitigate voltage collapse through the use of algorithms that can easily differentiate between balanced three phase faults and load dynamics under depressed voltage condition. In addition, intelligent automatic voltage regulators for transformer OLTC (On-Load Tap Changers) that can either trip to local control or temporarily block its operation during the emergency state should be integrated into the SPS.

2.2 Voltage stability overview

After a major disturbance occurred in a large power system, if proper operator or automatic control actions were not taken immediately, the consequences can be numerous, with parallel transmission corridors subjected to overload due to redistribution of power flow after the initial outage, and thus a process of cascading transmission line outages may result. At some point, issues related to dynamic performance would lead to a number of consequences namely: transient angular instability, small signal instability (power oscillations) and voltage instability or collapse. A clear understanding of different types of instability and how they are interrelated is essential for the satisfactory design and operation of power systems.

2.2.1 Basic definitions and classifications

The IEEE/CIGRE joint task force on stability and definitions [10] has come up with a blue print on the definitions and classification of power system stability. Therefore, to aid its analysis they defined power system stability as follows:

“Power system stability is the ability of an electric power system, for a given initial operating condition, to regain a state of operating equilibrium after being subjected to a physical disturbance, with most system variables bounded so that practically the entire system remains intact”[10].

Fig. 2.1 shows the classification of power system stability according to IEEE/CIGRE joint task force.

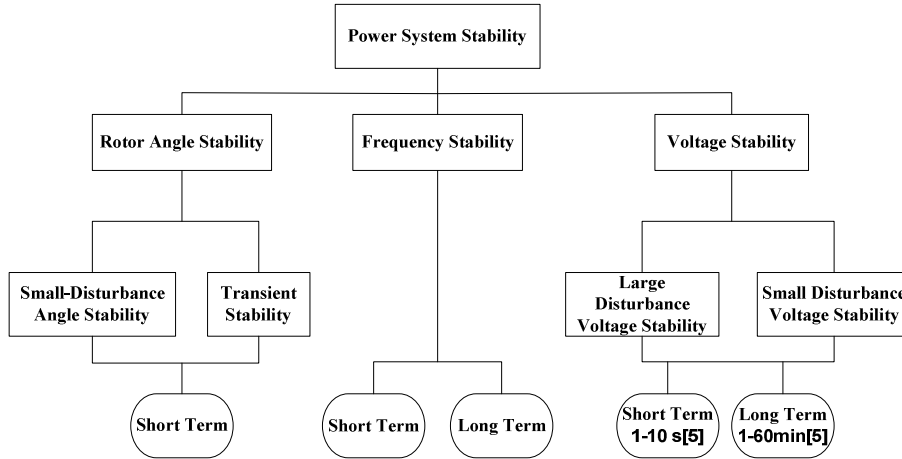


Figure 2.1 Power system stability classifications [10]

2.2.1.1 Voltage stability

According to the definition in [10], “*Voltage stability*” refers to the ability of a power system to maintain steady voltages at all buses in the system after being subjected to a disturbance from a given initial operating condition. It depends on the ability to maintain/restore equilibrium between load demand and load supply from the power system. A possible outcome of voltage instability is loss of load in an area, or tripping of transmission lines and other elements by their protective systems leading to cascading outages. Loss of synchronism of some generators or from operating conditions that violate field current limit may result in outages.

The other two stability issues are: the rotor angle and the frequency stability. Power system undergoing system instability usually experience more than one of these instability phenomena. In this thesis large disturbance voltage stability within a time frame of 2 seconds to 10 minutes is investigated, since this time frame is enough for structural changes to take place due to the isolation of the faulted elements and sometimes resulting in voltage collapse.

2.2.1.2 Voltage collapse

Voltage collapse may be described as a rapid and uncontrolled drop of bus voltage due to the dynamic behaviour and/or increase in load at the bus. It is generally characterized by inadequate reactive power support in a high load area. It is described in [5] as: “*A power system at a given operating state and subject to a given disturbance undergoes voltage collapse if post-disturbance equilibrium voltages are below acceptable limits.*” Voltage collapse can extend across the whole power system or be limited to a certain system area.

The term *voltage collapse* is also defined in [10] as the process by which the sequence of events accompanying voltage instability leads to a blackout or abnormally low voltages in a significant part of the power system. Stable (steady) operation at low voltage may continue after transformer tap changers reach their boost limit, with intentional and/or unintentional tripping of some load.

2.2.2 Causes of Voltage instability

The main factors that cause voltage instability are as follows:

- Inability of the power system to meet the demand for reactive power due to a mismatch between load demand and supply of reactive power.
- Progressive fall or rise of the voltage at some buses.

- Transfer of active and reactive power over a highly inductive transmission network to electrically long distance load resulting in voltage drop.
- Loss of load in an area, or tripping of transmission lines and other elements by their protective systems.
- Loss of synchronism of some generators may result from these outages or from operating conditions that violate field current limits.
- Heavily stressed and/or weak power systems.

If following a disturbance the power system reached a new equilibrium state without affecting the system integrity, i.e., with practically all generators and loads connected through a single continuous transmission system, the system is said to be stable. Some generators and loads may be disconnected by the isolation of faulted elements or intentional tripping such as load shedding to preserve the continuity of operation of the bulk of the system. Intentional splitting into two or more “islands” to preserve as much of the generation and load as possible due to certain severe disturbances may sometimes be necessary to mitigate large interconnected systems from voltage instability. The system can be restored to normal state of operation with the help of automatic controls and power system operator’s actions. On the other hand, if the system is unstable, it could lead to cascading outages and a shutdown of a major portion of the power system.

2.2.3 Power Electronics-based solutions to voltage stability

Flexible AC Transmission lines (FACTS) and HVDC are the emerging technology widely adopted for the control of real and reactive power flow of a large interconnected system. FACTS controllers are used to control reactive power, while the role of HVDC is used for economic reasons for the interconnection of submarine cables longer than 50km or overhead lines over 1000km.

The causes of voltage instability listed in the previous section can be overcome by adopting one or more of the following compensating devices:

- Series capacitive compensation: This results in reducing the series reactive impedance of the transmission corridor thereby minimizing the voltage drop along the line, the receiving-end voltage variation as well as the possibility of voltage collapse [11]. It can be utilized to provide power oscillation damping and towards increasing the transient stability limit. Examples of series compensations includes among others: TSSC (Thyristor Switched Series Capacitor), TCSC (Thyristor Controlled Series Capacitor) and SSSC(Static Synchronous Series Compensator)
- Shunt reactive compensation: This includes SVC (Static VAR Compensator) and STATCOM (Static Synchronous Compensator) based on Voltage Source Converters (VSC) - used mostly in custom power devices for the control of both active and reactive power- for the control of the voltage profile, the reactive power as well as increasing the steady state Available Transmission Capacity (ATC) of the transmission corridor. Shunt compensation technique is widely accepted as a means of supplying the reactive power demand and regulating the terminal bus voltage. It increases the rotor angle (transient) stability of the system and provides effective damping of power oscillations by changing the power flow during and immediately after disturbances [11].

2.3 Unit Protection scheme concept

This work is concerned with the investigation of the behaviour of zone3 distance protection relay of a transmission corridor with emphasis on simulating zone3 distance protection settings during a major system disturbance. Practical voltage collapse scenario using IEEE14-Bus and CIGRE Nordic32 test systems are simulated in the later chapters to critically examine the roles played by zone3 distance protection towards the system voltage collapse. Therefore, it would be appropriate at this juncture, to present in this section an overview of the fundamental objectives and performance of the protective relay as applied in practice.

Important requirements for the generation and transmission of electric power to various load centres includes meeting up with the standard protection code/procedures [12][13]. In addition, acceptable engineering practice and application guides supplied by the relay manufacture should also be followed.

2.3.1 Fundamental Objectives of unit protection schemes

The fundamental objective of power systems and system protection includes among others to [14]:

- Maintain a very high level of continuity of service and minimize the extent and time of the outage when a severe disturbance occurs.
- Provide isolation of only the affected faulty area in the power system quickly, so that as much as possible the rest of the system is left intact.

In addition, a good protection scheme should have the following characteristics:

- *Reliability*: This is further divided into two aspects; Dependability and Security
 - *Dependability*: refers to the ability of the protection system to perform its required function correctly when required.
 - *Security*: refers to its ability to restrain or avoid unnecessary operation during normal loading condition and for faults outside the designated zone of operation.

Thus, protection must be both dependable and secure keeping in mind that enhancing security tends to decrease dependability and vice versa [14].

- *Selectivity*
- *Speed of Operation*
- *Simplicity and*
- *Economics*

2.3.2 Performance Assessment of Protective Relay

This can be categorized as follows:

- *Correct Operation*: The conditions for correct operation are such that at least one of the primary relays operated correctly, none of the backup relays operated and the faulty area was properly isolated in the time expected. The 2003 blackouts in the US and Europe were clear examples of the “correct, not as planned or expected” operation. That is, the apparent impedance seen by the distance relays entered into the operation zones and timed out before the cascaded tripping occurred. The relays operated correctly, but were generally regarded as unwanted operation.
- *Incorrect Operation (mal-operation)*: This is due to a failure or a mal-operation of the protective system. The result may be either incorrect isolation of a healthy area of the system, or failure to isolate the faulty area. In both cases the consequences could be disastrous. The reasons for incorrect operation include among others: misapplication of relays, incorrect setting, human errors, and equipment failures (relays, breakers, CTs, VTs, station battery, wiring, pilot channel, auxiliaries, etc). Use is made of; Primary, local and remote backups in order to minimize the consequences of the protection failure [14].

2.3.3 Protection Zones

To ensure adequate security and safety during normal and abnormal operating conditions such that no blind spot is left unprotected power system networks are grouped into protection zones as illustrated in Fig. 2.2.

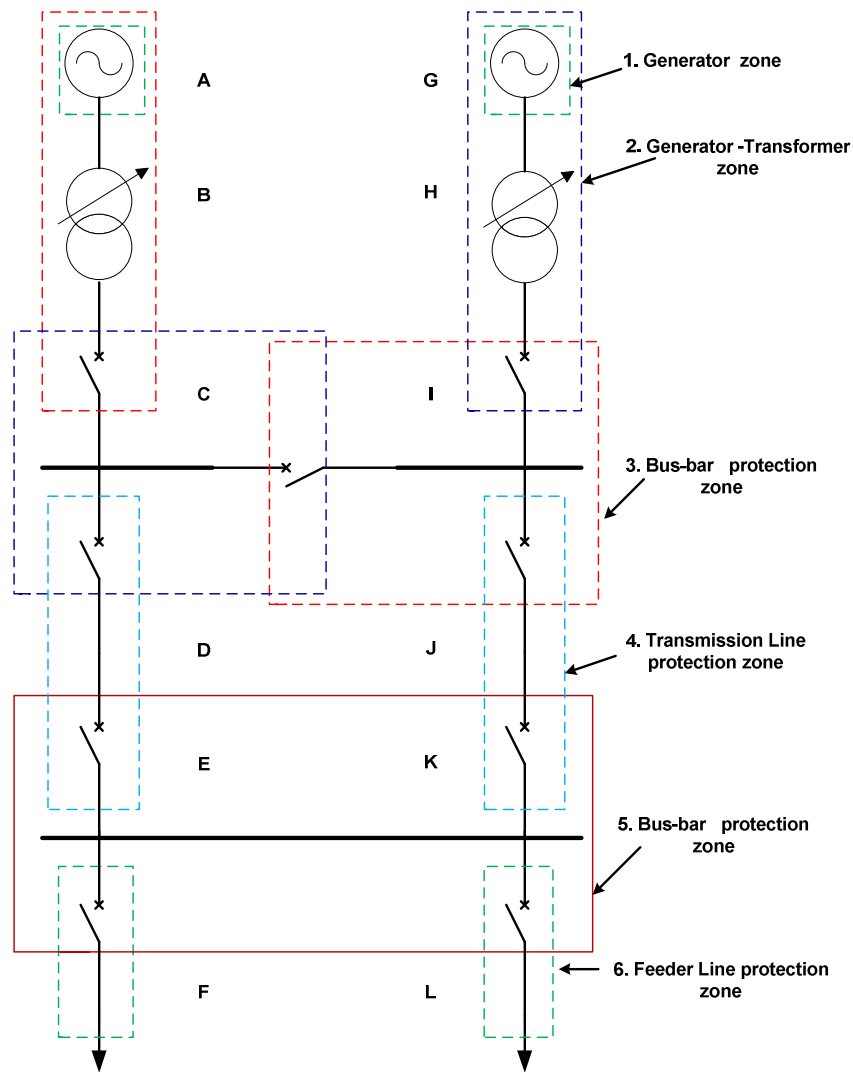


Figure 2.2 Categories of protection zones

2.4 Basics of System Protection Scheme

During a severe system disturbance actions of unit protection often further worsen the system stability. Also, both failure to operate and incorrect operation of unit protection can result in major system upsets involving increased equipment damage, increased personnel hazards, and possible voltage collapse. Line outages caused by tree contacts and high power flow are typical example in the blackout that occurred in the US in August 2003. Then there comes the concept of system protection schemes (SPS) discussed extensively in the literature [1][2][3][4].

In SPS intentional load shedding, tripping of excess generation, opening of transmission lines may be required as corrective actions for a stressed system condition.

As a means of improving power system security and reliability defence plans that utilise the emerging technology such as synchronous phasor measurement systems and reliable digital communication systems are described in the literature [1][2][3][4].

Among the widely used SPS applicable to voltage instability are:

- Underfrequency controlled load shedding
- Undervoltage controlled load shedding scheme
- Automatic switching(ON/OFF) of shunt reactors and capacitors
 - Overvoltage control
 - Undervoltage control
- Generation rejection; where one or more generating units are tripped by SPS
- Remote load shedding

2.4.1 Load shedding scheme

Two types of load shedding schemes based on system frequency and bus voltage magnitudes are used.

- Underfrequency load shedding: This is widely used to preserve the security of both the generation and transmission system during disturbances. When reduction in system frequency fall below 49Hz Underfrequency relays would be activated and after a short time delay TD without recovering a tripping signal would be issued to trip a circuit breaker with a specific load disconnected from supply. Such schemes are essential if a utility intends to minimise the risk of total system collapse, maximise the reliability of the overall network and protect system equipment from damage.
- Undervoltage load shedding: This is required when voltage magnitude continues to decay but the system frequency is within acceptable tolerance band. Use is made of Undervoltage relay fed from the bus/feeder voltage transformers to monitor, detect and disconnect some load when all other solutions have failed to preserve system stability and for mitigation against voltage collapse. The undervoltage relay will operate and trip a feeder circuit breaker when the input level falls below a pre-set threshold for more than a few seconds.

Fig. 2.3 shows a generic concept of Underfrequency and Undervoltage load shedding used in voltage collapse mitigation.

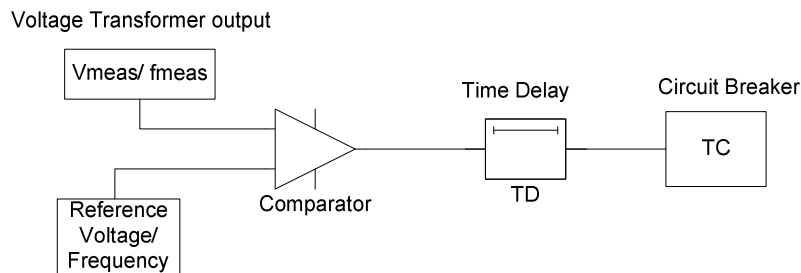


Figure 2.3 Concept of underfrequency and undervoltage load shedding

2.4.2 Tap changer operation and blocking scheme

The tap changer action is illustrated in Fig. 2.4. EHV/HV and HV/MV power transformers are usually equipped with on-load tap changers (OLTC). Each OLTC is accompanied with a tap changer panel with automatic voltage regulator relay. The secondary side voltage is monitored via a potential transformer and fed into the AVR (Automatic Voltage Regulator). If the controlled voltage is below /above the dead-band, the tap changer would tap up/ down and its operation can be automatic or manual.

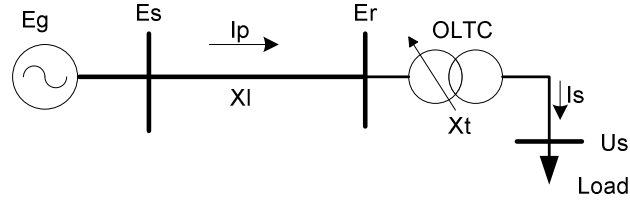


Figure 2.4 Tap changer scheme

As the transformer primary voltage level keeps on dropping, the current flow in the transmission line would continue to increase in order to supply the load power. This increase in current flow will further increase the transmission losses thereby reducing the voltage at the receiving end.

When U_s is low, the AVR will detect the low voltage and after a prescribed time delay it will send a command signal to the OLTC control to raise the transformer's tap position. This would in effect cause I_p and the voltage drop along the transmission line to increase. The losses on the transmission line further decrease E_r , thereby affecting U_s and calling for tap changer operation again. The cumulative effect would unfold itself into possible voltage collapse when allowed to continue.

A comprehensive method for the mitigation against this correct but unwanted tap changer operation is simply to block the automatic stepping up of the tap-changers due to the load dynamics [25].

The sending and receiving end real and reactive power flow assuming a lossless system is given in [5] as:

$$P_s = \frac{E_s E_r}{X_l} \sin \delta = P_r \quad (1)$$

And

$$Q_s = \frac{E_s^2 - E_s E_r \cos \delta}{X_l}$$

$$Q_r = \frac{E_s E_r \cos \delta - E_s^2}{X_l}$$

From (1) it can be observed that the reactive powers at the sending and receiving ends of the line are not equal. But the sending and receiving end active power are the same. The reactive power transmission is dependent mainly on the magnitude of the bus voltages and its direction is from the highest voltage to the lowest voltage. On the other hand, the active power transfer is closely coupled to the power angle δ . A typical value of the power angle for rotor angle stability is $\delta \approx 44^\circ$ [5]. This implies that the active power transfer depends mainly on the power angle.

2.4.3 Distance protection zones and settings

Distance protection has been widely used in the protection of EHV and HV transmission lines. The basic principle of operation of distance protection is shown in Figure 2.5.

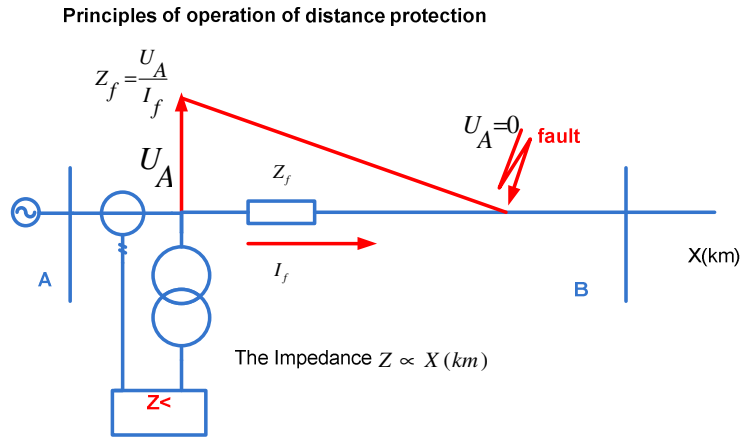


Figure 2.5 Principle of operation of distance protection

The input to the relay point is the phase voltages and line currents transformed with the help of voltage and current transformers. When a fault occurs on the protected line the fault current and voltage is fed to the protection. The voltage would fall towards zero at the point of the fault. The voltage drop along the line is equal to the product of the fault current I_f and the impedance Z_f . Figure 2.6 shows the three zones of protection widely used in distance protection schemes.

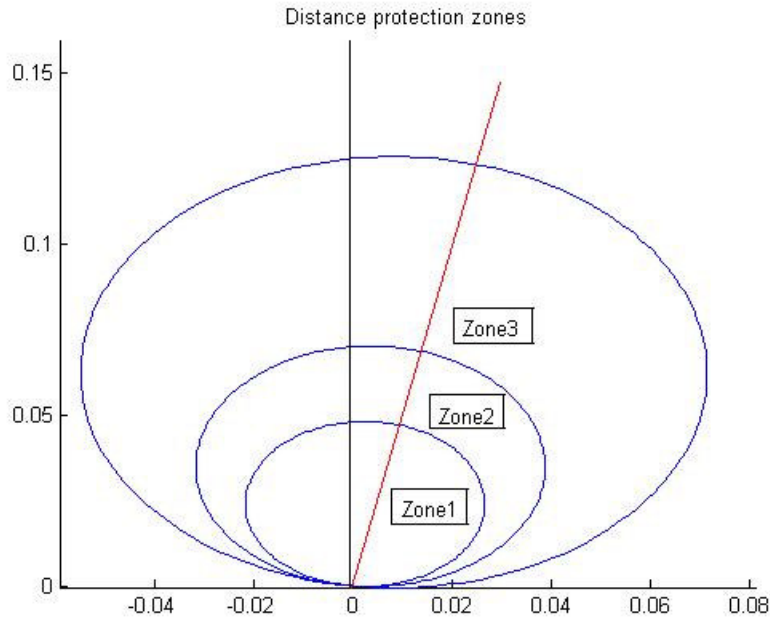


Figure 2.6 Distance protection zone

One of the advantages of using distance protection is that it has additional elements - zone2 and zone3 elements- that provide both local back-up as well as remote back-up protection. Zone2 is designed to provide a time delayed backup to local distance zone1 as well as remote bus bar faults, whilst zone3 is designed to provide a further time delayed protection and served as a larger backup zone than zone2 and covers a large part of the system.

Typically the reach settings of the three zones are chosen according to [16][17] as follows:-

- Zone 1(Z1) reach = 80% of the protected line (for overhead line),
- Zone 2 (Z2)reach = the protected line + 25% of the shortest next line
- Zone 3 (Z3) reach = the protected line + the longest next line (forward) + 25% of the longest third line.
- Backward Zone 3 reach = 10% of zone 3 forward reach (backward). The backward zone 3 reach provides back-up to local bus bar faults.

Selectivity is achieved by a combination of the distance reach setting and the time delay for each zone as illustrated in a simple radial network shown in Fig. 2.7.

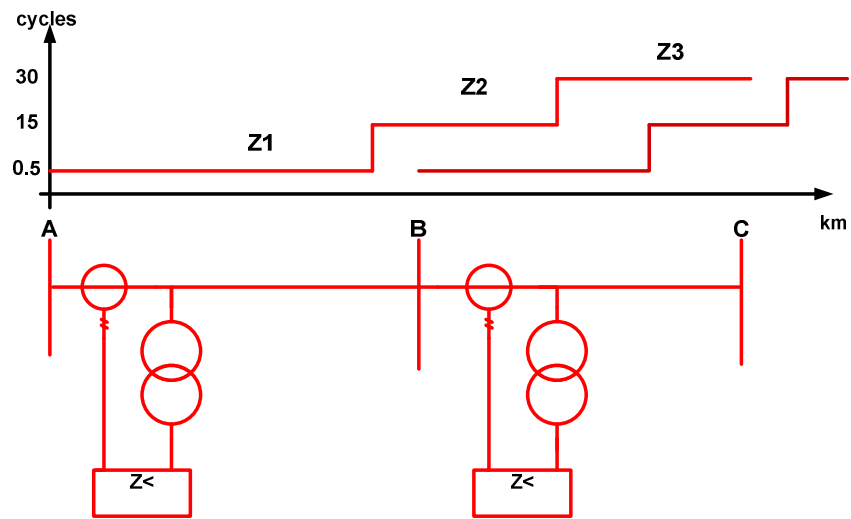


Figure 2.7 Distance reach settings with respective time delay units

Chapter Three: System Modelling

The key issue in power system simulation is the integrity of the data used in the system modelling. This requires accurate data to represent the dynamic behaviour of the generators, transmission lines, transformers and OLTC, protection schemes and load dynamics. It the purpose of this chapter to present a brief overview of the aspects of system modelling as it concern the dynamic behaviour of power system components.

3.1 System Modelling overview

The modelling starts from a single line diagram of a power network comprising generators, transmission lines, transformers and load centres. For a detailed system study all these components need to be accurately modelled and for voltage instability studies the modelling aspect is focussed on the following:

- Synchronous generators, automatic voltage regulators, exciters, governors and stabilizers.
- Transmission lines and transformers represented as π -equivalents
- On-load tap changer dynamics.
- Compensating devices, i.e. SVC, TCSC and STATCOM
- Dynamic load models comprising static and transient components and/or as induction motor load.

Each of these component modelling has been a subject of in-depth study in many publications [5][18][22][24]. This work make use of the available data extracted from selected publication in the literature and marry it to the data required in the PSS/E model library for conducting voltage instability studies of IEEE14-bus and Nordic32-bus test systems.

3.2 Generator model

Two types of generators: synchronous generator and induction machine are modelled. They are widely used for the generation of bulk electricity and as part of renewable energy source in large power network. A brief review of their fundamentals is followed next.

3.2.1 Synchronous generators

More than 95% of power generation is predominantly supplied from synchronous generators. In addition to their main task of generating active power to be consumed by load, synchronous generators have an important task of maintaining grid voltage within a tolerance value 1.0 ± 0.05 p.u of its nominal value.

The voltage control capability of the synchronous generator is an important pre-condition for stable operation, since without voltage control electric power transmission will not practically be possible. The equivalent circuit and phasor diagram of a simplified synchronous generator is shown in Fig. 3.1.

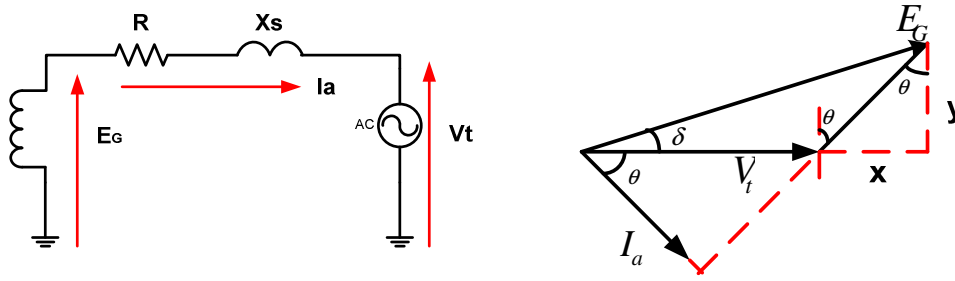


Figure 3.1 Simplified equivalent circuit and phasor diagram of a synchronous generator

The relevant basic background equations for the synchronous generator in steady state are as follows:

First it is assumed that $R \ll X_s$

$$\bar{E}_G = \bar{V}_t + \bar{I}_a \bar{X}_s$$

$$P = 3V_t I_a \cos \theta$$

$$Q = 3V_t I_a \sin \theta$$

$$y = I_a X_s \cos \theta = E_G \sin \delta$$

$$I_a \cos \theta = \frac{E_G \sin \delta}{X_s}$$

$$P = \frac{3V_t E_G \sin \delta}{X_s}$$

Similarly

$$x = I_a X_s \sin \theta = E_G \cos \delta - V_t$$

$$I_a \sin \theta = \frac{E_G \cos \delta - V_t}{X_s}$$

$$Q = \frac{3V_t (E_G \cos \delta - V_t)}{X_s}$$

The frequency-active power droop characteristics and voltage-reactive power characteristics of a synchronous generator are shown in Fig. 3.2.

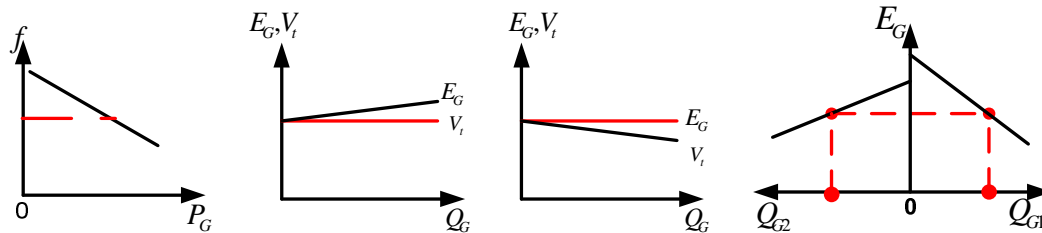


Figure 3.2 Droop characteristics of a synchronous generator

As an example, the synchronous generators shown in Fig. 3.3 provide the primary source of both active and reactive power for consumption at the load via a transmission line.

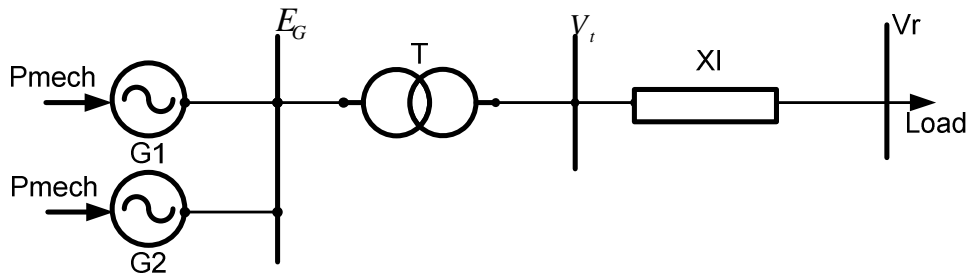


Figure 3.3 Synchronous generators providing reactive power

A typical capability curve of a synchronous generator is shown in Fig. 3.4. It specifies the machine rating and the limits enforced by armature current and field current heating. The armature heating limit corresponds to the circle in the P-Q plane where the radius is equal to the magnitude of the apparent power given as:

$$P^2 + Q^2 = (V_a I_a)^2$$

While the field heating limit when field current and hence field voltage are limited to their maximum value with constant V_a is derived as:

$$P^2 + \left(Q + \frac{V_a^2}{X_s}\right)^2 = \left(\frac{V_a E_G}{X_s}\right)^2$$

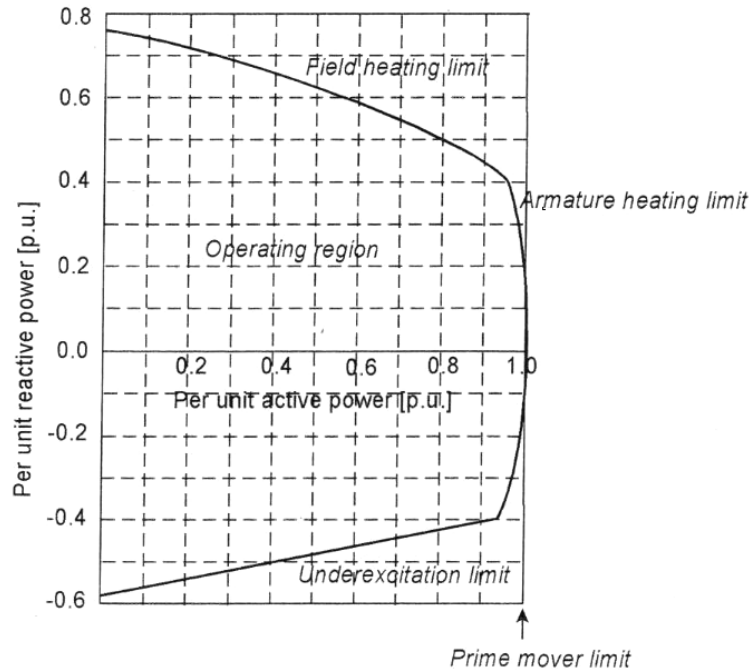


Figure 3.4 Typical capability curve of a synchronous generator.

3.2.2 Induction generators

The current trend in power generation focuses much attention on continuous usage of renewable energy and due to this; the induction generator and its modelling are now a subject of intensive research in both the academia and industries. For the purpose of carrying out dynamic studies, both the detailed model and the simplified model of the induction generators are briefly considered as follows:

3.2.2.1 Detailed induction generator model

This is referred to as the fifth order model in which both the stator and rotor electromagnetic transients are taken into consideration. It contains four electric variables and the generator speed.

The relevant machine equations are derived in [18][22][23][24] as follows:

- Stator Equations

$$\lambda_{ds} = X_s i_{ds} + X_m i_{dr}$$

$$\lambda_{qs} = X_s i_{qs} + X_m i_{qr}$$

$$v_{ds} = -R_s i_{ds} + \omega_s \lambda_{qs} - \frac{d\lambda_{ds}}{dt}$$

$$v_{qs} = -R_s i_{qs} - \omega_s \lambda_{ds} - \frac{d\lambda_{qs}}{dt}$$

- Rotor Equations

$$\lambda_{dr} = X_r i_{dr} + X_m i_{ds}$$

$$\lambda_{qr} = X_r i_{qr} + X_m i_{qs}$$

$$0 = -R_r i_{dr} + s\omega_s \lambda_{qr} - \frac{d\lambda_{dr}}{dt}$$

$$0 = -R_r i_{qr} - s\omega_s \lambda_{dr} - \frac{d\lambda_{qr}}{dt}$$

$$\tau_{em} = \lambda_{qr} i_{dr} - \lambda_{dr} i_{qr}$$

Where: By applying the following conventions, the slip is given as

$$s = \frac{\omega_s - \omega_r}{\omega_s} \text{ and } \omega_s = \frac{120f_s}{N_p}$$

N_p is the number of poles, f_s is the synchronous (stator) frequency

ω_s, ω_r are the synchronous and rotor speed

τ_{em} is the electromagnetic torque

$\lambda_{ds}, \lambda_{qs}, \lambda_{dr}, \lambda_{qr}$ are the flux linkages for stator and rotor aligned to dq coordinates

$i_{ds}, i_{qs}, i_{dr}, i_{qr}$ are the stator and rotor current components in the dq coordinates

v_{ds}, v_{qs} , are stator voltages in dq with shorted rotor windings.

R_s, X_s, R_r, X_r are the stator and rotor resistances and reactances, and X_m is the mutual reactance of the electrical equivalent circuit.

3.2.2.2 Simplified Induction generator Model

A simplified and widely accepted model for stability studies [22] is shown in Fig. 3.5.

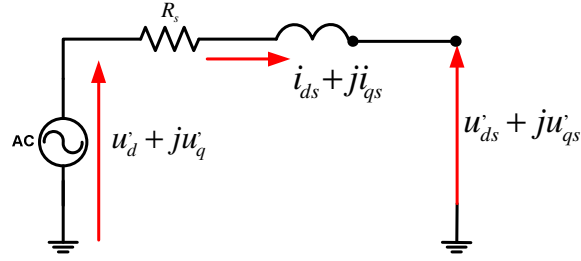


Figure 3.5 Simplified induction generator model

In this model the flux linkages are assumed to change instantaneously in which case all their derivatives terms in the above equations are zero.

The rate of change of the generator voltage source and the electromagnetic torque are governed by the following equations.

$$\frac{du'_d}{dt} = -\frac{1}{T'_o} [u'_d - (X_s - X'_s) i_{qs}] + js\omega_{base} u'_q$$

$$\frac{du'_q}{dt} = -\frac{1}{T'_o} [u'_q + (X_s - X'_s) i_{ds}] - js\omega_{base} u'_d$$

$$\tau_{em} = u'_d i_{ds} + u'_q i_{qs}$$

where; s is the slip and

$$X'_s = X_s - \frac{X_m^2}{X_r}$$

$$T'_o = \frac{X_r}{R_r}$$

In the latest versions of PSS/E model library there are built-in models for induction generators. The models are suitable for performing dynamic analysis for wind power generation. However, this work was done with PSS/E 29 and use was made of the available generator model for the voltage stability studies.

3.2.3 Dynamic generator modelling

For all dynamic analysis, generator model must take into account transients and sub-transient phenomena. Detailed mathematical derivation for dynamic generator models is beyond the scope of this thesis but is described in [18][22][23][24].

The classical model is represented with a constant voltage source (E_G) behind a constant Impedance Z (where $Z = R_a + jX_d$).

The dynamics of the classical model is represented by the swing equation

$$\frac{d^2\delta}{dt^2} = \frac{\omega_o}{2H} (P_m - P_e) - T_D \frac{d\delta}{dt}$$

where

δ is the rotor angle with respect to a reference

ω_0 is the synchronous speed(=1pu)

H is the inertia constant in per unit(pu)

P_m is the mechanical power in pu

P_e is the electrical power

T_D is the damping coefficient

The differential equations for the transient model are given as:

$$\frac{de'_d}{dt} = \frac{1}{T'_{q0}} \left[\left(\frac{X_q - X'_q}{X'_q - X_l} \right) e_{ld} + \left(\frac{X'_q - X_l}{X'_q - X_l} \right) e'_d \right]$$

and

$$\frac{de'_q}{dt} = \frac{1}{T'_{d0}} \left[e_{fd} + \left(\frac{X_d - X'_d}{X'_d - X_l} \right) e_{lq} - \left(\frac{X_d - X_l}{X'_d - X_l} \right) e'_q \right]$$

where

e'_d and e'_q are the transient voltages in d- and q-axis

e_{ld} and e_{lq} are the voltages behind the d- and q-axis leakage reactance.

The transient and subtransient models take into consideration the transient and subtransient effects of direct (d) and quadrature (q) axes added to the swing equation.

Data required for the complete machine model (subtransient generator model) are as follows:

R_a = Stator (armature) resistance

X_l = Stator (armature) leakage reactance

X_d, X_q = Synchronous reactance in d- and q-axis

X'_d, X'_q = Transient reactance in d- and q-axis

X''_d, X''_q = Subtransient reactance in d- and q- axis

T'_{d0}, T'_{q0} = Open circuit time constant in d- and q-axis

T''_{d0}, T''_{q0} = Subtransient open circuit time constant in d- and q-axis

S_m = Apparent power (nominal complex power)

U_m = Nominal voltage

H and T_D = Inertia constant and damping coefficient.

Fig. 3.6 shows the functional block diagram of a typical excitation control system for a large synchronous generator.

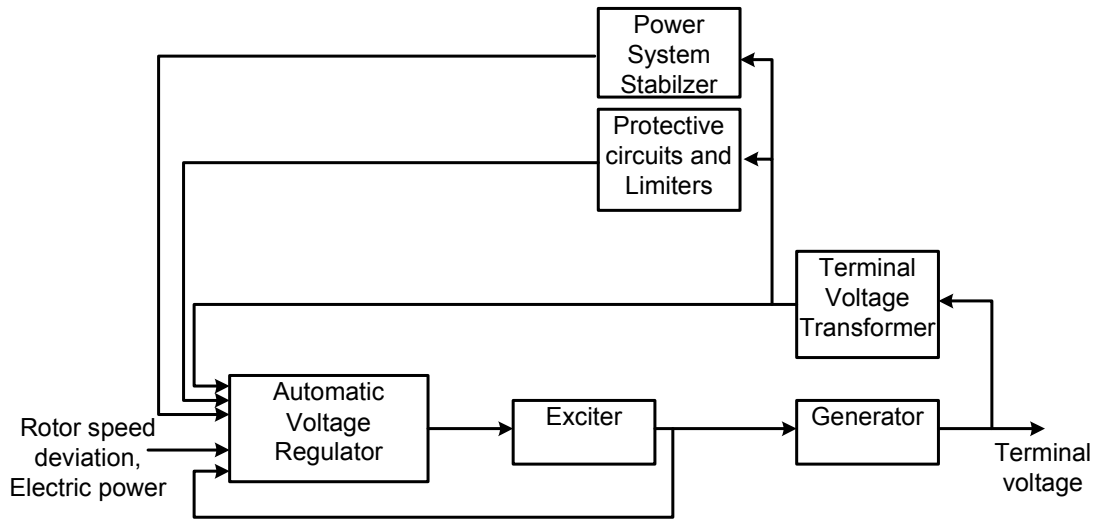


Figure 3.6 Functional block diagram of excitation control system

The regulator (AVR) is fed with input control signals such as rotor speed deviation and its function is to process and amplify the error signal to a level suitable for the control of the exciter.

The power stage of the excitation control system is the exciter. It provides the necessary dc power to the synchronous machine field windings.

The power system stabilizer (PSS) provides an additional input signal to the regulator to damp oscillations.

Terminal voltage transducer senses the generator terminal voltage, rectifies it to dc quantity and compares it to a reference desired terminal voltage.

Limiters and protective circuit ensure that the capability limits of the exciter and the synchronous generator are not violated.

In this thesis, use is made of the GENROU and the GENSAL build-in models in PSS/E model library [20] to model the generation units. The excitation control system used for the modelling are selected from the model library and includes; stabilizers (STAB2A), exciters (SEXS) and governors (HYGOV).

GENROU represents a round rotor generator model with quadratic saturation, while the salient pole generator model with quadratic saturation on the d-axis is represented as GENSAL. The hydro units are modelled as GENSAL while the thermal units are modelled as GENROU. The block diagram of GENROU and GENSAL together with the excitation system and their appropriate data are given in Appendix A.

3.3 Transmission line protection model

Transmission lines are represented by their positive sequence impedance and modelled as π -equivalents. The positive sequence impedance of the transmission lines are used to set the distance protection zones of the distance relays.

3.3.1 Distance relay model and setting calculations

Distance relays from different relay manufacturers basically measure the apparent impedance at the relaying point. This is achieved by computing the ratio of the measured positive sequence phase voltage to the line current. The relays are supposed to detect not only transmission system faults but also they should provide a local back-up protection for bus-bar faults as well as remote back-up for downstream faults.

The philosophies of distance relay models in PSS/E model library are the same but differ only in their characteristics. Some of these characteristics are as follows:

- Double circle or lens out-of-step tripping or blocking relay (CIROS1)
- The mho, impedance, or reactance distance relay (DISTR1)
- Polygonal distance relay model (RXR1)

The mho characteristics distance relay is selected in this study since these relays are still widely in use in power utilities and its settings are readily available and fully documented. Details of the relay data are given in Appendix B.

3.3.1.1 Other system relay models and settings

Protection in addition to the distance protection relays include among others:

- *Generator protective relays*: generator over speed, overload, loss-of-excitation, apparent impedance, generator terminal current, out-of-step relay and generator tripping relay.
- *Transmission line relays*: Line overload relay, circuit breaker failure relay, and directional earth fault relay.
- *Bus relays*: Over/Underfrequency relay, Over/Undervoltage relay.
- *Transformer and reactor protection relays*: Transformer guard, differential and restricted earth fault relays, OLTC relays.

Since the aim of the thesis is to study voltage instability scenario, only few of the protective relays are included in the modelling. The data sheets of these relays are given in Appendix B.

3.3.2 Protective relay fault-clearing times

The total time required to clear a fault in the system is given as:

$$t_C = t_R + t_{CB}$$

Where

t_C = Fault-clearing time

t_R = Relay time in the range of 1 to 30 cycles

t_{CB} = Breaker interruption time (3 to 5 cycles)

For distance relay studies in this thesis, zone1 relay time is instantaneous (0.5cycle); zone2 relay time is 15cycles and zone3 relay time is 30cycles at a system frequency of 50Hz. The circuit breaker time is chosen as 5cycles.

3.3.3 System backup protection

The two types of relays that are commonly used for system phase fault backup are: the distance relay and voltage restrained or voltage-controlled time-over current relay. The choice of the relay is usually dependant on the type of relaying used on the lines connected to the generator. The distance backup relay is used where distance relaying is used for line protection, while the over current type of backup relay is used where over current relaying is used for line protection [12].

The time delays of these relays are one second or less- this implies that they don't coordinate with excitation limiting controls. These relays are meant to detect transmission system faults, but could operate on overload (high generator reactive output) and low terminal voltage. Unwanted operation of these relays have contributed to several voltage collapses and a call was made for the settings of these relays to be reviewed [5].

3.4 The On-load tap-changer model

The distance protection behaviour in a stressed system, in the range of 0.1 seconds to 10 minutes as well as the impact of automatic on-load tap-changer (OLTC) regulation are of great interest in voltage instability analysis.

While tap-changers provide voltage control by restoring the load voltage level, they can contribute significantly to the cause of long-term voltage instability during their actions when attempting to restore the load voltages. During this process the transmission voltage upstream is further deteriorated which can degenerate into possible voltage collapse.

A simplified OLTC representation and equivalent diagram is shown in Fig. 3.8.

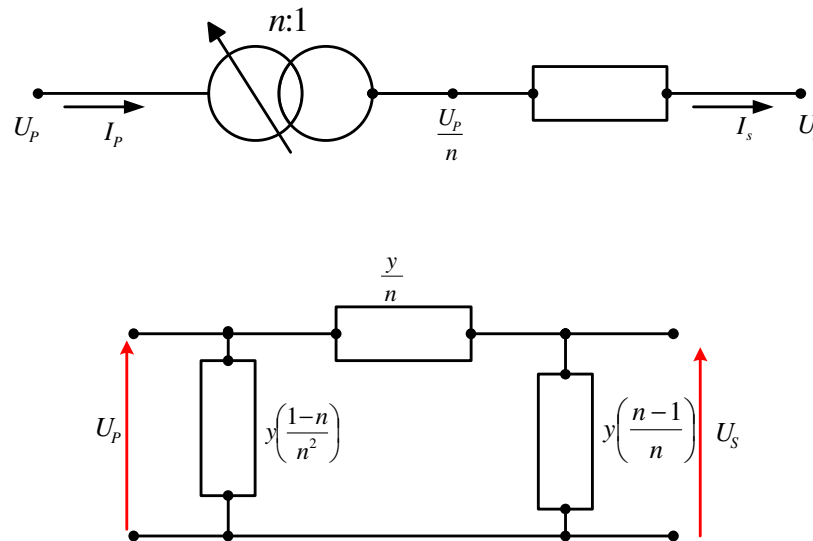


Figure 3.8 OLTC single line diagram and equivalent representation

Typical modelling of OLTC require some specifications to be made that includes: time delays for issuing raise/lower command, setting the reference voltage, dead band voltage range and time between successive taps. A non linear system model of OLTC is derived in [30][38]. Fig. 3.9 shows a basic arrangement of OLTC.

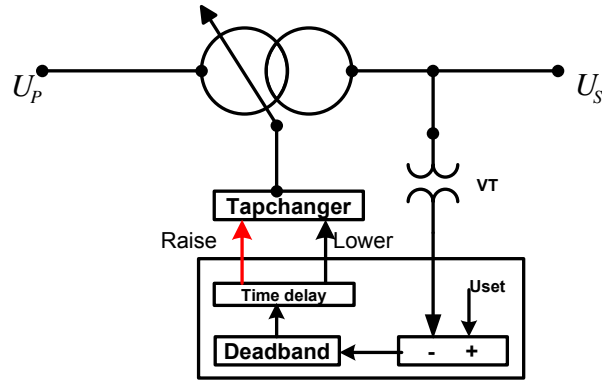


Figure 3.9 Typical arrangement of OLTC

PSS/E has an inbuilt OLTC model in its model library. To capture the behaviour of the tap changer operation during long term voltage dynamics the OLTC models at some strategic buses for the IEEE14-bus and Nordic32-bus test systems are set according to Table 3.1 and 3.2 respectively.

Table 3.1 IEEE14-bus OLTC model settings

Code	Model Type	IB	JB	CID	TD	TC	TSD
0	OLTC1	4011	9011	1	20	0	2
0	OLTC1	4011	9011	1	20	0	2.5
0	OLTC1	5011	6011	1	20	0	1.5

Table 3.2 Nordic32-bus OLTC model settings

Code	Model Type	IB	JB	CID	TD	TC	TSD
0	OLTC1	1044	4044	1	40	0	8
0	OLTC1	1044	4044	2	40	0	8
0	OLTC1	1045	4045	1	40	0	8
0	OLTC1	1045	4045	2	40	0	8
0	OLTC1	41	4041	1	40	0	7.9
0	OLTC1	42	4042	1	40	0	6.5
0	OLTC1	43	4043	1	40	0	7.5
0	OLTC1	46	4046	1	40	0	6.1
0	OLTC1	51	4047	1	40	0	7.4
0	OLTC1	61	4051	1	40	0	6.6
0	OLTC1	62	4061	1	40	0	7.1
0	OLTC1	63	4062	1	40	0	6.2

Typical time delay (TD) for OLTC is 40 seconds per step as given in Table 3.2. But it is reduced in the simulations in Chapters 5 and 6 in order to see quick effect of the tap changing transformer.

3.5 Load Models

Load models are classified as either static, dynamic, or composite. However, from the system operator point of view, feeder loads are expressed as aggregate of several electrical apparatus in MW and Mvar.

Example of feeder loads includes: industrial, commercial and residential feeders. Each feeder load is made up of a combination of apparatus such as lighting, heating, room air conditioning, fridges, motors, etc. The power consumed by these loads is a function of both frequency and voltage.

Loads are described to be the main driving force for voltage instability [10]. In response to a disturbance, power consumed by the loads tends to be restored by the action of on-load tap changing transformers, motor slip adjustment, distribution voltage regulators, and thermostats. Load restoration results in high voltage network being subjected to further increase in stress due to increasing demand of the reactive power consumption by the load. This in turn leads to further reduction in voltage. Therefore, when load dynamics attempt to restore power consumption beyond the capability of the transmission network and available generation, a run-down situation causing voltage instability occurs [5][22][24].

Several studies, [27][28][29][30][31] have shown the critical effect of load representation in voltage stability studies. But, load modelling has been a tedious task due to the nature of the power system loads. In this work load response to voltage and its dynamic behaviour is monitored by distance protection relay. In view of this, a brief review of load modelling is appropriate at this juncture.

3.5.1 Static load models

As the name implies, a *static load model* is not time dependent, it expresses the characteristics of the load at any instant of time as an algebraic functions of the bus voltage magnitude and system frequency at that instant.

In the range of minutes, load voltage characteristics have strong dynamic influence on system behaviour particularly during voltage instability and voltage collapse phenomenon [5]. This has led to several load models being developed and appearance of numerous publications on the subject in the literature [27][28][29][30][31]. Common static load models are described as follows:

3.5.1.1 Exponential load

In general form, exponential load is expressed in [24] as:

$$\text{Consumed load active power; } P = zP_0 \left(\frac{U}{U_0} \right)^\alpha \text{ and}$$

$$\text{Consumed load reactive power; } Q = zQ_0 \left(\frac{U}{U_0} \right)^\beta$$

Where:

P, Q are the consumed load active and reactive power

zP_0 , zQ_0 are the active and reactive power consumed when $U = U_0$.

z is dimensionless load demand variable

U_0 is the reference (nominal) voltage(kV)

α , β are load-voltage dependence variables that determine the sensitivity of load power to voltage.

This expression led to further classification of the exponential load into:

- Constant power load denoted as P, when $\alpha = \beta = 0$
- Constant current load denoted as I, when $\alpha = \beta = 1$

- Constant impedance denoted as Z, when $\alpha = \beta=2$

In order to carry out base case stability analysis all loads are modelled as voltage dependent with $\alpha=1$ for active power and $\beta=2$ for the reactive power.

If the demand variable z is set z=1, and α and β were split into static (α_s, β_s) and transient (α_t, β_t) components, then a detailed exponential load would take the form of that given in [27][28] as follows:

$$P_s(U) = P_0 \left(\frac{U}{U_0} \right)^{\alpha_s}, \quad Q_s(U) = Q_0 \left(\frac{U}{U_0} \right)^{\beta_s}$$

$$P_t(U) = P_0 \left(\frac{U}{U_0} \right)^{\alpha_t}, \quad Q_t(U) = Q_0 \left(\frac{U}{U_0} \right)^{\beta_t}$$

Where:

P_s and Q_s are the consumed static active and reactive power

P_t and Q_t are the consumed transient active and reactive power

P_0 and Q_0 are the active and reactive power when $U=U_0$.

α_s, β_s = static active and reactive load-voltage dependence

α_t, β_t = transient state active and reactive load-voltage dependence

U is the bus voltage at the load point [kV]

U_0 is the nominal supply voltage (pre-fault supplying voltage) [kV]

3.5.1.2 Polynomial load

The most common load model representations used in dynamic analysis is the polynomial load. This type of load is expressed as [24]:

$$P = zP_0 \left[a_p \left(\frac{U}{U_0} \right)^2 + b_p \left(\frac{U}{U_0} \right) + c_p \right]$$

$$Q = zQ_0 \left[a_q \left(\frac{U}{U_0} \right)^2 + b_q \left(\frac{U}{U_0} \right) + c_q \right]$$

Typical static load models that have both exponential and polynomial components are commonly referred to as "**ZIP**" models. Therefore, by setting the demand variable z=1, a simple and efficient load model that represents composite load comprising of constant power(P), constant current(I) and constant impedance(Z), is obtained as:

$$P = P_0 \left[a_p \left(\frac{U}{U_0} \right)^2 + b_p \left(\frac{U}{U_0} \right) + c_p \right]$$

$$Q = Q_0 \left[a_q \left(\frac{U}{U_0} \right)^2 + b_q \left(\frac{U}{U_0} \right) + c_q \right]$$

Where

P and Q are the consumed load (demand) active and reactive power [MW and Mvar].

P₀ and Q₀ are the active and reactive power when U=U₀.

The coefficients a_p , b_p , c_p and a_q , b_q , c_q are equal and sum up to 100 %. (i.e.

$$a_p + b_p + c_p = a_q + b_q + c_q = 100\%)$$

U₀ is the nominal supply voltage (pre-fault supplying voltage) [kV]

U is the bus voltage at the load point [kV]

3.5.2 Dynamic load model

This load model is time dependent and is represented as a set of non-linear equations, where the active power and reactive power are nonlinearly dependent on voltage. Common examples of dynamic loads are electrical heating, air conditioning, refrigerator and freezers. Load model with exponential recovery proposed in [28] is referred to as dynamic load model. The recovery time (T_{pr} and/or T_{qr}) is in the range of minutes. Based on [28] the load model is made up of two components, namely; *static* part of the active and reactive power denoted by P_s (U) and Q_s (U), and *transient* part denoted with P_t (U) and Q_t (U). By introducing load states x_p and x_q as in [28], the exponential load recovery is

given by:

(a) For active power

$$\frac{dx_p}{dt} = -\frac{1}{T_{pr}} x_p + N_1(U)$$

$$x_p = T_{pr} (P_d - P_t(U))$$

$$-\frac{1}{T_{pr}} x_p = -P_d + P_t(U)$$

$$N_1(U) = P_s(U) - P_t(U)$$

Hence

$$\frac{dx_p}{dt} = -P_d + P_s$$

Where P_d is the active power demand

(b) For reactive power

$$\frac{dx_q}{dt} = -\frac{1}{T_{qr}} x_q + N_2(U)$$

$$x_q = T_{qr} (Q_d - Q_t(U))$$

$$N_2(U) = Q_s(U) - Q_t(U)$$

Hence

$$\frac{dX}{dt} = -Q_d + Q_s(U)$$

By setting $X_p = T_{pr} P_r$ a more accurate model for voltage stability is developed in [27] as:

$$T_{pr} \left(\frac{dP_r}{dt} \right) + P_r = P_0 \left(\frac{U}{U_0} \right)^{\alpha_s} - P_0 \left(\frac{U}{U_0} \right)^{\alpha_t}$$

$$T_{qr} \left(\frac{dQ_r}{dt} \right) + Q_r = Q_0 \left(\frac{U}{U_0} \right)^{\alpha_s} - Q_0 \left(\frac{U}{U_0} \right)^{\alpha_t}$$

$$P = P_r + P_0 \left(\frac{V}{V_0} \right)^{\alpha_t} \quad \text{and} \quad Q = Q_r + Q_0 \left(\frac{V}{V_0} \right)^{\beta_t}$$

Where

α_s, β_s = steady state active and reactive load-voltage dependence

α_t, β_t = transient state active and reactive load-voltage dependence

T_{pr} and T_{qr} = active and reactive load recovery time constant[s]

V, V_0 = supplying voltage and the pre-fault value of supplying voltage [kV].

P_0, Q_0 = active and reactive power consumption at pre-fault voltages [MW, Mvar].

P_r, Q_r = active and reactive power recovery [MW, Mvar].

P and Q are the consumed load (demand) active and reactive power [MW and Mvar].

In general, when there is a voltage drop of 5 to 10% on load nodes, α_t obtained during measurement was found to be equal to 2 [28]. This implies that the transient load component can be regarded as a constant impedance load. A high sensitivity (α_s, β_s) will generally help the system to survive, after a reduction of the supplying voltage, by means of reduced power consumption.

3.5.3 Induction motor load model

For modelling of induction motors, most stability programs include a dynamic model based on the equivalent circuit shown in Fig. 3.10 [5]. Other features available in some programs are additional rotor circuits, saturation, low voltage tripping, and variable rotor resistance.

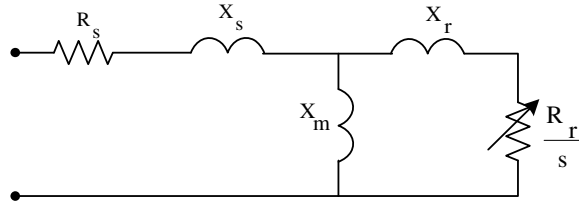


Figure 3.10 Equivalent circuit of an induction motor

R_s , R_r , X_s and X_r are the stator and rotor resistances and reactances respectively. X_m is the magnetizing reactance, and s is the slip of the motor. It is important to note that the “slip” used in this model is the frequency of the bus voltage minus the motor speed.

The stator flux dynamics are normally neglected in stability analysis, and the rotor flux is neglected in long-term analysis. Fig. 3.11 shows the transient state equivalent circuit, where the induction motor is modelled by a transient emf E' behind a transient impedance X' [5].

Several levels of detail, based on this equivalent circuit, may be available, including:

- A dynamic model including the mechanical dynamics but not the flux dynamics,
- Addition of the rotor flux dynamics,
- Addition of the stator flux dynamics.

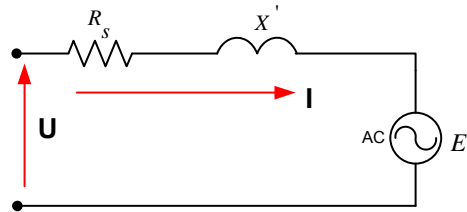


Figure 3.11 Equivalent circuit of a transient-state induction motor

Stator flux dynamics are normally neglected in stability analysis and the rotor flux dynamics may sometimes be neglected, particularly for long-term dynamic analysis.

Low voltage tripping is an important feature for voltage stability analysis and other studies involving sustained low voltage.

3.5.3.1 CLODBL MODEL

A load model that represents a complex load in the PTI PSS/E stability program is designated as CLODBL model. It includes dynamic models of aggregations of large and small motors, non-linear model of discharge lighting, transformer saturation effects, constant MVA, shunt capacitors, and other static load characteristics and series impedance and tap ratio to represent the effect of intervening sub transmission and distribution elements.

3.5.3.2 CIM5BL MODEL

This induction motor load model is also available in the PSS/E model library and is used in this thesis to model some selected load. The equivalent diagram is as shown in Fig. 3.12.

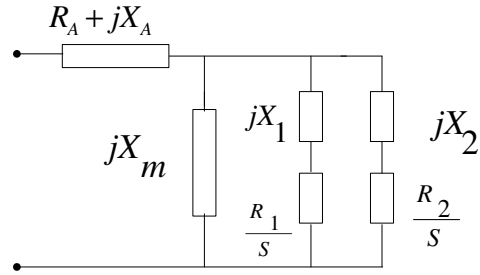


Figure 3.12 Type 1 model CIM5 Induction motor load. Impedances on motor MVA base

Model Notes:

- To model single cage motor: set $R_2 = X_2 = 0$.
- When $MBASE = 0$; motor MVA base = $PMULT \times MW$ load. When $MBASE > 0$; motor MVA base = $MBASE$.
- Load torque, $TL = T_{nom} (1 + \Delta\omega) D$: where T_{nom} is the load torque at 1 pu speed.
- T_{nom} is specified by the user only for motor starting.
- To disable relay; set $VI = 0$

The values of the induction motor parameters are obtained using motor parameter (IMD) PSS/E utility program. Typical parameters for some load obtained using IMD are given in Appendix C.

Chapter Four: Standard Test system and network Modelling descriptions

A simplified IEEE14-bus test system model is considered for learning the PSS/E software particularly the load flow and base case dynamic simulation. The knowledge acquired was extended to study Nordic32 bus test systems for investigating the influence vis-à-vis the role of distance protection relay zone3 during voltage instability. A description of these test systems are briefly given in the next section.

4.1 IEEE14-bus Test System

A single line diagram of the IEEE14-bus standard system is shown in Fig. 4.1. It consists of 14 buses, five synchronous generators with AVR, exciters and stabilizers, two 2 winding transformers equipped with on-load tap changers and a 3 winding transformer. A total of 16 transmission lines connect 11 loads in the system to the generation units. The loads are initially considered as an aggregated load of 259 MW and 81.3 Mvar. During the dynamic analysis the load were converted into a “ZIP” model. Three of the synchronous generators are synchronous condensers used only for reactive power support. The dynamic data for the generators exciters was selected from [34][35].

The IEEE14-bus was studied using PSS/E to obtain the steady state and base case dynamic performance of the system during voltage instability. The test system is equipped with distance protection relays installed on eight 130kV transmission lines. Bus 13011 and 14011 are selected as monitoring points for the voltage collapse scenario with their associated load modelled as aggregated load. The effect of OLTC is monitored at bus 6011 and 9011. All corresponding data necessary for carrying out the static load flow and dynamic stability studies are selected from existing publications [5][22][24][34][35]. A summary of the demand-supply and losses during steady state and N-1 contingency is given in Table 4.1.

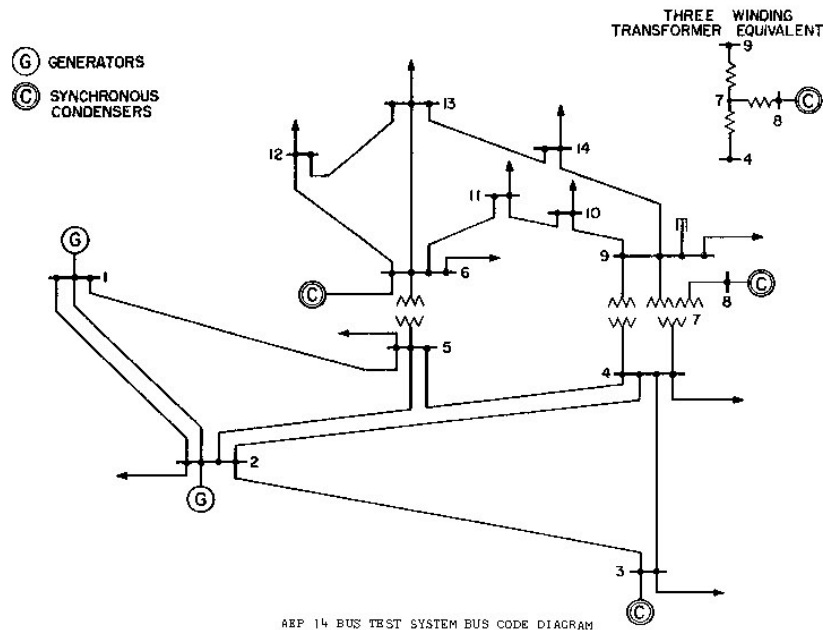


Figure 4.1 IEEE14-bus test network

Highest losses were observed when line 2011 and 3011 were on outage. Dynamic analysis of the network is presented in Chapter five with distance relays installed on these lines.

Table4.1 Demand –supply balance during steady state and N-1 contingency

	Steady state condition		N-1 contingency line outage 1011-2011		N-1 contingency line outage 1011-5011		N-1 contingency line outage 2011-3011		N-1 contingency line outage 2011-4011		N-1 contingency line outage 2011-5011		N-1 contingency line outage 3011-4011		N-1 contingency line outage 5011-4011	
	P(MW)	Q(MVAr)	P(MW)	Q(MVAr)	P(MW)	Q(MVAr)	P(MW)	Q(MVAr)	P(MW)	Q(MVAr)	P(MW)	Q(MVAr)	P(MW)	Q(MVAr)	P(MW)	Q(MVAr)
Generation	273.8	130.3	276.2	140	282.4	162.1	289.8	185.1	275.1	136.5	275.3	144.6	274	133.6	277.9	155.6
Load	-259	-130.6	-259	-130.6	-259	-130.6	-259	-130.6	-259	-130.6	-259	-130.6	-259	-130.6	-259	-130.6
Reac. Comp	0	0	0	0	0	0	0	0	0	0	0	0	0	0	0	0
Cap Comp	0	0	0	0	0	0	0	0	0	0	0	0	0	0	0	0
Losses	-14.8	0.3	-17.2	-9.4	-23.4	-31.5	-30.8	-54.5	-16.1	-5.9	16.3	-14	-15	-3	-18.9	-25
Connected capacity	785MVA		785MVA		785MVA		785MVA		785MVA		785MVA		785MVA		785MVA	

4.2 CIGRE Nordic32-bus power system

To further carry out a more detailed and close to practical analysis of zone3 distance relay during voltage instability, the Nordic32-bus test system is used. This is due the availability of relevant data from previous studies and its close resemblance to a real power system in Sweden where more generation units are in the north and heavy load centres in the south. The voltage collapse scenario that occurred in the southern part of Sweden in 2003 where two critical transmission corridors were on outage and a generating unit tripped on internal fault is simulated in PSS/E. Distance protection relays (zone1, 2 and 3) for monitoring and tripping the critical lines are installed with a view to monitor the dynamic load behaviour and the anticipated operation of the distance relays.

As a starting point the simplified single diagram of the CIGRE Nordic32-bus test system given in [36][37] is shown in Fig. 4.2.

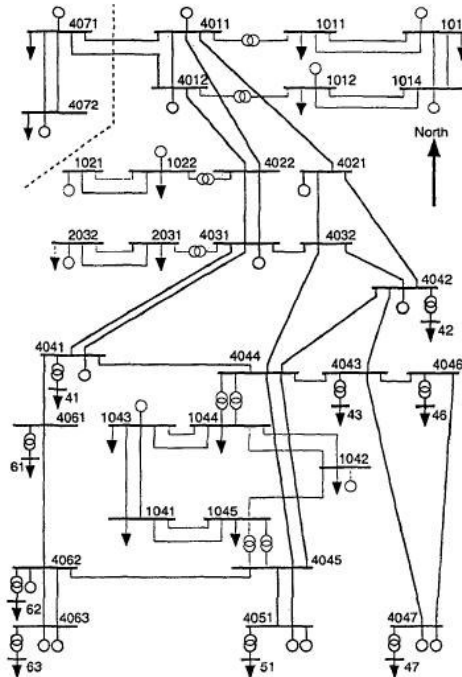


Figure 4.2 CIGRE Nordic32-bus test network

The model consists of 22 synchronous generators and 1 synchronous compensator all equipped with AVR, excitors and stabilizers. 17 transformers equipped with on-load tap changers, 52 branches and a total of 22 aggregated loads. Distance protection relays with mho characteristics were installed on the

critical lines connecting north and south. The modelling was achieved using the inbuilt models in the PSS/E library where the generation in the north which are predominantly hydro are represented with GENSAL models while the GENROU models are used to represent the generation in the south. The base case load flow with moderate from north to south gives a demand–supply balance as tabulated in Table 4.2.

Table 4.2 Normal operation demand- supply and losses

Normal operation		
	Moderate Transfer	
	P(MW)	Q(MVAr)
Generation	11571.8	1656.75
Load	-11260.68	-3459.6
Reactive Compensation	0	-500
Capacitive compensation	0	1400
Losses	-311.12	902.85
Connected capacity	17250MVA	

The active and reactive power flow and their respective line losses on the five transmission corridors from north to south during moderate transfer are tabulated in Table 4.3.

Table 4.3 Active and reactive flow of critical lines

Moderate Transfer flow from North to south via critical lines							
Name	Bus no	Transmitting end		Receiving end		Line loss	
		P(MW)	Q(MVAr)	P(MW)	Q(MVAr)	P(MW)	Q(MVAr)
Line CL12	4021-4042	590.1	-117	-556.5	12.5	-33.6	104.5
Line CL14	4031-4041_1	659.2	-109	-633.6	37.1	-25.6	71.9
Line CL15	4031-4041_2	659.2	-109	-633.6	37.1	-25.6	71.9
Line CL16	4032-4042	656.7	-49	-631.5	16.5	-25.2	32.5
Line CL17	4032-4044	523.6	-132	-497	34.3	-26.6	97.7
Total Transfer		3088.8	-516	-2952.2	137.5	-136.6	378.5

In addition to the critical lines for moderate transfer from north to south, other transmission lines of interest in this thesis for investigating voltage collapse, OLTC operation and dynamic load behaviour are considered. In Table 4.4 the flow and losses on these lines are given during normal operation.

Table 4.4 Power flow and losses for normal operation

Flow on some selected lines of interest							
Name	Bus no	Transmitting end		Receiving end		Line loss	
		P(MW)	Q(MVAr)	P(MW)	Q(MVAr)	P(MW)	Q(MVAr)
Line FL9	4047-4043	388.6	80.8	-385.5	-110.2	-3.1	29.4
Line FL10	4062-4061	254.6	46.9	-253.2	-91.6	-1.4	44.7
Line FL11	4062-4045	176.5	-137.3	-173	-78.7	-3.5	-58.6
Line RL3	1044-1043_1	181.4	-21.2	-178	46.8	-3.4	-25.6
Line RL4	1044-1043_2	181.4	-21.2	-178	46.8	-3.4	-25.6

In the next chapter, base case stability analysis for the normal operation described above and pre-fault condition after two critical lines were granted line outages for maintenance is presented.

Chapter Five: Dynamic Simulation in PSS/E

This chapter begins with a short description of the basic procedures for conducting dynamic simulation. The strategy used is two folds. The steady state analysis is studied using the load flow where N-1 contingency criterion is applied to IEEE14-bus test system. Then the concept is extended to perform the dynamic simulation using similar sequence of events used in the steady state analysis. This provides the opportunity to study the behaviour of the distance protection relay operation during voltage collapse scenario.

5.1 Basic procedure

The following procedure need to be fulfilled before conducting dynamic simulation.

- Creating from scratch a RAW file according to the methods outlined in [20] or using an already created RAW file.
- Running a successful load flow case and checking to ensure that all violations are resolved.
- Converting Loads and generators in the saved load flow case (.sav) file as outlined in [20].
- Creating a DYRE file.
- Running the base case stability analysis.
- Running the full stability analysis and plotting of results.

5.2 Dynamic Stability studies of IEEE14-bus test case

Set of files given in Table 5.1 are required to carry out load flow analysis and dynamic stability run. This is accessed in PSS/E using *psslf4* and *pssds4* respectively. In addition, the converted version of the file *IEEE14bus_converted.sav* is used for performing dynamic stability studies.

Table 5.1 Data files for power flow studies of IEEE14bus

File Name	Description
IEEE14bus.raw	Base case input data file
IEEE14bus_unconverted.sav	Main load flow solved case
IEEE14bus.sld	Single line diagram drawing datafile
IEEE14_stability.dyr	Base case Dynamic data file
IEEE14_mitigation.dyr	mitigation dynamic data file
IEEE14_converted.sav	Converted saved case file with loads and generators converted
IEEE14_basecase.snap	Basecase snap shot file
IEEE14_Vcollapse.snap	Voltage collapse snap shot file
IEEE14_mitigation.snap	Mitigation of voltage collapse snapshot file
IEEE14_baseresult.out	Base case stability result
IEEE14_VCresult.out	Voltage collapse result
IEEE14_mitigationresult.out	Mitigation result for voltage collapse
IEEE14bus_Relaydata.dat	Distance protection relay data file

Distance protection relays are installed on the positive direction of the power flow on all the 130kV lines and the relay zone reach and time settings are tabulated in Table 5.2.

Table 5.2. Zone reach settings for mho distance relays used in IEEE14-bus test system

Name of Line	Relay Location	Model	Type (mho)	Zone1 (pu) reach			Zone2(pu) reach			Zone3(pu) reach		
				Magnitude	Angle	centre radius	Magnitude	Angle	centre radius	Magnitude	Angle	centre radius
HV_L1	1011-2011-1-1	DISTR1	1	0.09962	71.9	0.04981	0.1703	71.9	0.08515	0.8514	79.6	0.4257
HV_L2	1011-2011-2-1	DISTR1	1	0.09962	71.9	0.04981	0.1703	71.9	0.08515	0.8514	79.6	0.4257
HV_L3	1011-5011-1-1	DISTR1	1	0.1836	76.4	0.0918	0.2405	76.2	0.12025	0.3192	74.7	1596
HV_L4	2011-3011-1-1	DISTR1	1	0.1628	76.6	0.0814	0.249	75.2	0.1245	0.4631	75.7	0.23155
HV_L5	2011-4011-1-1	DISTR1	1	0.54672	81.8	0.27336	0.6943	81.6	0.34715	0.91412	78.8	0.45705
HV_L6	2011-5011-1-1	DISTR1	1	0.1464	71.9	0.0732	0.194	71.9	0.097	0.4958	79.8	0.2479
HV_L7_1	3011-4011-1-1	DISTR1	1	0.147	68.6	0.0735	0.2806	76.2	0.1403	0.4524	77.4	0.2262
HV_L7_2	4011-3011-1-1	DISTR1	1	0.147	68.6	0.0735	0.2341	70.3	0.11705	0.5556	75.6	0.2778
HV_L8	5011-4011-1-1	DISTR1	1	0.03534	72.4	0.01767	0.14413	84.7	0.072065	0.4312	84	0.2156
Tme settigs				5 cycles (100mS)			15 cycles (300mS)			30 cycles (600mS)		

It can be observed in Fig. 5.1, that the direction of the power flow is from bus 1011 and 2011, i.e. towards the load side with bus 1011 serving as the slack bus.

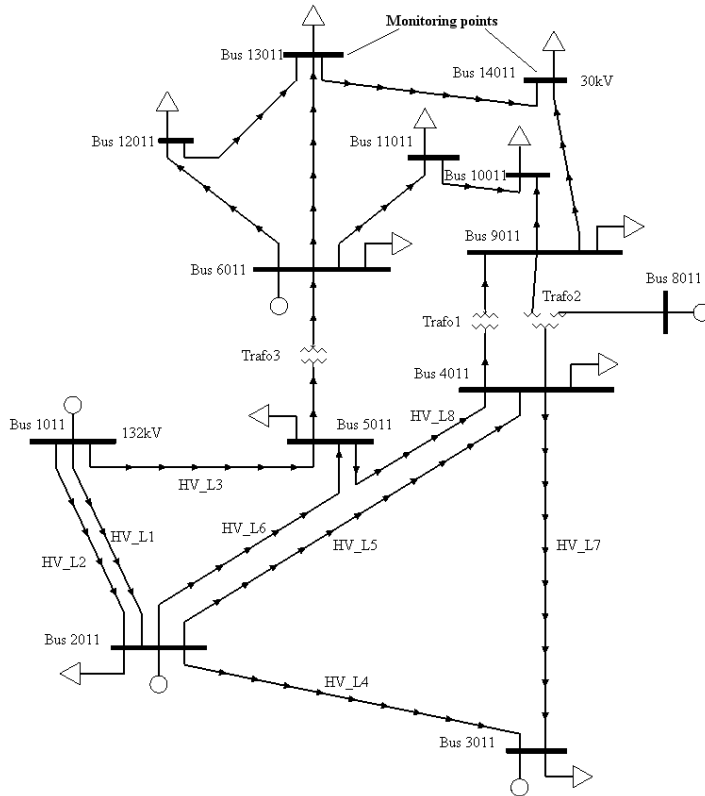


Figure 5.1 IEEE14-bus test networks showing positive direction of power flow

The two winding transformers (Trafo1 and Trafo3) as shown in Fig. 5.1 are equipped with OLTC and the longest line is from bus 2011 to 4011. The actions of these on-load tap changers will be studied in the simulation presented in the next section.

5.2.1 IEEE14-bus base case stability run

The apparent impedance for the base case, of the 130kV lines as measured by the distance protection relay is plotted together with the relay characteristics in Fig. 5.2 for the longest line HV_L5.

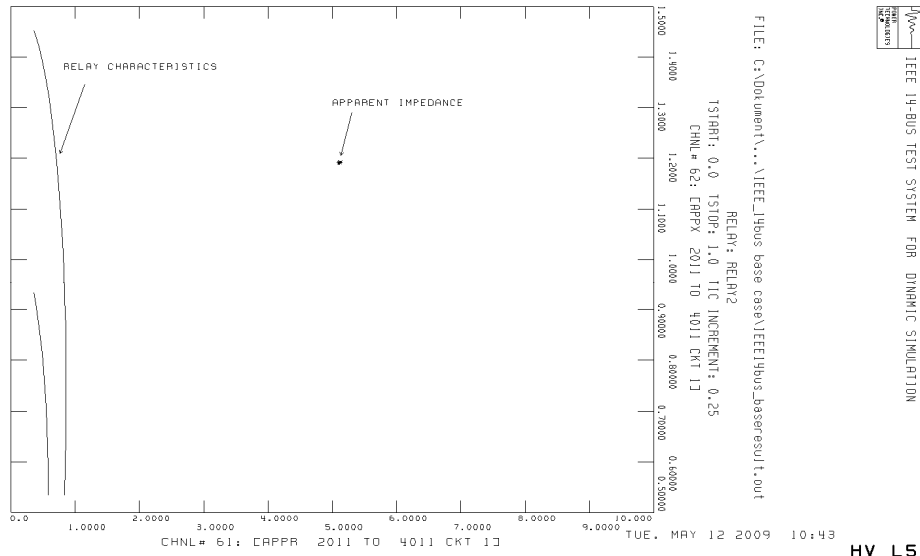


Figure 5.2 Apparent impedance of the line from bus 2011 to 4011(HV_L5)

As seen in Fig. 5.2, the apparent impedance is stationary and situated far away from the relay characteristics. This is the steady state situation where the load behaved like a constant power load model.

The IEEE14-bus test system base case load flow result shows that the system is operated satisfactorily under normal operating conditions and the voltages are within the 1.0 ± 0.05 p.u, thus there is no voltage violation. A summary of the load flow result is given in Fig. 5.3.

```
***** SUMMARY FOR COMPLETE SYSTEM *****
```

SYSTEM SWING BUS SUMMARY													
BUS	X---	NAME---	X	AREA	---	X	ZONE	---	X	MW	MVAR	MVABASE	
1011	BUS1011	130	1	[]	1	[]	231.9	-6.7	615.0
13 BUSES		5 PLANTS		5 MACHINES		11 LOADS							
19 BRANCHES		3 TRANSFORMERS		0 DC LINES		0 FACTS DEVICES							
MW		MVAR		X----- ACTUAL -----X		X----- NOMINAL -----X							
FROM GENERATION				273.6		131.1		273.6		131.1			
TO CONSTANT POWER LOAD				259.0		81.5		259.0		81.5			
TO CONSTANT CURRENT				0.0		0.0		0.0		0.0			
TO CONSTANT ADMITTANCE				0.0		0.0		0.0		0.0			
TO BUS SHUNT				0.0		0.0		0.0		0.0			
TO FACTS DEVICE SHUNT				0.0		0.0		0.0		0.0			
TO LINE SHUNT				0.0		0.0		0.0		0.0			
FROM LINE CHARGING				0.0		14.2		0.0		13.7			
VOLTAGE		X----- LOSSES -----X		X-- LINE SHUNTS --X		CHARGING							
LEVEL BRANCHES		MW		MVAR		MW		MVAR		MVAR			
130.0		8		13.99		51.84		0.0		0.0		13.9	
30.0		11		0.65		11.96		0.0		0.0		0.3	
TOTAL		19		14.64		63.81		0.0		0.0		14.2	

Figure 5.3 Summary of the load flow result for the base case

5.2.2 Pre-fault condition

In order to establish a pre-fault condition which resembles a stressed system, transmission lines HV_L2 and LV_L13 were granted on outage for maintenance as shown in Fig. 5.4. The system still operates satisfactorily and the voltages are within the 1.0 ± 0.05 p.u.

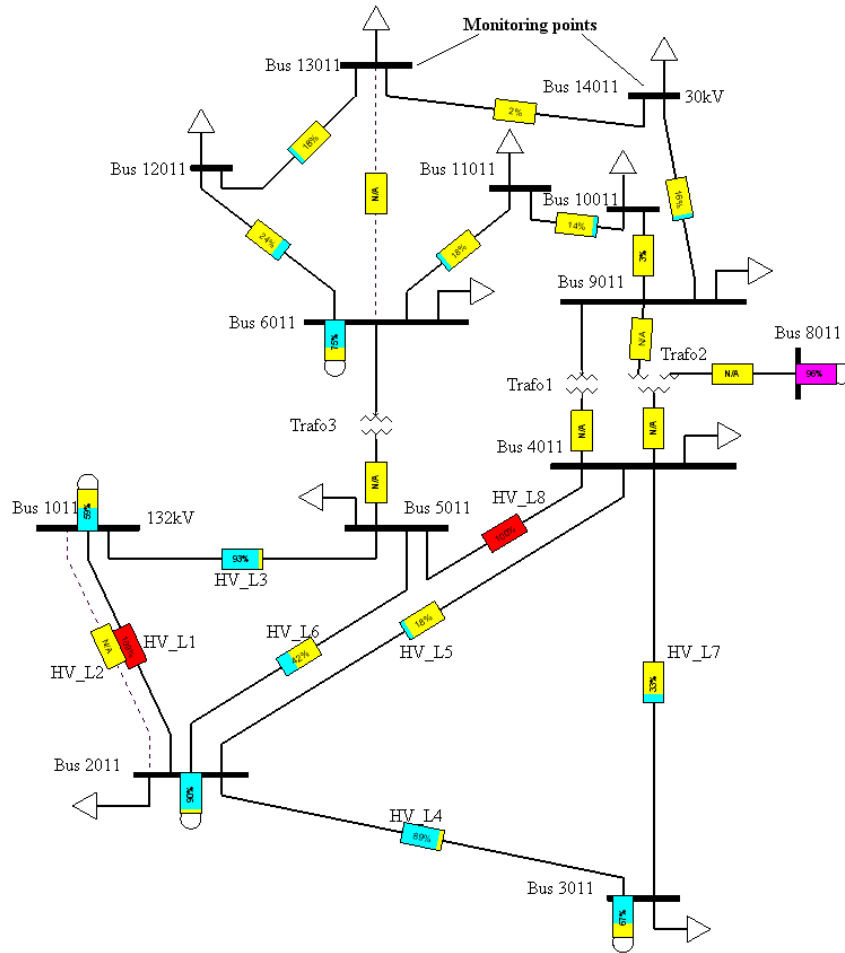


Figure 5.4 Two line outages as pre-fault condition

The loads in the system are modelled as “ZIP” models as described in Chapter 3 and also as LDFRAL model (i.e. frequency sensitive load model) with the following parameters as:

0 'LDFRAL' * 0.75000 0.0000 0.75000 0.0000 /

Where: the real power load exponent (m) and the real current load exponent (r) are taken as 0.75 each, while the reactive power load exponent (n) and reactive current load exponent (s) are zero.

Of particular interest in this study are the loads ‘LJ’ and ‘LK’ connected to bus 13011 and 14011. These loads were further modelled as induction motor load and complex load respectively. The induction motor parameters are obtained using the PSS/E auxiliary software (IMD). Details of the induction motor characteristics and parameters are given in Appendix C. For the complex load model a free assumption is made such that the load is represented as:

14011 'CLODBL' * 50 0 5 0 0.0 2 0.0 0.1 /

Where, 50% of the load at bus 14011 is assumed to be made up of large motor load having a step down distribution transformer with 5% excitation current and 10% impedance. The remaining fraction of the load are considered as constant impedance load having $K_p=2$.

A summary of the load flow result for the pre-fault condition is shown in Fig. 5.5. This when compared with the base case load flow result shows that for the same loading condition the active and reactive power losses increases by 29.5% and 21.05% respectively.

```

***** SUMMARY FOR COMPLETE SYSTEM *****
SYSTEM SWING BUS SUMMARY
BUS X---NAME---X X--- AREA ---X X--- ZONE ---X      MW      MVAR  MVABASE
1011 BUS1011 130   1 [   ] 1 [   ]      236.2    -33.7   615.0
  13 BUSES          5 PLANTS          5 MACHINES      11 LOADS
  17 BRANCHES       3 TRANSFORMERS      0 DC LINES      0 FACTS DEVICES
X----- ACTUAL -----X X----- NOMINAL -----X
      MW      MVAR      MW      MVAR
FROM GENERATION      278.0    145.6    278.0    145.6
TO CONSTANT POWER LOAD 259.0    81.5    259.0    81.5
TO CONSTANT CURRENT      0.0      0.0      0.0      0.0
TO CONSTANT ADMITTANCE  0.0      0.0      0.0      0.0
TO BUS SHUNT            0.0      0.0      0.0      0.0
TO FACTS DEVICE SHUNT   0.0      0.0      0.0      0.0
TO LINE SHUNT           0.0      0.0      0.0      0.0
FROM LINE CHARGING      0.0     13.1      0.0     12.3

VOLTAGE      X----- LOSSES -----X X-- LINE SHUNTS --X CHARGING
LEVEL BRANCHES MW      MVAR      MW      MVAR      MW      MVAR
130.0        7      17.37    63.29    0.0      0.0     12.9
 30.0        10     1.59    13.95    0.0      0.0      0.2
TOTAL      17     18.96    77.24    0.0      0.0     13.1

```

Figure 5.5 Summary of the load flow result for the pre-fault condition

5.3 The IEEE14-bus Voltage collapse scenario

The term voltage collapse as described in [10] is the process by which the sequence of events accompanying voltage instability leads to complete blackout or abnormally low voltages in a significant part of the power system.

In the voltage collapse scenario, it is assumed that underfrequency and undervoltage relay protection schemes are deactivated. The dynamic load behaviour of the induction motor load and complex load are observed at buses 13011 and 14011. While the action of tap-changer is monitored at bus 6011 and 9011.

The triggering event that can lead to voltage collapse may be any or all of the following:

- Sudden increase in load
- Loss of a critical transmission line due to line fault such as tree contact
- Loss of generation and lack of reactive power support

For the purpose of conducting preliminary studies on voltage stability, the following sequence of switching actions is implemented in the dynamic simulation:

- 0-60 seconds: represent the pre-fault and normal loading condition
- At 60 seconds: Synchronous condenser unit at bus 8011 dropped out.
- At 180 seconds: 130kV line HV_L3(1011-5011) tripped out of service
- At 360 seconds: 130kV line HV_L8 (5011-4011) tripped out of service
- At 480 seconds: 130kV line HV_L4 (2011-3011) tripped out of service. This last switching action caused rapid operation of tap changer and led to voltage instability and voltage collapse.

5.3.1 Distance relay operation

The apparent impedance and distance relay operation during the switching operation for the longest 130kV transmission line (HV_L5) is shown in Fig. 5.6. Interesting to observe in the figure is that the tripping occurred without any line fault and the apparent impedance traverse through zone3, 2 and 1 within a time frame of 0.7 second (360 to 360.7). This corresponds to zone2 operation with zone3 yet to timeout. The strategy used is by assuming zone1 is equipped with power swing blocking, in which case zone1 time is set to be equal to zone2 timing (15cycles).

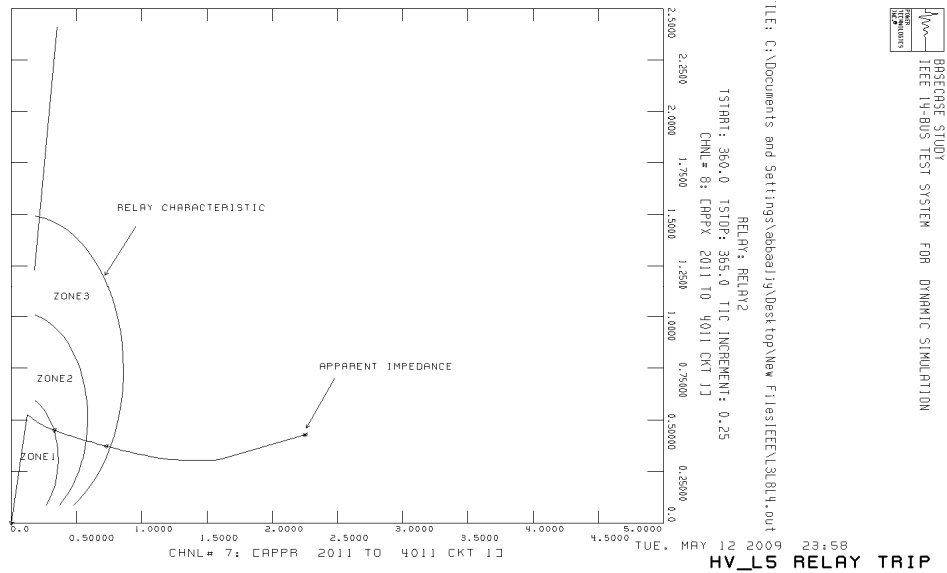


Figure 5.6 Tripping characteristics of distance relay on line HV_L5

By taking a closer look at the trajectory of the apparent impedance shown in Fig. 5.7, the instances at which it enters the various zone are determined as follows:

- It is out of zone3 at T1=360.1seconds
- It enters zone3 at T2= 360.23 seconds
- It enters zone2 at T3=360.33seconds
- It enters zone1 at T4= 360.5 seconds
- It enters zone1 and stays up to T5=360.65 seconds before tripping occurred.
- At 360.661 the circuit breaker trips in zone2.

Expected total time of operation of zone2 = Time zone2 picked up+ zone2 time out+ Circuit breaker time = 360.33+0.3+0.1=**360.73** seconds.

Expected time of operation of zone3= Time zone3 picked up+ zone3 time out+ Circuit breaker time= 360.23+0.6+0.1=**360.93** seconds.

This shows that at the time zone3 will time out (360.83 seconds) the circuit breaker that already received tripping signal from zone2 must have opened.

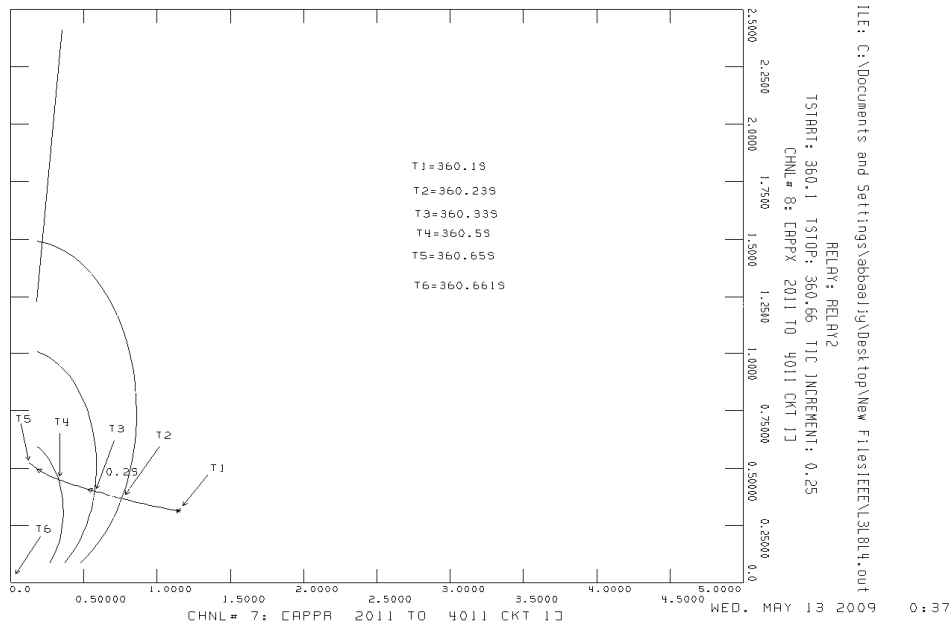
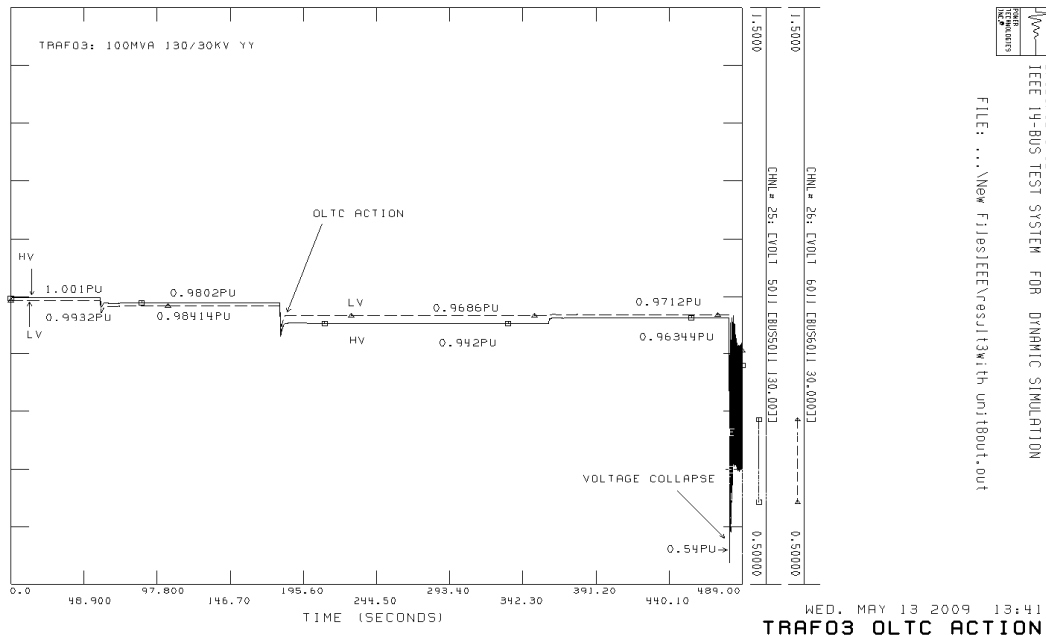


Figure 5.7 130kV distance relay time operation of line HV_L5

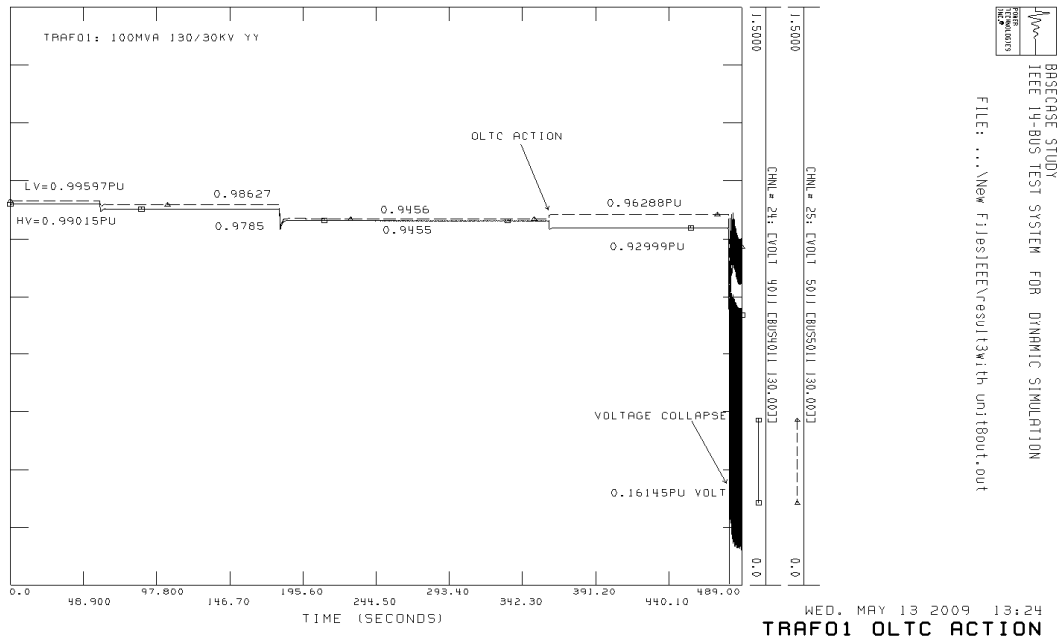
If zone2 is blocked, the tripping would still occur in **0.2** seconds (the difference between 360.73 seconds to 360.93 seconds). For some lines the apparent impedance traversed through zones2 and 3 then move out of the zones before the timed out.

5.3.2 Voltage profile and OLTC action

Initially the voltage at the HV side of the transformer is slightly higher than the LV side. But as the switching event progresses, the tap changer began to operate to maintain the LV side voltage close to the nominal value. At certain point the voltage at the HV side would be lower than that of the LV side. Fig. 5.8 shows the action of the tap changing transformer at buses 6011 and 9011.



(a) OLTC action at bus 6011



(b) OLTC action at bus 9011
Figure 5.8 Voltage profile of tap changing transformers

At bus 6011 the voltages collapses to 0.5pu and at bus 9011 the voltage collapses to 0.1614pu. In both cases the action of OLTC towards restoring nominal voltage on the LV side is shown labelled in the figure.

5.3.3 Dynamic load behaviour

A snapshot of the induction motor load taken between 176.0 seconds to 183.0 seconds illustrates the restoration properties of the load. The load is sensitive to each of the switching actions and attempt to restore back its load after each disturbance.

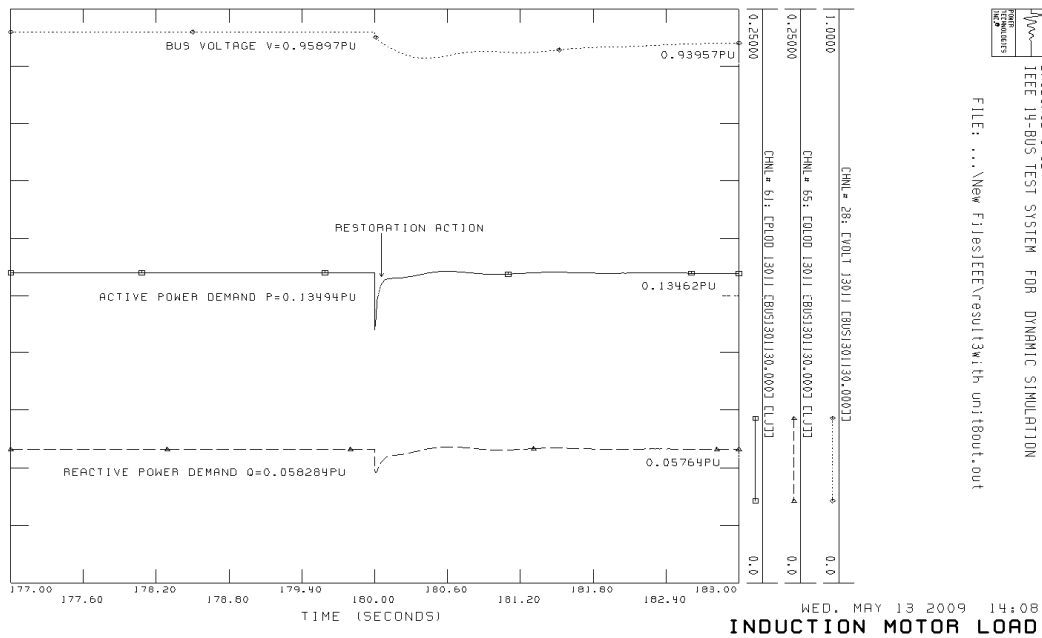


Figure 5.9 Induction motor load behaviour at bus 13011

Fig. 5.9 shows the behaviour of the induction motor load at bus 13011. Within a time frame of 485 seconds as shown in Fig. 5.10 the voltage collapses occur between 480 to 485 seconds.

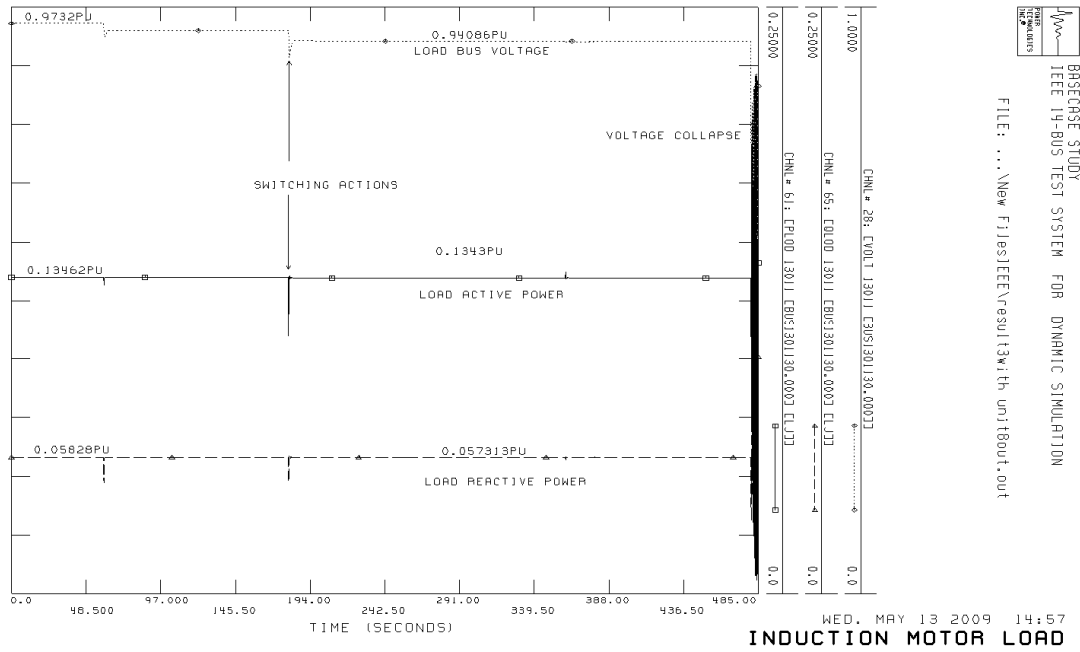


Figure 5.10 Voltage collapse at bus 13011 connected with induction motor load

In practice, the induction machine load are usually protected against over/undervoltages as well as internal failure with over current/ earth fault protection, fuses and for very small motors using mcb (medium circuit breaker).

An effective means of voltage collapse mitigation is to use system protection scheme which automatically control and disconnects/connects generation, load or compensating devices in order to achieve the load- generation balance under emergency condition. Part of the strategy includes blocking of on-load tap changer operation and using load shedding techniques discussed in Chapter 2. However, load shedding is always recommended to be the last defence action and its application is surrounded with lots of controversies especially in a deregulated power system.

The mitigation strategy would be presented in the next chapter, where the voltage collapse incidence similar to the Sweden/Denmark blackout will be simulated using Nordic32 bus system.

Chapter Six: Case study of Nordic32-bus system

In this chapter, concepts of voltage stability as well as behaviour of distance relay during small and large disturbances will be investigated via a case study of Nordic32-bus system. Important issues such as OLTC action, high reactive power losses, cascaded tripping of critical lines during the system disturbance is presented.

It was shown in Chapter 5 that heavily loaded IEEE14-bus test system results in voltage instability due to a bus-bar fault triggering event. The findings includes among others the following observations; high active and reactive power demand as well as power losses, distance protection operation in zone1, 2 and 3 when the tap changer is considered blocked. The influence of load shedding as a means of voltage collapse mitigation is highlighted.

6.1 Base case and pre-fault condition of Nordic32-bus system-static analysis approach

To begin with the voltage stability issue, load flow analysis of the moderate transfer Nordic32-bus system is first studied. The choice of Nordic32-bus system in this work is due to its wide acceptability in the literature, availability of data and more importantly its close resemblance as well as its simplicity to mimic the practical Swedish network system. It is assumed that the system is designed to withstand N-1 contingency which includes but not limited to the tripping of an important transmission line or loss of generation unit. Also considered in the analysis are that the load are modelled as constant power load for the static load flow solutions and a mixture of aggregate induction motor load, complex load and 'ZIP' load model for the dynamic simulation.

Similar pre-fault condition as reported in [21] before the blackout incidence in southern Sweden in 2003 is applied to the Nordic32-bus test system in order to observe the important parameters such as voltage profile, frequency, active and reactive power generation, transmission line loading condition and total system losses. Then, simulation of voltage collapse scenario based on the triggering event reported in [21] is implemented.

The investigation of voltage stability and zone3 distance protection studies in this Chapter would be carried out as follows:

- *Base case stability:* The behaviour of the system is observed under normal loading and operation condition.
- *Pre-fault condition:* An N-1 contingency criterion is implemented by granting outages on a 400kV transmission line and a generation unit on annual overhaul when the system is moderately loaded.
- *Triggering event condition:* This is a transmission line fault with fault duration of 0.1sec.
- *Post fault condition:* This includes the possibility of voltage collapse- i.e. for bus voltages less than 0.5p.u.
- *Operation of distance protection relays:* This applies to the critical lines connecting north to south with the zone time settings set to standard recommended settings- Zone timings Zone1 = 0mS, Zone2= 300 milliseconds and Zone3 = 500milliseconds -1second. The voltage collapse incidence is monitored using three different timing conditions , namely:
 - Zone3 set at 0.6 seconds (30cycles)
 - Zone3 blocked i.e. set at 1.2 seconds (60cycles)
 - Only zone2 in service. Zone1 and zone3 blocked, each set at 1.2 seconds (60cycles).

The setting calculations of the distance protection zones for selected critical lines of the Nordic32-bus test systems used in this study are tabulated in Table 6.1.

Table 6.1 Zone reach settings for mho distance relays used in Nordic32-bus test system

Relay Location	Model	Type (mho)	Zone1 (pu) reach			Zone2(pu) reach			Zone3(pu) reach		
			Magnitude	Angle	centre radius	Magnitude	Angle	centre radius	Magnitude	Angle	centre radius
4011-4021-1-1	DISTR1	1	0.04824	84.26	0.02413	0.0703	84.29	0.03515	0.1261	82.48	0.06305
4011-4022-1-1	DISTR1	1	0.03216	84.26	0.0161	0.0432	84.69	0.0216	0.0905	83.97	0.04525
4012-4022-1-1	DISTR1	1	0.02818	83.48	0.0141	0.03821	83.99	0.01911	0.0855	83.62	0.04275
4021-4032-1-1	DISTR1	1	0.03216	84.3	0.01608	0.051	82.6	0.0255	0.09558	83.7	0.04805
4021-4042-1-1	DISTR1	1	0.04866	80.5	0.025	0.0646	80.7	0.0325	0.081	81.1	0.0405
4022-4031-1-1	DISTR1	1	0.03216	84.29	0.01608	0.0427	84.29	0.02135	0.09197	82.82	0.04598
4022-4031-2-1	DISTR1	1	0.03216	84.29	0.01608	0.0427	84.29	0.02135	0.09197	82.82	0.04598
4031-4032-1-1	DISTR1	1	0.00804	84.26	0.00402	0.0203	80.1	0.01015	0.0779	84.29	0.03895
4031-4041-1-1	DISTR1	1	0.03236	81.47	0.01618	0.04292	81.96	0.02146	0.05543	76.97	0.02771
4031-4041-2-1	DISTR1	1	0.03236	81.47	0.01618	0.04292	81.96	0.02146	0.05543	76.97	0.02771
4032-4042-1-1	DISTR1	1	0.03298	76	0.01649	0.045	76.5	0.0225	0.0662	79.11	0.0331
4032-4044-1-1	DISTR1	1	0.0403	83.16	0.02014	0.0516	83.32	0.0258	0.09185	83.44	0.04593
4041-4044-1-1	DISTR1	1	0.02412	84.29	0.01206	0.0314	84.52	0.0157	0.04522	84.29	0.02261
4042-4044-1-1	DISTR1	1	0.0161	84.29	0.00805	0.02134	84.62	0.01067	0.06159	83.94	0.0308

It should be noted that the zone reach settings are expressed in per-unit of the system base and represent the secondary impedance fed into the relay model according to the method outlined in section 2.4.3.

In the base case all available generating units and transmission lines are in service and are connected to the loads. Fig. 6.1 shows the summary of the load flow results showing total generation, constant power load, shunt compensation and active and reactive power losses.

```

***** SUMMARY FOR COMPLETE SYSTEM *****
                SYSTEM SWING BUS SUMMARY
BUS X---NAME---X X--- AREA ---X X--- ZONE ---X      MW      MVAR  MVBASE
4011 BUS4011 400 1 [      ] 1 [      ] 450.5    -89.9  1000.0
 41 BUSES      20 PLANTS          23 MACHINES      22 LOADS
 69 BRANCHES   17 TRANSFORMERS    0 DC LINES      0 FACTS DEVICES
X----- ACTUAL -----X X----- NOMINAL -----X
FROM GENERATION      11250.5    987.3    11250.5    987.3
TO CONSTANT POWER LOAD 10940.0    3358.4    10940.0    3358.4
TO CONSTANT CURRENT      0.0      0.0      0.0      0.0
TO CONSTANT ADMITTANCE  0.0      0.0      0.0      0.0
TO BUS SHUNT            0.0    -931.2    0.0    -900.0
TO FACTS DEVICE SHUNT  0.0      0.0      0.0      0.0
TO LINE SHUNT          0.0      0.0      0.0      0.0
FROM LINE CHARGING     0.0    4391.8    0.0    4311.0

VOLTAGE X----- LOSSES -----X X-- LINE SHUNTS --X CHARGING
LEVEL BRANCHES MW      MVAR      MW      MVAR      MW      MVAR
400.0  50    243.14  2474.51  0.0    0.0    4340.6
220.0  2    15.28   114.62  0.0    0.0     3.5
130.0  17    52.03   362.67  0.0    0.0     47.7
TOTAL  69    310.45  2951.80  0.0    0.0    4391.8

```

Figure 6.1: Complete base case system summary

The following pre-fault conditions similar to those described in [21] are adopted in both the static load flow and the dynamic simulation:

- A generation unit at RT132_bus1042 out of service for annual overhaul
- A single 400kV line CL15 out of service for maintenance work

The system adjusted to the N-1 contingency criterion and no violation of the system loading and voltage constraints was observed. The summary of the load flow result for the pre-fault condition is displayed in Fig. 6.2.

```

***** SUMMARY FOR COMPLETE SYSTEM *****
                SYSTEM SWING BUS SUMMARY
BUS X---NAME---X X--- AREA ---X X--- ZONE ---X      MW      MVAR  MVABASE
4011 BUS4011 400 1 [      ] 1 [      ] 990.1    213.6  1000.0
 41 BUSES      20 PLANTS                22 MACHINES  22 LOADS
 68 BRANCHES   17 TRANSFORMERS          0 DC LINES   0 FACTS DEVICES
                X----- ACTUAL -----X X----- NOMINAL -----X
                MW      MVAR      MW      MVAR
FROM GENERATION      11430.1  2472.0  11430.1  2472.0
TO CONSTANT POWER LOAD 10940.0  3358.4  10940.0  3358.4
TO CONSTANT CURRENT    0.0      0.0      0.0      0.0
TO CONSTANT ADMITTANCE 0.0      0.0      0.0      0.0
TO BUS SHUNT           0.0     -1085.6  0.0     -900.0
TO FACTS DEVICE SHUNT  0.0      0.0      0.0      0.0
TO LINE SHUNT          0.0      0.0      0.0      0.0
FROM LINE CHARGING    0.0     4149.7  0.0     4071.0

VOLTAGE X----- LOSSES -----X X-- LINE SHUNTS --X CHARGING
LEVEL BRANCHES MW      MVAR      MW      MVAR      MVAR
400.0  49  409.27  3779.49  0.0      0.0      4096.5
220.0  2  16.03  120.22  0.0      0.0      3.4
130.0  17  64.82  449.19  0.0      0.0      49.8
TOTAL  68  490.12  4348.90  0.0      0.0      4149.7

```

Figure 6.2: System summary of the pre-fault condition

It can be observed from the system summary result that the active and reactive power generation increases due to the pre-fault condition. Also the MW & Mvar losses for the pre-fault condition increases to 1.57 and 1.47 times each, when compared with the normal operation.

The loading for normal and pre-fault conditions of the 5 major transmission lines: CL12, CL14, CL15, CL16 and CL17 are tabulated in Table 6.2 and Table 6.3 respectively.

Table 6.2 Normal power transfer, line losses and loading condition

Transmission lines	sendind end profile			Receiving end profile			Line Loss		Line loading
	MW	MVAR	Bus Voltage(p.u)	MW	MVAR	Bus Voltage(p.u)	MW	MVAR	%
CL12	533.6	-137.2	1.07	-508.6	-48	1.043	25	-185.2	34
CL14	577.9	-135.9	1.05	-559.7	-5.4	1.042	18.2	-141.3	36
CL15	577.9	-135.9	1.05	-559.7	-5.4	1.042	18.2	-141.3	36
CL16	609.2	-80.6	1.065	-589.4	-21.1	1.043	19.8	-101.7	38
CL17	483.3	-134.4	1.07	-462.7	-5.2	1.043	20.6	-139.6	31

Table 6.3 Pre-fault power transfer, line losses and loading condition

Transmission lines	sendind end profile			Receiving end profile			Line Loss		Line loading
	MW	MVAR	Bus Voltage(p.u)	MW	MVAR	Bus Voltage(p.u)	MW	MVAR	%
CL12	709	-98.8	1.013	-659.7	90.9	1	49.3	-7.9	47
CL14	1055.2	-73.6	0.987	-986.4	294.8	1	68.8	221.2	71
CL15	0	0	0.987	0	0	1	0	0	0
CL16	828.8	-36.1	0.995	-786.8	148.9	0.993	42	112.8	56
CL17	680.3	-179.9	0.995	-633	170.3	1	47.3	-9.6	47

Fig. 6.3 shows the single line diagram for the pre-fault condition. It can be seen that generation units CT11, FT44, FT47 and FT62 are close to their reactive power limits and are bound to trip due to action of other protections.

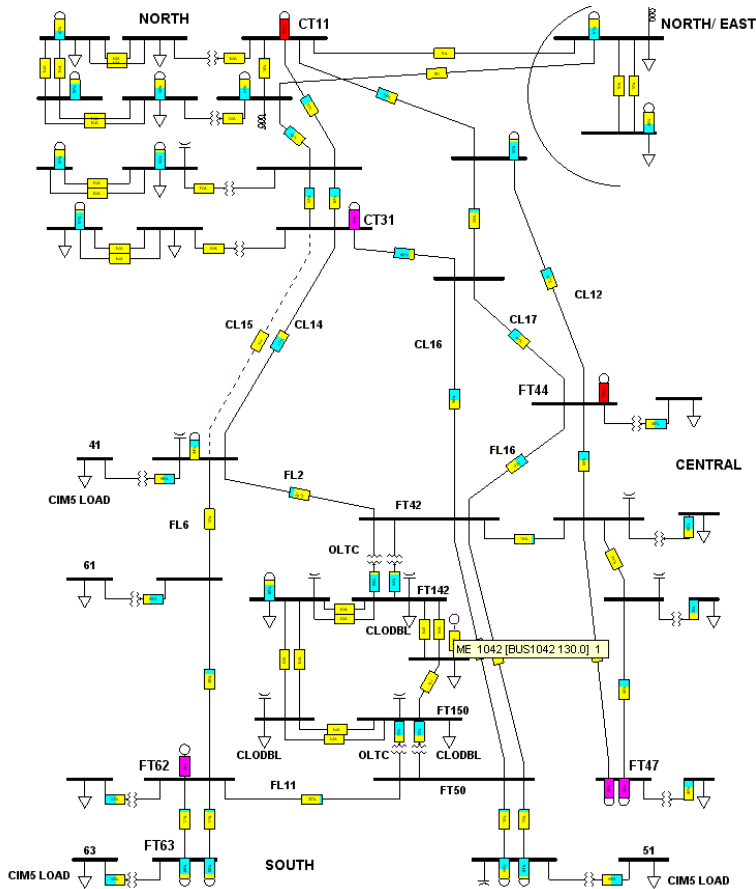


Figure 6.3 Pre-fault single line diagram of Nordic32-bus test system

This implies that the system is under stress condition, any low probability credible contingency may lead to voltage collapse unless protection and control scheme intervened. However, the load flow result with transformer OLTC in automatic operations shows further increase in the system losses as shown in Fig. 6.4.

```

***** SUMMARY FOR COMPLETE SYSTEM *****
                SYSTEM SWING BUS SUMMARY
BUS X---NAME---X X--- AREA ---X X--- ZONE ---X      MW      MVAR  MVBASE
4011 BUS4011 400 1 [ ] 1 [ ] 1007.5    217.4    1000.0
41 BUSES      20 PLANTS      22 MACHINES  22 LOADS
68 BRANCHES  17 TRANSFORMERS  0 DC LINES  0 FACTS DEVICES
X----- ACTUAL -----X X----- NOMINAL -----X
                MW      MVAR      MW      MVAR
FROM GENERATION      11447.5    2829.9    11447.5    2829.9
TO CONSTANT POWER LOAD      10940.0    3358.4    10940.0    3358.4
TO CONSTANT CURRENT      0.0      0.0      0.0      0.0
TO CONSTANT ADMITTANCE      0.0      0.0      0.0      0.0
TO BUS SHUNT      0.0    -888.2      0.0    -900.0
TO FACTS DEVICE SHUNT      0.0      0.0      0.0      0.0
TO LINE SHUNT      0.0      0.0      0.0      0.0
FROM LINE CHARGING      0.0    4128.3      0.0    4071.0
VOLTAGE X----- LOSSES -----X X-- LINE SHUNTS --X CHARGING
LEVEL BRANCHES      MW      MVAR      MW      MVAR
400.0  49    415.29    3837.93      0.0      0.0    4082.9
220.0  2     16.03     120.22      0.0
0.0    3.4
130.0  17     76.13     529.82      0.0      0.0    42.0
TOTAL   68    507.45    4487.97      0.0      0.0    4128.3

```

Figure 6.4: system summary with transformer OLTC in operation

This when compared with the base case load flow result shows that for the same loading condition the active and reactive power losses increases by 63.46% and 52.04% respectively. These losses are on the high side.

If under this stress condition a line fault due to tree encroachment causes line CL17 to trip. The system entered into emergency state and the voltage collapse -static load flow result blown up after six iterations. It should be observed that the solution does not converge even though no protection of any kind is implemented in the static analysis model.

6.2 Dynamic simulation of the Nordic32-bus system

In the dynamic simulation, the following modelling considerations are made:

- Distance protection relays were installed on 15 transmission lines in the forward direction of power flow using 'DISTR1' build-in model of the PSS/E model library. Complete DISTR1 protocol for the 15 transmission lines are given in Appendix B.
- On-load tap changer models 'OLTC1' are loaded into the dynamic data file (.dyr). Details for the on-load tap changer models are given in Appendix C.
- The loads in the system are represented as frequency sensitive as described in Chapter 5 using

```
0 'LDFRAL' * 0.75000 0.0000 0.75000 0.0000 /
```

And the loads are further grouped into:

- Constant impedance, constant current and constant power “ZIP” models with the following parameters:

100%I, 0, 0 and 0,100%Z, 0 for the demand active and reactive power respectively.

- Complex loads are assumed at Area 4 on buses 1041, 1044 and 1045 with the parameter selection as follows:

```
1041 'CLODBL' * 0.0 0.0 5 0.0 0.0 2 0.0 0.1 /
```

```
1044 'CLODBL' * 90 0.0 5 0.0 0.0 2 0.0 0.1 /
```

```
1045 'CLODBL' * 0.0 90 5 0 0.0 2 0.0 0.1 /
```

It can be observed that; at bus 1044, 90% of the load is dedicated to be a large motor load, while small motor load at bus1045 constitute 90% of the load. All the buses have a step down distribution transformer with 5% excitation current and 10% impedance. The remaining fraction of the load are considered as constant impedance load where $K_p=2$.

- Aggregate Induction motor loads were assumed at Area 8 on buses 41, 51 and 63. Typical parameter settings obtained using IMD- the auxiliary PSS/E tool-are given in Appendix C.
- For defense action against voltage collapse underfrequency and undervoltage load shedding schemes were applied to some selected load. Details of the appropriate settings are given in Appendix D. The underfrequency relay operates in three stages from 48.8Hz to 48.0Hz in accordance with Nordic grid code [32]. While the undervoltage relay also operates in three stages- based on free assumption- from 0.9p.u to 0.8p.u.

6.3 Pre-fault and voltage collapse scenario

In the pre-fault and voltage collapse simulation, the on-load tap changer is allowed to operate in stepping mode (unlocked), while underfrequency and undervoltage relays for load shedding are deactivated in order to show the role of the on-load tap changer operation towards accelerating voltage collapse incidence. In addition, the loads are all represented with ZIP models.

6.3.1 Time frame for the simulation

Based on the time frame for protective relaying and overload protection given in [5], 600-740seconds time frame is adopted throughout the simulation to study the voltage instability phenomena. The following switching actions are carried out:

- 0-60 seconds: Normal loading condition representing base case
- At 60 seconds: Unit RT132 connected to bus 1042 switched out for annual overhaul. Tap changer operation adjusted the system to normal operating condition.
- At 180 seconds: 400kV line CL15 (circuit2 4031-4041) out of service for maintenance work. Rapid operation of tap changer was observed.
- At 360 seconds: Line CL12 (circuit 2, 4021-4042) out of service for line maintenance work. The system is stressed at this stage due to the action of tap changer and non application of load shedding scheme.
- At 480 seconds: Line CL 16 (circuit 2, 4032-4044) tripped on overload. This triggered a cascaded trippings of 400kV transmission lines.

From 482 - 490 seconds the system begins to experience cascaded trippings of 400kV lines which led to voltage collapse after approximately 3 seconds from the triggering event.

6.4 Simulation results for the voltage collapse scenario

6.4.1 Distance relay operations

Table 6.4 below shows a summary of zone timer pick up and the timed out operations that led to the cascading events of the critical lines which connects high generation area in the north to the high load area in the south. This timing operation is extracted from voltage collapse event records.

Table 6.4 Cascaded tripping events during voltage collapse, between 0-490 seconds

Transmission lines numencature	Branch number	Manual operation time in seconds	Pick up operation			Time out operation			Time of circuit breaker tripping	Comments
			zone3	zone2	zone1	zone3	zone2	zone1	Opening time(seconds)	
CL12	4021-4042_L1		481.929	482.019	482.41			482.419	482.519	Loss of supply
CL12	4021-4042_L2	360								6th cascading event
CL14	4031-4041_L1		481.729	481.949	482.199		482.249	482.239	482.339	2nd cascading event
CL15	4031-4041_L2	180								
CL16	4032-4044_L1		481.779	481.939	482.039		482.239	482.049	482.149	1st cascading event
CL16	4032-4044_L2	480								
CL17	4032-4042_L1		482.019	482.089	482.239			482.249	482.349	3rd cascading event
CL17	4032-4042_L2		482.019	482.089	482.239			482.249	482.349	3rd cascading event
FL2	4041-4044		482.279	482.279	482.269			482.279	482.379	4th cascading event
FL16	4042-4044		482.219	482.269	482.289			482.299	482.399	5th cascading event

It can be observed that within 2.52 seconds all the remaining critical lines connecting north and south tripped in cascade thereby leading to a voltage collapse in the south.

In the case of voltage collapse incidence, the apparent impedances shown in Fig. 6.5 for lines CL12 and CL14 are seen to traverse through all the zones since the relay characteristics are static while the apparent impedances are dynamic. The plots are taken between the periods of 480 seconds to 490 seconds after the initiation of the triggering event.

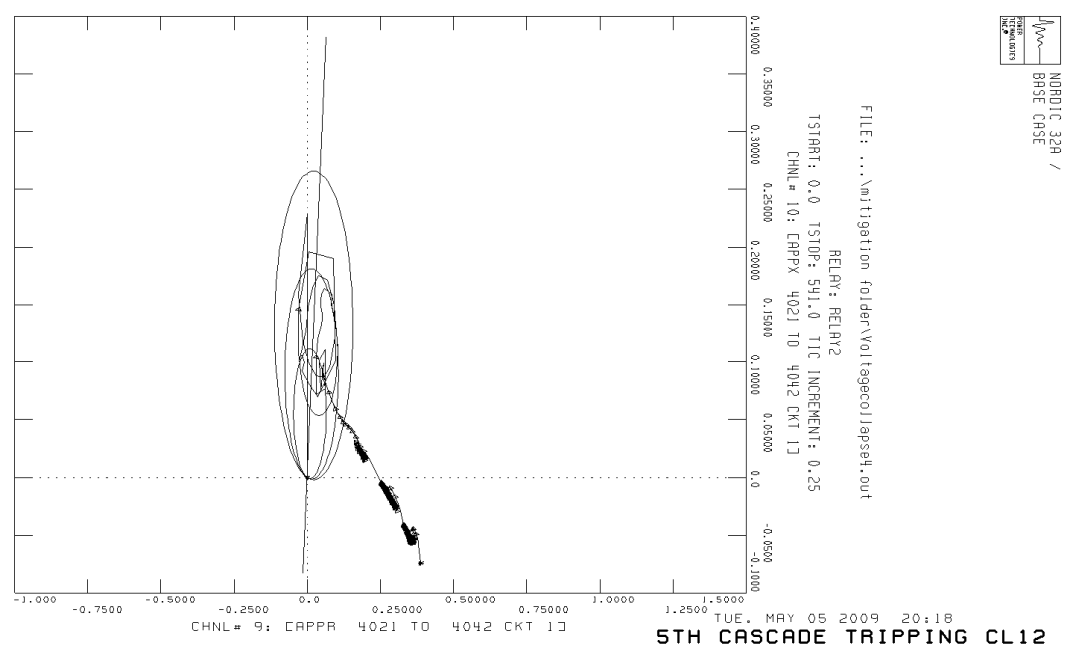
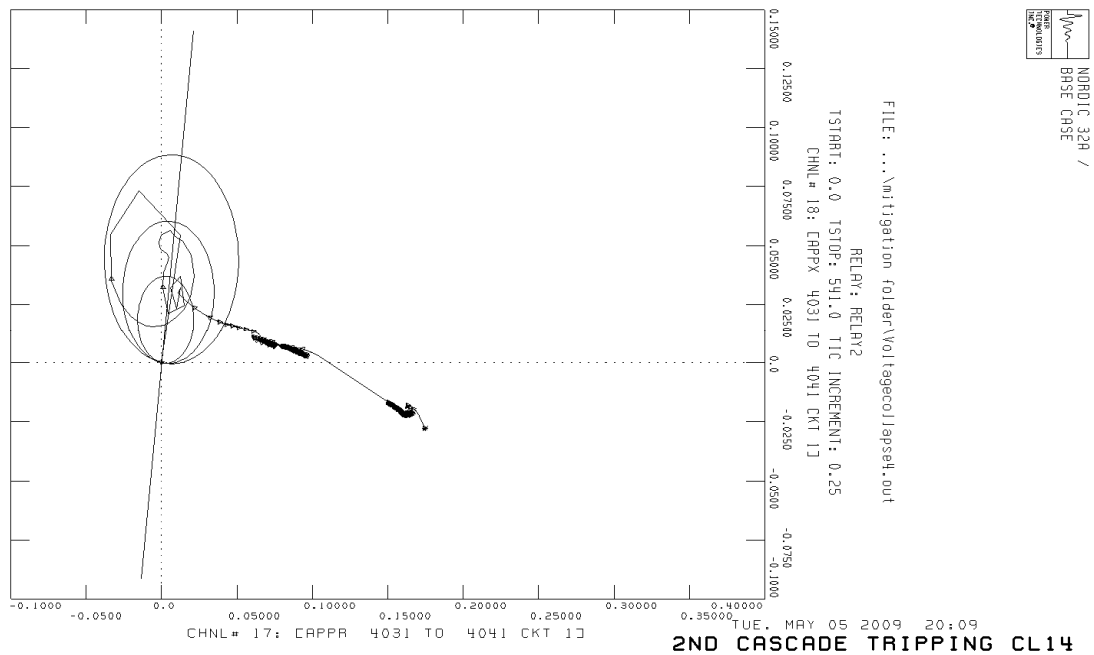


Figure 6.5 Cascaded tripping events for lines CL12 and CL14

Based on the result tabulated in Table 6.4, within 2.52 seconds with respect to the triggering event all the critical lines tripped in cascade and 370 milliseconds is the time lag observed between the commencements of the cascaded trippings to the last event.

6.4.2 Generator active, reactive power and terminal voltage output

During the voltage collapse incidence the demand for reactive power increases as shown in Fig. 6.6 beyond what the generation units' capability curve specifies. This would cause generator protection to operate on overexcitation and field limit. The cumulative effect results in voltage collapse.

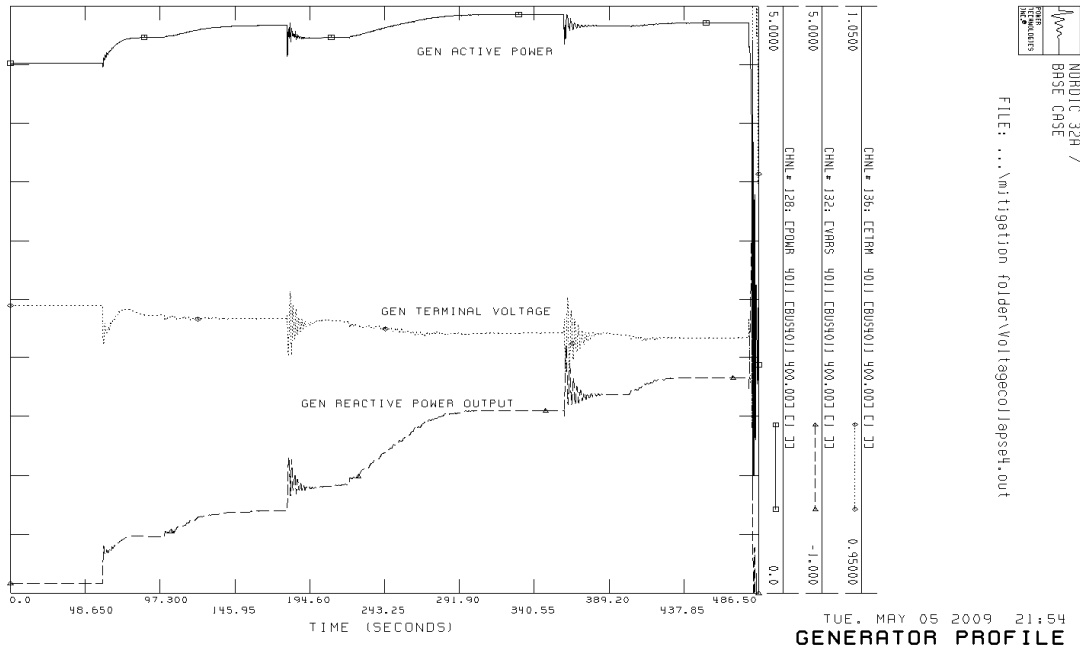
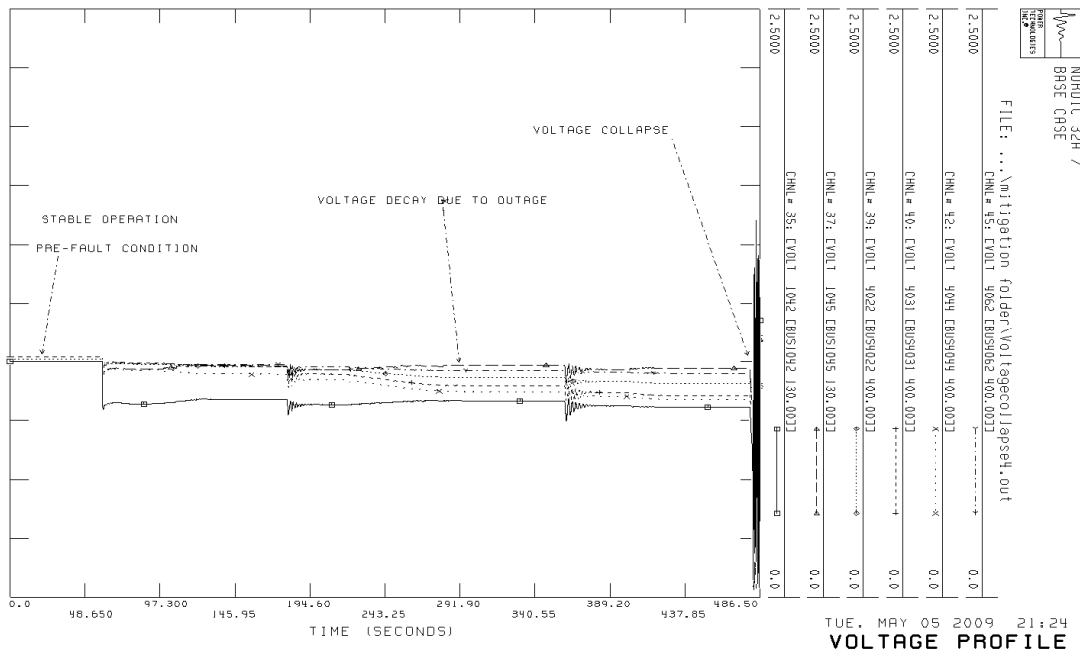


Figure 6.6 Typical generator profile for unit CT11 (bus 4011)

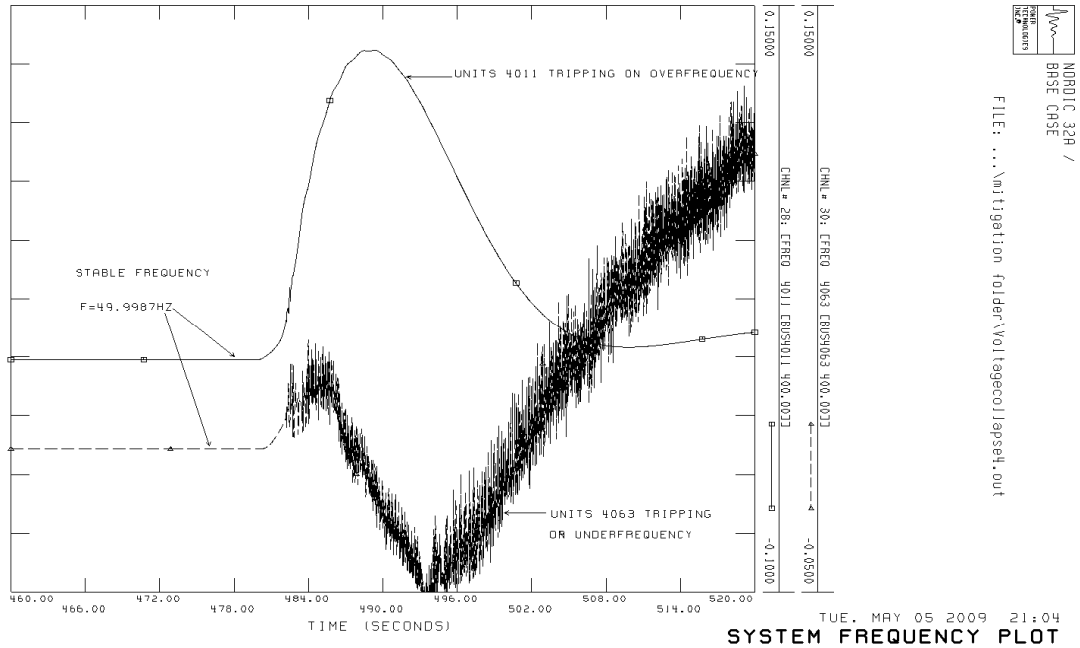
6.4.3 Voltage profile, system frequency and OLTC action

The voltage profile for the system and a typical action of an OLTC can be seen in Fig. 6.7. While on one hand the grid voltage on the HV side decreases continuously, on the other hand the OLTC continue to move in order to restore the correct voltage at the low voltage side.

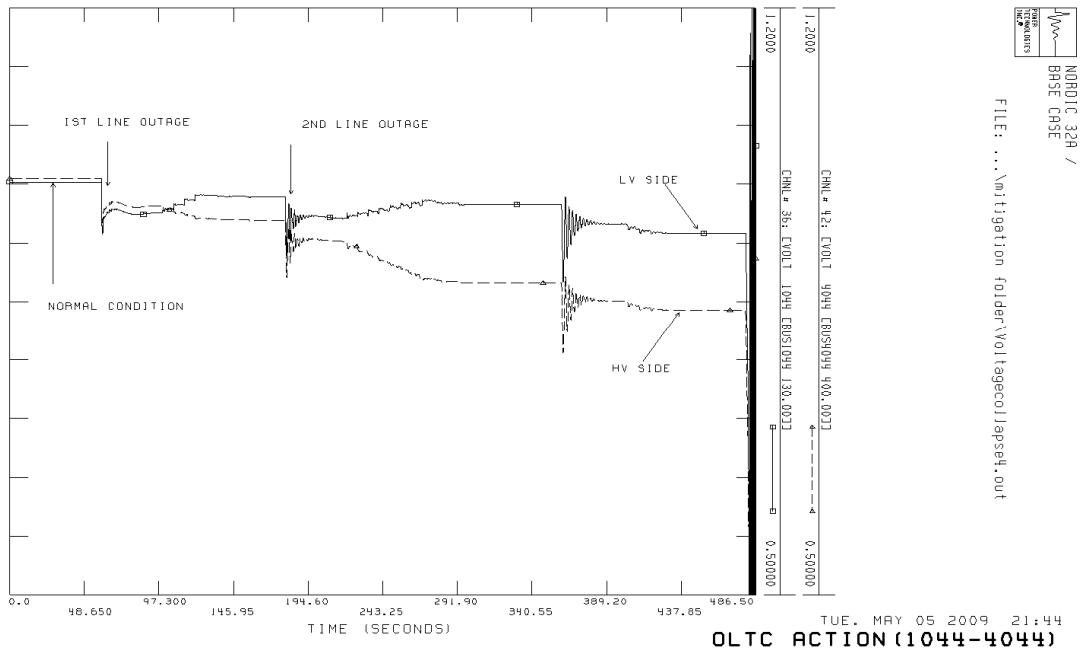
Before the occurrence of the fault, the system frequency is maintained within a tight steady value as shown in Fig. 6.7(b). However, it can be observed during the disturbance that the system frequency at CT11 (bus 4011) is very high, while at FT63 (bus 4063) very low. In both cases overfrequency and underfrequency relay would operate and trip the units.



(a) System voltage profile



(b) System frequency

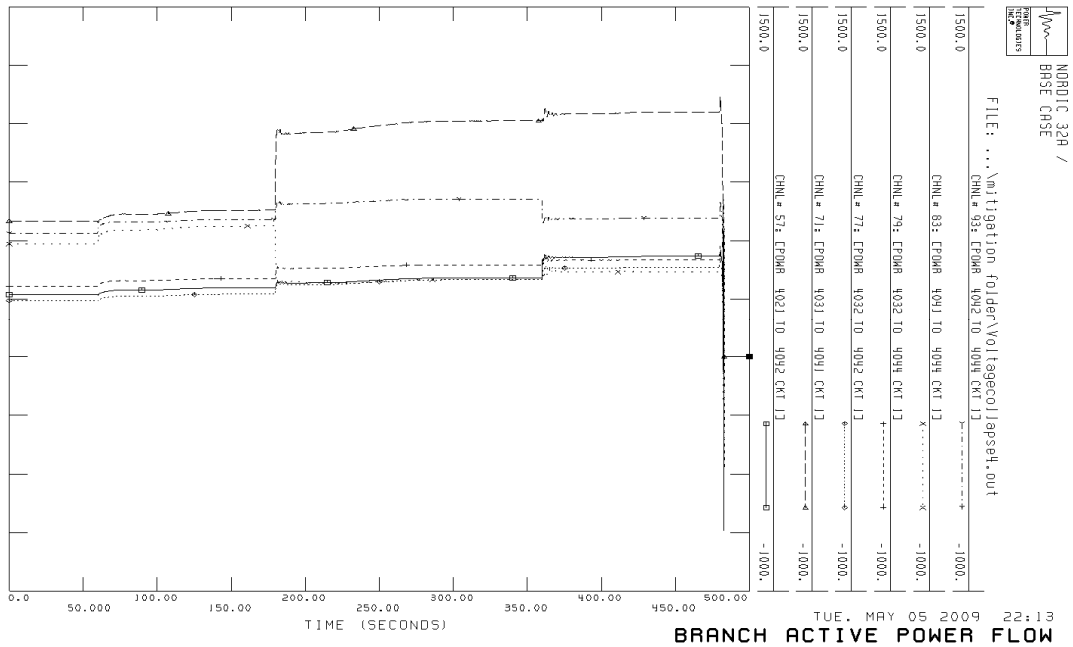


(c) Typical OLTC action

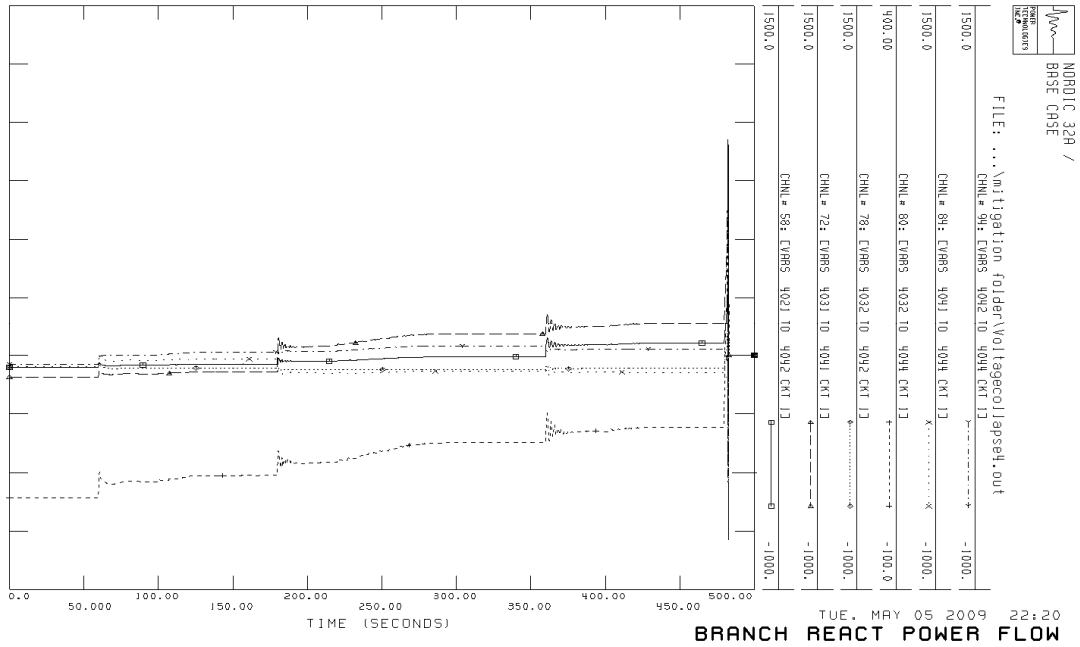
Figure 6.7: Voltage profile, system frequency and OLTC action during voltage collapse

6.4.4 Branch flows and losses

The branch flows in the transmission line corridors which interconnect northern to the southern areas as monitored on lines CL12, CL14, CL16 and CL17 are shown in Fig. 6.8. The transmission losses associated with the line outages and during the voltage instability are also shown in Fig. 6.9.



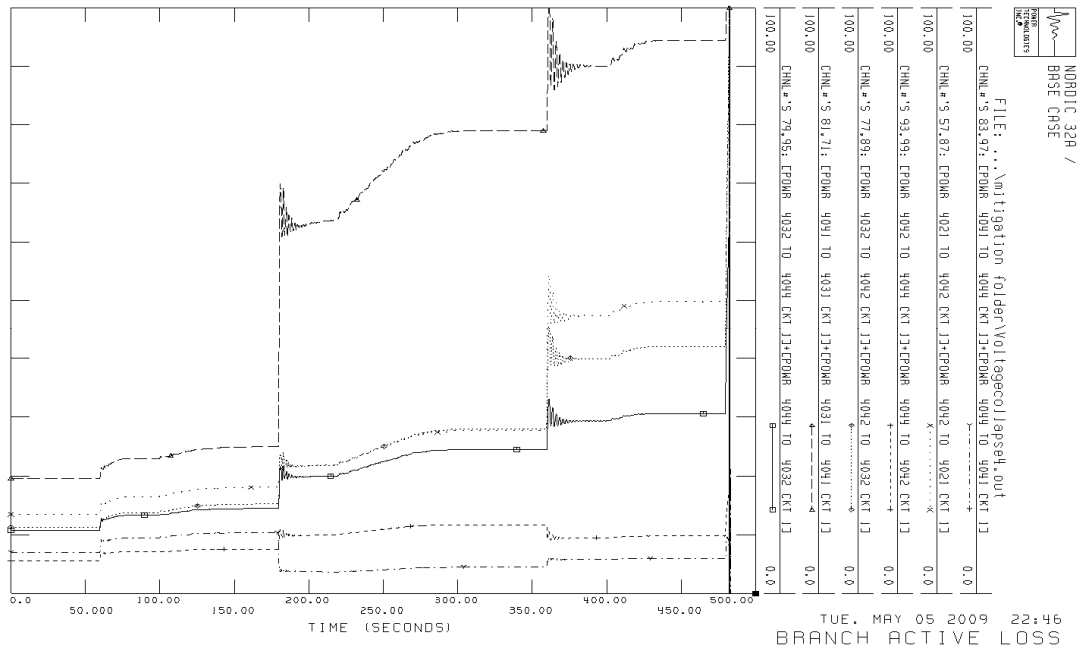
(a) Active power flow during voltage collapse



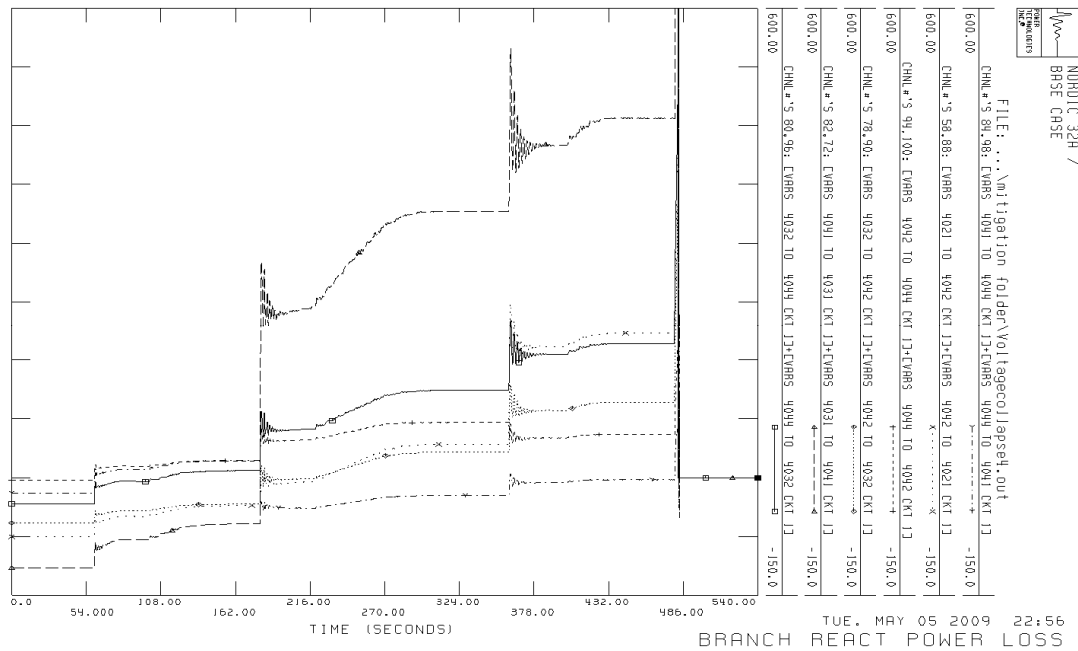
(b) Reactive power flow voltage collapse

Figure 6.8 Branch power flow (a) active power flow and (b) reactive power flow

For each line outage, increase in the active and reactive power flow on the remaining critical lines is observed. This is reflected on the line losses which also increase. The transmission lines are therefore operated close to their design limits.



(a) Active power losses during voltage collapse scenario



(b) Reactive power flow during voltage collapse scenario

Figure 6.9 Active and reactive power losses

6.4.5 Dynamic load profile

Further insight into the voltage collapse phenomenon can be observed from the load behaviour shown in Fig. 6.10 at bus 41 during the line outages. Due to the switching actions, the loads tends to restore back to normal operation after each voltage dip.

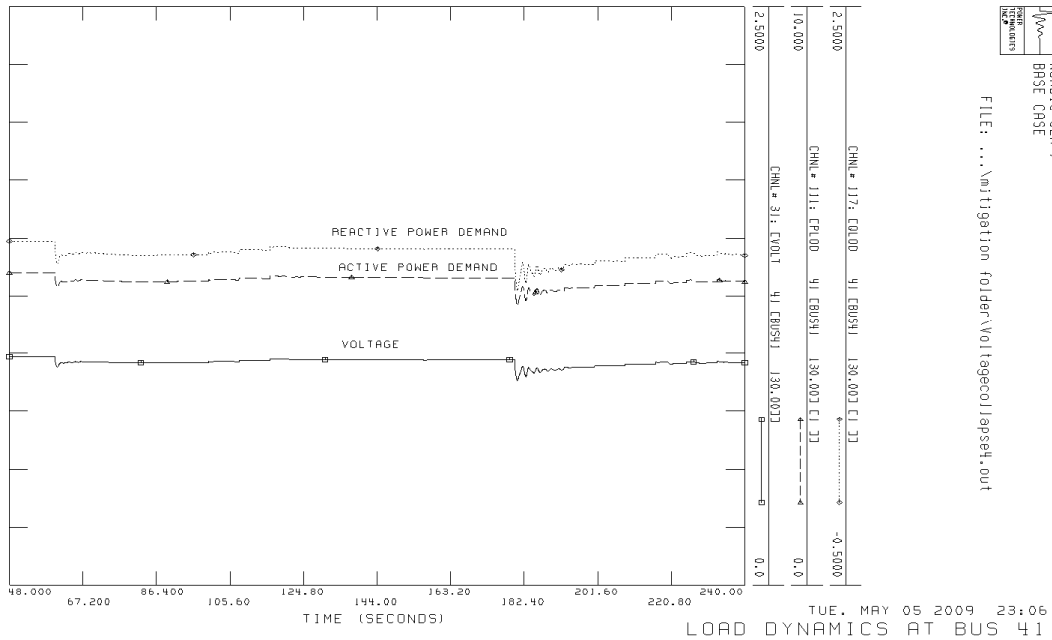


Figure 6.10 Load dynamic profile

6.5 Mitigation scenario of voltage collapse

An effective means of voltage collapse mitigation is to use system protection schemes which automatically control and disconnects/connects generation, load or compensating devices in order to achieve the load- generation balance under emergency condition. Part of the strategy includes blocking of on-load tap changer operation and using load shedding techniques discussed in Chapter 2. However, load shedding is always recommended to be the last defence action and its application is surrounded with lots of controversies especially in a deregulated power system.

It was demonstrated in the previous section that OLTC actions and cascaded tripping of distance relays resulted in a voltage collapse after 480 seconds. In view of this, a short term solution to voltage collapse using a mitigation scheme which utilises the underfrequency and the undervoltage load shedding relays is implemented in this section.

Based on the existing Nordic grid code standard [32] which specifies the rules at which underfrequency relay should operate, the dynamic data file (.dyr) used in the voltage collapse scenario is updated and equipped with underfrequency protective relay as follows:

```
0 'LDSHAL' * 48.8 0.1 0.25 48.4 0.1 0.25 48.00 0.1 0.3 1.5 /
```

The circuit breaker time is set to 0.1 seconds and the underfrequency relay **LDSHAL** is set to operate in three stages namely:

- *Stage1*: The first load shedding point (Hz) is set at 48.8Hz, its first pick up time set to 1.2 seconds and first fraction of load to be shed is 25%.
- *Stage2*: Second load shedding point (Hz) is set at 48.4Hz, second fraction pickup time (sec) is 0.9 seconds and second fraction of load to be shed is 25%.
- *Stage3*: The third load shedding point (Hz) is set at 48.0Hz, third point pickup time (sec) is 0.6 seconds and third fraction of load to be shed is 50%.

Undervoltage load shedding is not applicable in Nordic system, rather provision for emergency power is made such that when the system voltage fall below 0.975pu and last for more than 2sec, the system protection scheme send a command for additional generation reserve.

However, for the purpose of understanding voltage collapse mitigation phenomena, use is made of the in-built undervoltage relay model **LVSHBL** in the PSS/E model library to carry out load shedding at bus 41, 51, 63, 1022, 1041, 1044 and 1045. The undervoltage load shedding relay ‘LVSHBL’ is set to operate in three stages as follows:

- *Stage1*: The first load shedding point (pu) is set at 0.9pu, first point pickup time (sec) is 0.55s, and first fraction of load to be shed is 25%.
- *Stage2*: The second load shedding point (p.u) is set at 0.85pu, second fraction pickup time (sec) is 0.45s, and second fraction of load to be shed is 25%.
- *Stage3*: The third load shedding point (pu) is set at 0.8pu, third point pickup time (sec) is 0.35s and third fraction of load to be shed is 50%.

Hence, the dynamic data file (.dyr) used in the voltage collapse scenario is further updated and equipped with load shedding schemes. Typical values of the relay settings are given in Appendix D.

The strategy used in identifying the effectiveness of the mitigation actions are summarised in Table 6.5. A slight modification of the sequence of events was made where a fault occurred on the line and lasted for 100 milliseconds instead of the mild disturbance that occurred at 480 seconds when line CL16_2 (Circuit 2, 4032-4042) was switched out in the previous section, and the time frame extended to 720 seconds.

Table 6.5 voltage collapse mitigation

Under frequency relay	Tap changer operation	Under voltage relay	Comments on voltage collapse occurrence
OFF	OFF	OFF	Likely
OFF	OFF	ON	Unlikely
OFF	ON	OFF	Highly likely
OFF	ON	ON	Unlikely
ON	OFF	OFF	Unlikely
ON	OFF	ON	Highly unlikely
ON	ON	OFF	Likely
ON	ON	ON	Unlikely

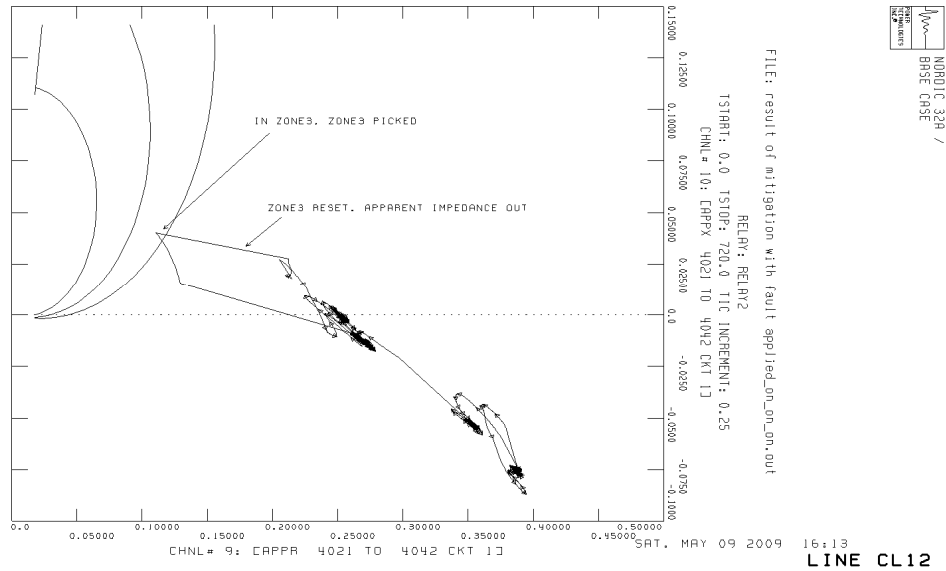
6.6 Simulation results for the mitigation of voltage collapse

The simulation results during the mitigation scenario with underfrequency and undervoltage load shedding in action when the OLTC is in operation shows that:

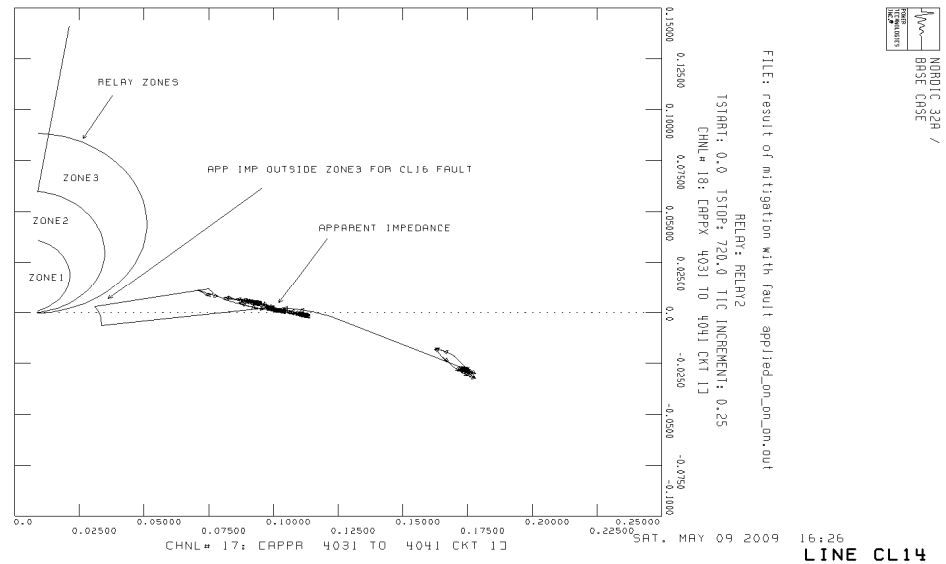
- The system survives the N-1 contingency and for the 720 second time frame there was no system breakdown.
- The mitigation action was dominated by undervoltage load shedding action. No record of underfrequency load shedding operation.
- The system collapse after undervoltage relay was blocked and only underfrequency load shedding in operation due to the action of OLTC.
- The system survives with undervoltage relay and OLTC action blocked relying only on underfrequency load shedding action.

6.6.1 Distance relay operations

The plots of the apparent impedance and zone reach of distance protection relays for the case when underfrequency and undervoltage load shedding are implemented with OLTC allowed to operate are shown in Fig. 6.11 for critical lines CL12 and CL14.



(a) No tripping on CL12



(a) Apparent Impedance out of zone reach setting for line CL14

Figure 6.11 Distance relay operation during voltage collapse mitigation

6.6.2 Generator active, reactive power and terminal voltage output

The timely intervention of the load shedding scheme during the switching events prevented the generation units from operating near their limits and this further shows the effectiveness of the voltage collapse mitigation scheme towards improving system security at the expense of switching out of some consumers. Fig. 6.12 shows the profile of a typical unit 4011 at CT11 where- in contrast with

the profile shown in Fig. 6.6- the terminal voltage, active and reactive power are shown to fall within the acceptable range.

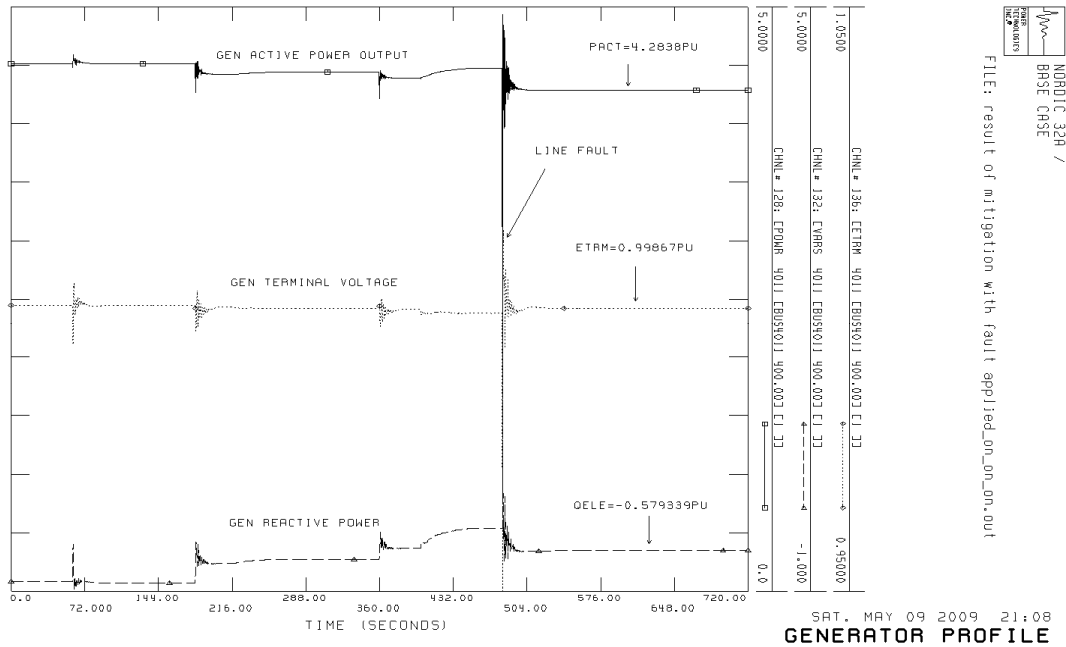
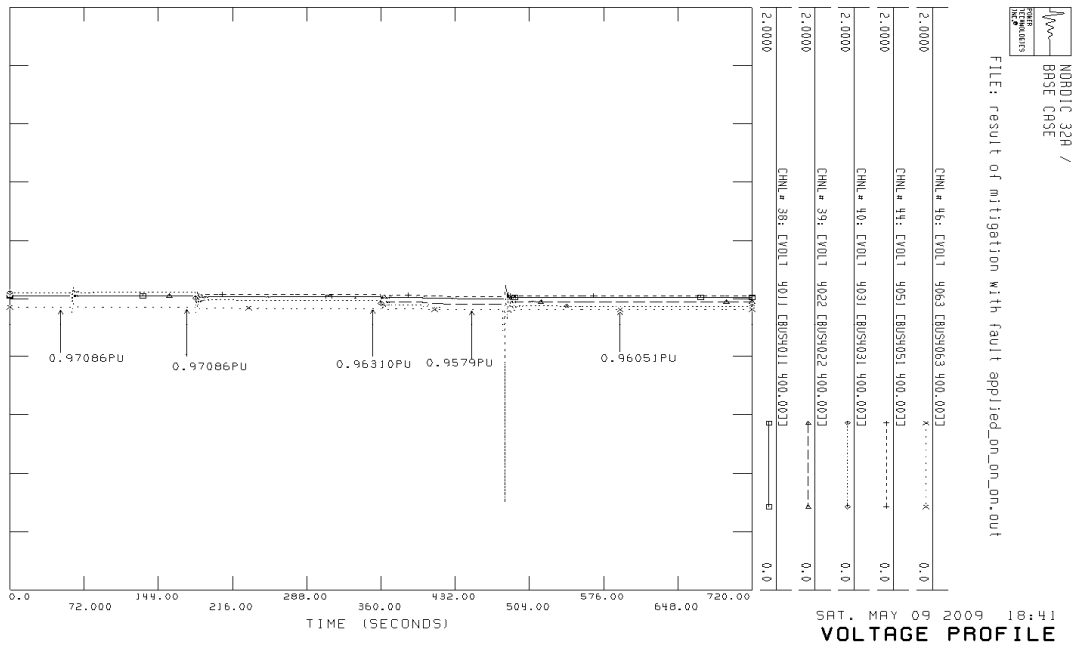


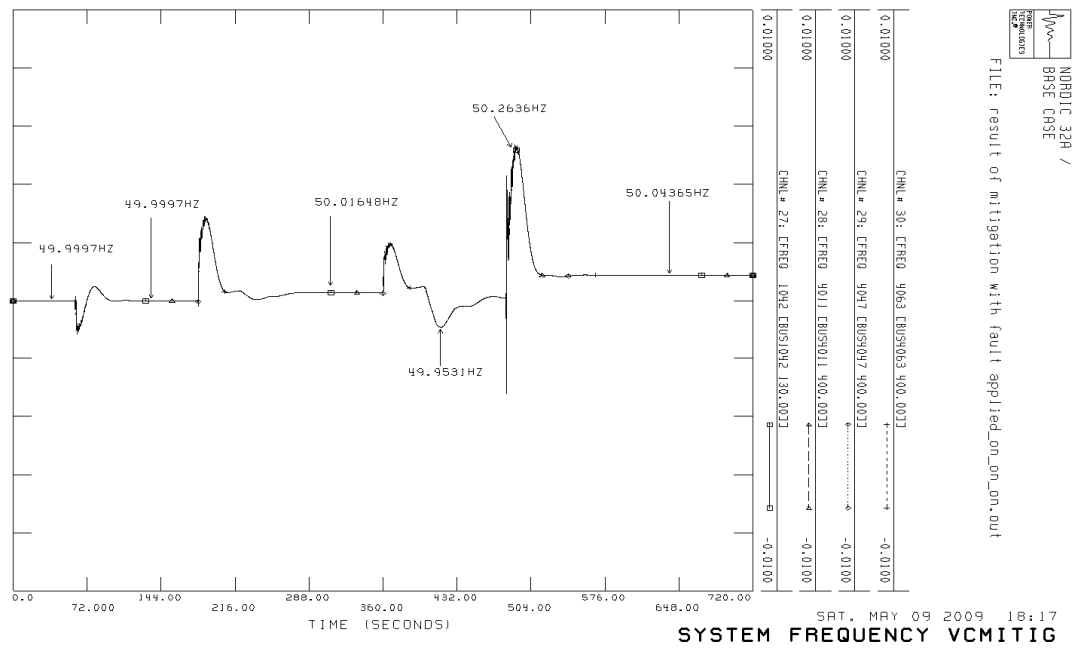
Figure 6.12 Typical generator profile obtained from voltage collapse mitigation measures

6.6.3 Voltage profile, system frequency and OLTC action

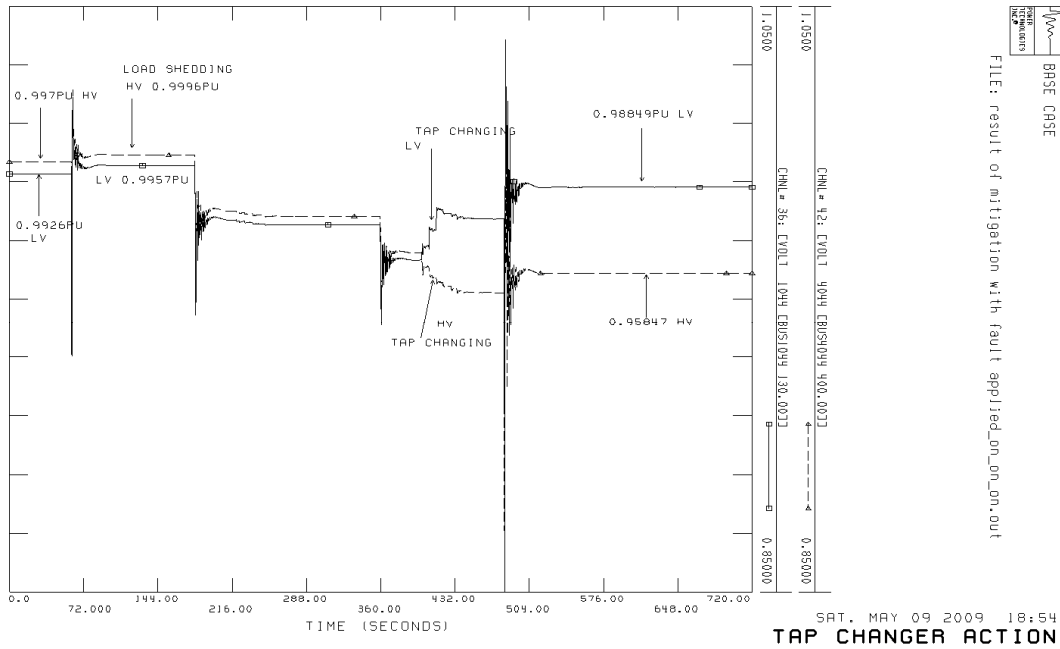
The effect of voltage collapse mitigation using undervoltage and underfrequency load shedding can be seen in Fig. 6.13(a). The voltage magnitude and the frequency profile shown in Fig. 6.13(b) were observed to fall within the acceptable range. While the OLTC continue to move to restore the voltage at the LV side and at a certain stage the voltage magnitude at the HV side as can be seen in Fig. 6.13(c) decreases below the LV side.



(a) System voltage profile



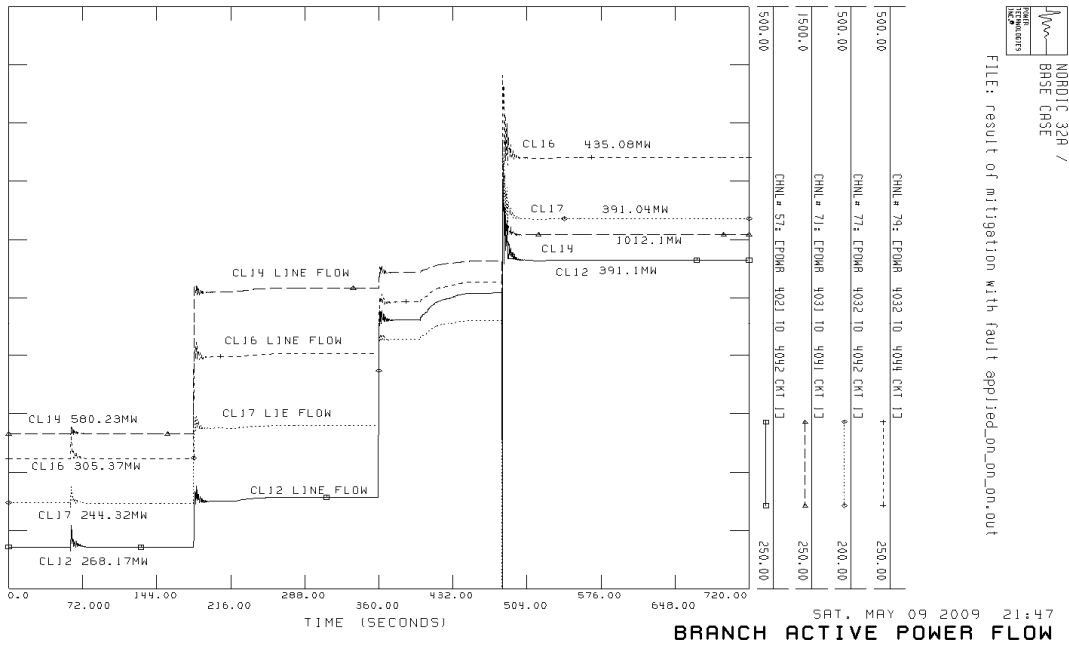
(b) System frequency



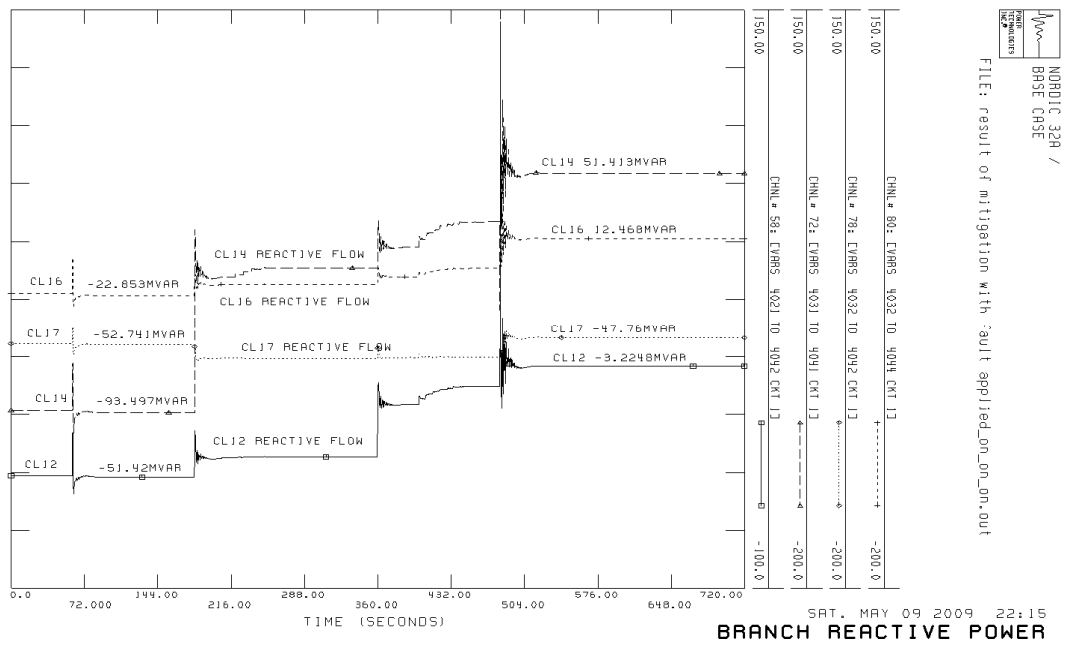
(c) OLTC action
Figure 6.13 System profile during voltage collapse mitigation

6.6.4 Branch flows and losses

The power flow through the critical lines particularly line CL14 during the mitigation process shows increase in both the active and reactive power. Fig. 6.14 (a) shows that the power flow remains within the rated available transmission capacity with CL14 having the highest active power flow of 1012.1MW and reactive power flow (Fig. 6.14(b)) of 51.413Mvar (approximately 50% of the active power flow). However, increase in line losses as shown in Fig. 6.15 were observed significantly.



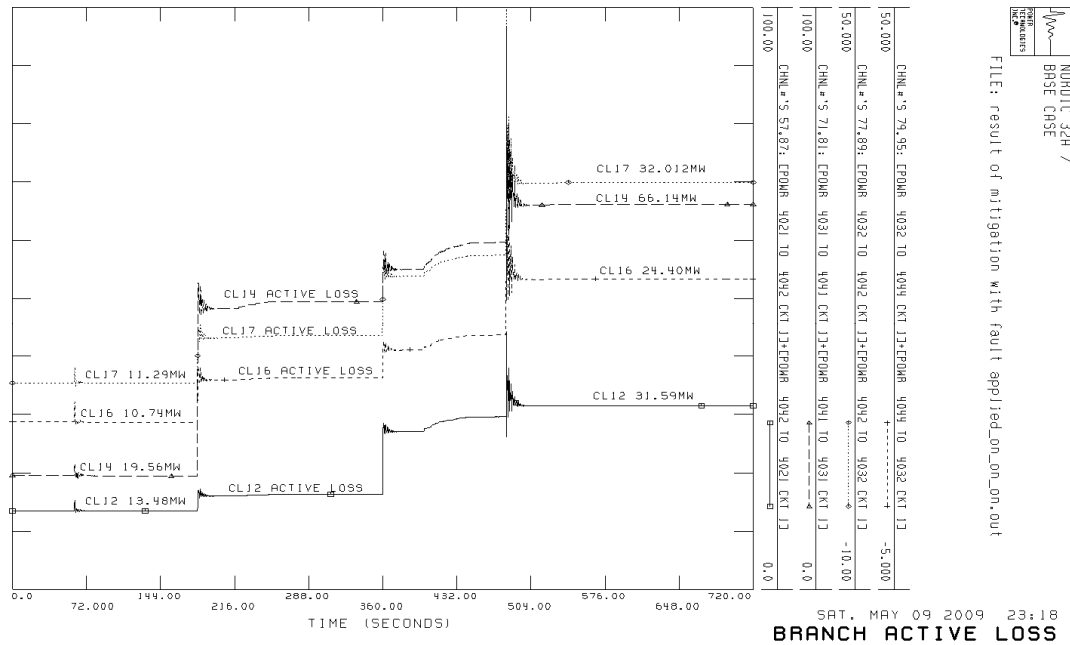
(a) Active power flow on critical lines



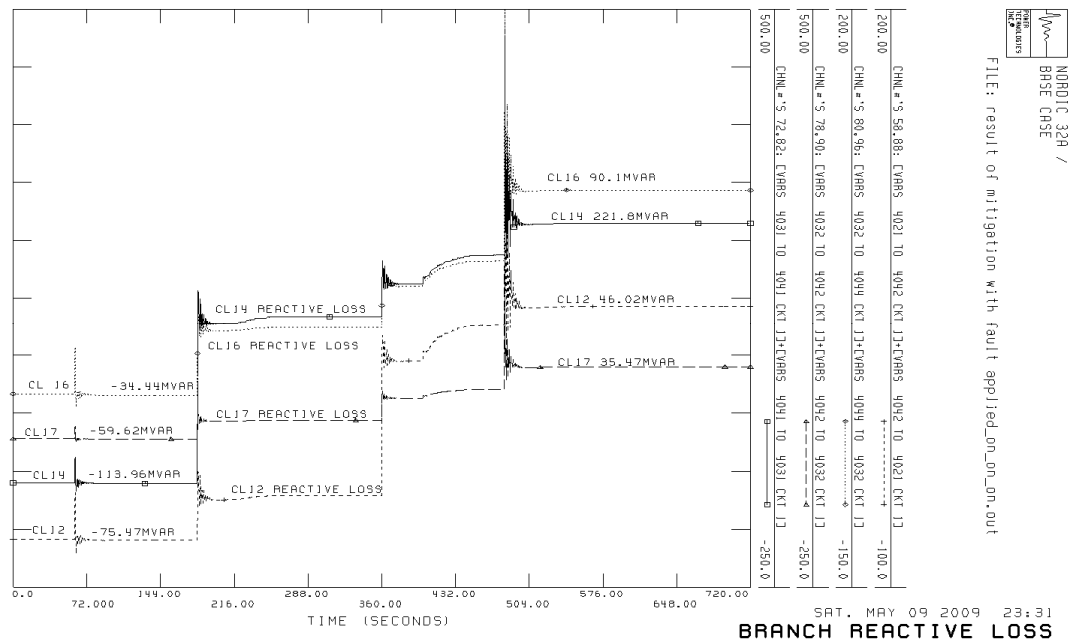
(a) Reactive power flow on critical lines

Figure 6.14 Power flow through critical branches during the mitigation process

In the same fashion the active and reactive power losses for line CL14 are observed to be 66.14MW and 221.8Mvar respectively (Fig. 6.15 (a) and (b)). This indicates that line CL14 is under stress and if additional defence actions- such as provision of additional reactive power support, SVC, STATCOM- are not provided, any mild disturbance could trigger cascaded trippings.



(a) Active power losses on critical lines



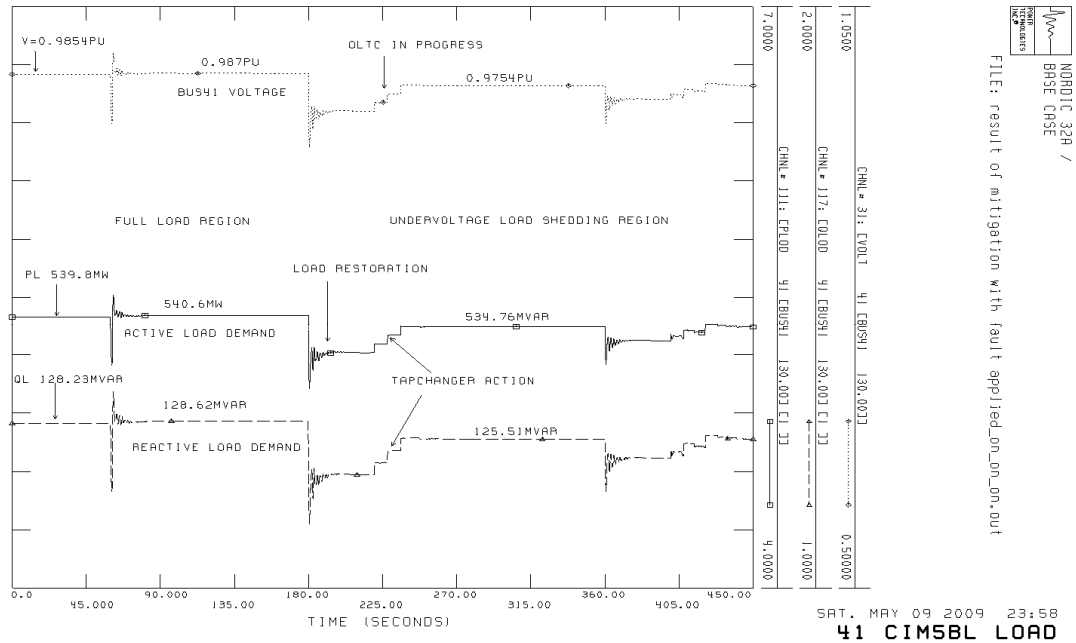
(a) Reactive power losses on critical lines

Figure 6.15 Power losses of critical transmission lines during mitigation process

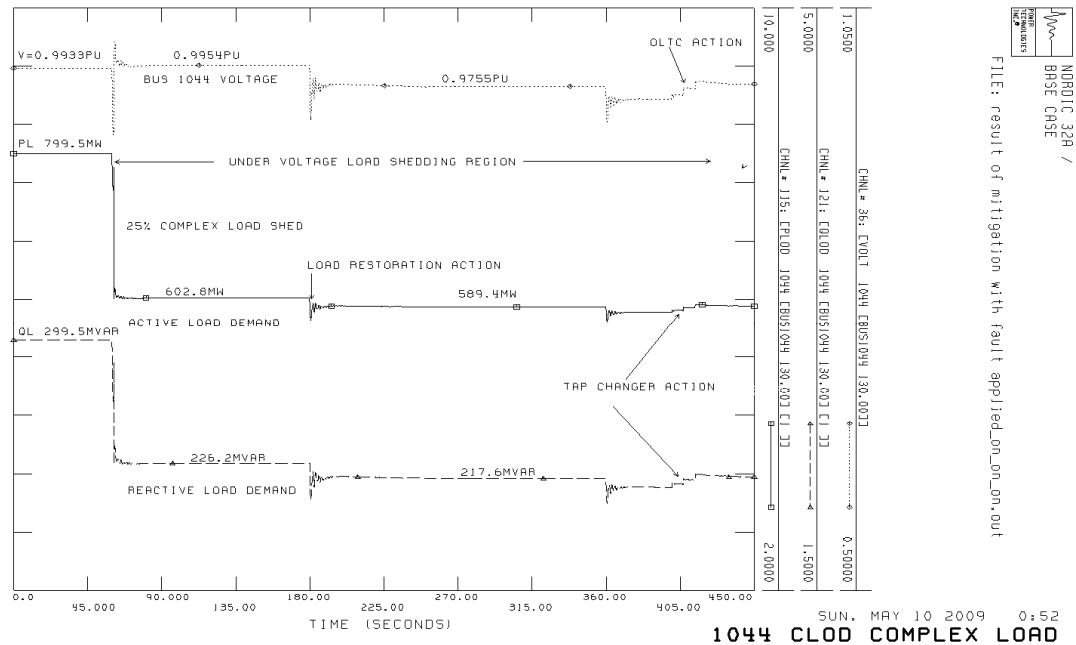
6.6.5 Load shedding actions

In order to have a better understanding of the load behaviour during load shedding actions, the plots of bus voltage, active and reactive power demand of loads at bus 41 comprising purely induction motor load and at bus 1044 comprising complex load are displayed in Fig. 6.16.

Undervoltage load shedding proved to be an effective means of mitigating voltage collapse. By careful selection of the load areas earmarked for load shedding and applying some optimisation techniques, the appropriate percentage of the load to be shed could be obtained. In this work the use of an assumption that 25% of the load would be shed in the first stage is purely to demonstrate the idea, as the criteria for load shedding varies for different networks and moreover it is often considered as the last resort since a majority of utilities are not willing to shed load, hence not widely implemented.



(a) Induction motor load at bus 41



(b) Complex motor load at bus 1044

Figure 6.16 Load shedding actions applied in voltage collapse mitigation.

It can be observed in Fig. 6.16 that there was no load shedding in the first 59 seconds. After dropping a unit at RT132 (bus 1042) at 60 seconds the complex load at bus 1044 switched out 25% of its load (Fig. 6.16(b)). This is reflected in the voltage profile. The bus voltage appreciates from 0.9933pu to 0.9954pu. The load restoration behaviour and tap-changer action can also be observed in the figure.

6.7 Effects of zone3 distance relay operation

In order to determine whether blocking the operation of distance protection relay zone3 would prevent the occurrence of cascaded tripping events and critically look at whether or not zone3 distance protection is to be blamed for the recent major blackouts in Europe additional simulation is repeated according to the same sequence of events conducted when all the zones are active and mitigation schemes deactivated. The effect of zone3 distance protection operation during the disturbance is further studied based on the following strategy:

- Zone1 is blocked by setting its timing 30cycles higher than zone3, while zone2 and zone3 are actively in operation.
- Both zone1 and zone2 timings are set at 30cycles higher than zone3 timing and the simulation of voltage collapse scenario repeated.
- The voltage collapse scenario simulation is repeated with zone3 and zone1timings set very high (60cycles) while zone2 is active.

The results of the simulation extracted from the event sequence is tabulated in Tables 6.5 and 6.6.

Table 6.5 cascaded tripping events during voltage collapse, between 0-540 seconds with zone1 blocked

Transmission lines nomenclature	Branch number	Manual operation time in seconds	Pick up operation (seconds)			Timed out operation (seconds)			Time of circuit breaker trippings (seconds)	Comments
			zone3	zone2	zone1	zone3	zone2	zone1		
CL12	4021-4042_L1		481.929	482.229	482.239					
CL12	4021-4042_L2	360								
CL14	4031-4041_L1		482.339	481.949	482.229	482.329	482.249	482.349	2nd cascading event	
CL15	4031-4041_L2	180								
CL16	4032-4044_L1		481.939	481.939	482.229		482.239	482.339	1st cascading event	
CL16	4032-4044_L2	480								
CL17	4032-4042_L1		482.019	482.229	482.239					
CL17	4032-4042_L2		482.019	482.229	482.239					
FL2	4041-4044		482.279	482.279						
FL16	4042-4044		482.259	482.339	482.269					

The simulation failed at 503.83 seconds, hence the timed out operation of the remaining critical lines could not be ascertained. It can be seen that zone2 timed out for line CL16 and followed shortly is line CL14 after 10ms.

For the second strategy zone1 and zone2 are blocked leaving only zone3 active. The pick up and timed out operation is tabulated in Table 6.6. It can be seen that cascading tripping event began with line CL14 and followed closely with line CL16 after 40ms.

Table 6.6 Cascade tripping events during voltage collapse, between 0-500 seconds with zone1 and zone2 blocked

Transmission lines nomenclature	Branch number	Manual operation time (seconds)	Pick up operation (seconds)			Timed out operation (seconds)			Time of circuit breaker trippings (seconds)	Comments
			zone3	zone2	zone1	zone3	zone2	zone1		
CL12	4021-4042_L1		482.369	482.229	482.239					
CL12	4021-4042_L2	360								
CL14	4031-4041_L1		482.369	482.379	482.389	482.329		482.429	1st cascading event	
CL15	4031-4041_L2	180								
CL16	4032-4044_L1		481.779	482.389	482.399	482.379		482.48	2nd cascading event	
CL16	4032-4044_L2	480								
CL17	4032-4042_L1		482.019	482.229	482.239					
CL17	4032-4042_L2		482.019	482.229	482.239					
FL2	4041-4044		482.279	482.279						
FL16	4042-4044		482.259	482.339	482.269					

In a similar fashion, the simulation failed at 500 seconds. Therefore, the tripping events of the remaining critical lines could not be determined. This scenario shows that once the system cascading began many transmission lines could possibly tripped in millisecond range.

The third option is due to the call made to get rid of zone3. Therefore by blocking zone3 and repeating the simulation the result is similar to the result of the first option tabulated in Table 6.5. The system would breakdown. This implies that even if zone3 is blocked, provided zone2 and zone1 are active, voltage collapse can still happen. The summary of the tripping events when zone3 is blocked is given in Table 6.7.

Table 6.7 Cascaded tripping events during voltage collapse in 504 second time frame with zone1 and zone3 blocked

Transmission lines nomenclature	Branch number	Manual operation time in seconds	Pick up operation			Time out operation			Time of circuit breaker trippings (seconds)	Comments
			zone3	zone2	zone1	zone3	zone2	zone1		
CL12	4021-4042_L1		481.929	482.229	482.239					
CL12	4021-4042_L2	360								
CL14	4031-4041_L1		482.339	481.949	482.229		482.249	482.349	2nd cascading event	
CL15	4031-4041_L2	180								
CL16	4032-4044_L1		481.939	481.939	482.229		482.239	482.339	1st cascading event	
CL16	4032-4044_L2	480								
CL17	4032-4042_L1		482.019	482.229	482.239					
CL17	4032-4042_L2		482.019	482.229	482.239					
FL2	4041-4044		482.279	482.279						
FL16	4042-4044		482.259	482.339	482.269					

Table 6.8 gives the comparison of the summary of the circuit breaker trippings for the conditions discussed above. The time lag between the condition when only zone3 is active with that when all the zones are active for line CL14 and 16 are 0.09 seconds and 0.33 seconds respectively.

Table 6.8 Comparison table of the summary of circuit breaker tripping times

Transmission lines nomenclature	Branch number	Time of circuit breaker tripping operation (seconds)			
		zone1, 2 and 3 active	zone2 and 3 active	Only zone2 active	Only zone3 active
CL16	4032-4044_L1	482.149	482.339	482.339	482.479
CL14	4031-4041_L1	482.339	482.349	482.349	482.429
CL17	4032-4042_L1	482.349			
CL17	4032-4042_L2	482.349			
FL2	4041-4044	482.379			
FL16	4042-4044	482.339			
CL12	4021-4042_L1	482.519			

Chapter Seven: Conclusion and Recommendation

The continuous connection of large wind farms to existing power systems and the deregulated power market operation when combined together would be a serious challenge to the power system protection engineers especially at ensuring correct and well coordinated relay settings that can provide adequate system reliability during heavy stressed system condition. Hence, the aspects of distance protection relay behaviour during mild and large system disturbances which may lead to voltage instability is carried out. In particular, the net effect of zone3 distance relay operation during voltage collapse incidences was investigated using the IEEE14-bus and the Nordic32-bus test systems.

7.1 Conclusion

In this work, the dynamic simulation of scenarios that lead to voltage collapse for the IEEE14-bus and the Nordic32-bus are carried out using PSS/E software for a time frame of 10 minutes. The exact causes of the voltage collapse vary from one network to another and from another point of view zone3 distance relay operation was among the several negative forces that could trigger the voltage collapse due to its cascaded tripping event.

However, based on the result of the simulation carried out in this work, it is shown that the effect of zone3 is to some extent exaggerated. As long as the system was allowed to operate near its design limit without enough reactive power support and without taking corrective actions, a credible contingency outage- be it mild or severe- would lead to cascaded tripping and the system would breakdown even with the zone3 distance relay deactivated. It was found that; at that critical condition the apparent impedance seen by the distance relay traverse through all the three zones and if zone1 is not equipped with power swing blocking the cascaded tripping is dominated by zone1 operation.

Another interesting finding is that, with zone1 blocked, zone2 will time out before zone3 and the system will breakdown. The cascaded trippings are dominated by zone2 operation. In addition, the effect of zone3 is similar to that of zone2 but the cascaded tripping event commenced after a very short time delay of 0.08 seconds. Based on the foregoing observation, zone3 distance relay operation should not entirely be blamed for the cascading tripping events.

It has also been established from the simulations carried out in this work that allowing tap changers to operate freely contributes to a large extent to the gradual degradation of the voltage. In addition, load dynamics having their load characteristics dependant on voltage and frequency plays the leading role during major disturbances due to their restoration properties.

While on the one hand blocking of tap changer operation combined with load shedding scheme – particularly the undervoltage load shedding- has been found to be a promising means of short term voltage collapse mitigation. However, the question to be addressed include among others the following: what percentage of load should optimally be shed and which customers would accept to be shed?

On the other hand it was found that blocking only zone3 distance relay operations when tap changers are allowed to move is not a viable solution for short term voltage collapse mitigation. A humble proposal is that the three zones of operation need to be blocked in order to prevent the commencement of cascaded tripping during large system disturbances. But from another point of view, this is not an acceptable solution.

It was also shown that switching out major transmission lines is associated with large increase in reactive power losses. If these losses are determined using simulations prior to granting a planned outage and adequate reactive compensation is provided, then the need for load shedding and the risk of voltage collapse could be reduced.

7.2 Recommendation

Based on the simulation studies conducted under the binding assumptions and the findings observed in this thesis, it would not be fair to solely blame distance protection zone3 for playing a major role at cascaded trippings during large system disturbances.

In line with the findings of this work, the following recommendations are proposed:

- Distance protection zone3 should be allowed to continue to operate since getting rid of it is not a solution at eliminating cascading tripping during large system disturbances. And also in the view of its usefulness at providing remote back up protection at no additional cost and its presence is an added advantage to field protection relay engineers when conducting maintenance and calibration of downstream protective relays.
- System operators should be trained and equipped with modern tools such that before granting a planned maintenance outage a simulation could be carried out to determine the reactive power support requirements that would be needed to minimise the power losses, as well as ensuring that sufficient security margin, in the form of spinning reserve, is maintained. This would greatly aid at achieving the desired voltage stability.
- Undervoltage load shedding proved to be an effective means of mitigating voltage collapse. Therefore, utilities should incorporate undervoltage relays at strategic loads into their system protection schemes.

7.3 Future work

In order to have a complete picture and a deeper understanding of the behaviour of the network during large disturbances, it would be appropriate to carry out further work to validate practically the results and finding of this work using a smaller system available in the power laboratory. Further work would also be required on the modelling aspects to include the following:

- Generators and generator-transformers and include their detailed protection scheme.
- Expand the transmission lines to closely mimic the actual network and include detailed distance protection relays for the transmission lines including HVDC links and protection schemes such as intertripping and breaker failure relays.
- Modelling of substation equipment such as transformer should include protection relays such as overload relay, Standby earth fault relay and backup overcurrent relays which may likely operate during the large system disturbance.
- The OLTC action should include other levels of downstream on-load tap changing transformers.
- The load aspects due to its stochastic nature should be further studied particularly taking into consideration distribution network and injection substations.
- The optimal strategy for conducting load shedding should be further looked into.

REFERENCES

- [1]. CIGRE SCTF 38.02.19, *System protection schemes in power networks*, 2001
- [2]. D. H. Karlsson, 'System protection schemes in power networks' , *IEEE power engineering review*, Nov 2001, pp37-38
- [3]. P. Crosley, D. Karlsson, F. Ilar "System Protection Schemes in Power Networks: existing installations and ideas for future developments" *IEE conference publication* no 479, 2001, pp 450-453
- [4]. CIGRE TF C2.02.24, *Defence plan against extreme contingencies*, Dec 2006
- [5]. C. W. Taylor, *Power System Voltage Stability*, McGraw Hill, 1994
- [6]. D. S. Kirschen, "Do investments prevents blackouts?" *Power Engineering society General meeting, IEEE*. June 2007, pp 1-5
- [7]. P. Pourbeik, P.S. Kundur, C.W. Taylor, " The anatomy of a Power grid blackout" *IEEE Power and Energy Magazine*, 2006, pp 22-29
- [8]. J. W. Bialek, "Blackouts in the US/Canada and continental Europe in 2003: is liberalization to blame?" *Power Tech*, 2005 IEEE Russia, 2005
- [9]. P. Fairley, " the Unruly Power Grid" *IEEE Spectrum* 2004, pp 22-27
- [10]. IEEE/CIGRE Joint Task Force on Stability Terms and Definitions, "Definitions and Classification of Power System Stability" *IEEE Transactions on Power Systems*, vol. 19, no. 2, May 2004, pp 1387-1401
- [11]. N.G. Hingorani and L. Gyugyi, *Understanding FACTS. Concepts and Technology of Flexible AC Transmissin systems*. New York: IEEE Press, Wiley-Interscience, 2000
- [12]. *IEEE guide for protective relay application to transmission lines*, IEEE Standard C37.113-1999
- [13]. *IEEE guide for AC generator protection*, IEEE C37.102-2006
- [14]. J. L. Blackburn and T. J. Domin, *Protective Relaying; Principles and Applications*, CRC Press, 3rd Edition, 2007
- [15]. M. Begovic et-al, "Summary of System Protection and Voltage Stability", *IEEE Transactions on Power Delivery*, vol 10, no.2, 1995, pp631-637
- [16]. K.W. Leung, "Computer-Aided setting calculation for distance zone2 and zone3 protection", *IEE International conference on Advances in Power system control, operation and management*, Nov 1991, pp 156-157
- [17]. M. Jonsson, J. Daalder, "Distance Protection and Voltage Stability", *Power system technology conference 2000*, vol 2, 2000, pp971-976
- [18]. L. Harnefors, *Control of Variable-Speed drives*, Mälardalen University Västerås, Sweden, 2002.
- [19]. IEEE PSRC K12, *Voltage Collapse Mitigation*, 1996
- [20]. PSS/E 29, *Program application guide: & Program operation manual* , vol 1 and 2, Oct. 2002, Power Technologies, INC
- [21]. S. Larsson, A. Danell, "The black-out in southern Sweden and eastern Denmark, September 23, 2003" *IEEE Power Engineering society*, General meeting, 2004.
- [22]. P. Kundur, *Power system stability and control*, McGraw-Hill, 1994
- [23]. A.R. Bergen and V. Vittal, *Power System Analysis*, 2nd edition, Prentice Hall, 2000

- [24]. T.V. Cutsem, C. Vournas, *Voltage Stability of Electric Power Systems*, Kluwer Academic Publishers, 1998
- [25]. C. Vournas, M. Karystianos, "Load tap changers in emergency and preventive voltage stability control" *IEEE Transactions on power systems*, vol.19, no.1, February 2004. pp492-498
- [26]. D. Karlsson, "A system protection schemes in power network based on new principles" ABB Automation products AB, Sweden, 2000
- [27]. D. Karlsson, *Voltage stability simulations using detailed models based on field measurements*, PhD dissertation, School of Electrical and Computer Engineering, Chalmers University of Technology, 1992.
- [28]. D. Karlsson, D.J. Hill, "Modelling and identification of nonlinear dynamic loads in power systems" *IEEE Transaction on Power Systems*, vol9, no.1, pp157-166, 1994
- [29]. S. Johansson, *Long-term Voltage Stability in Power systems*, PhD Technical report, Chalmers University of Technology, 1998
- [30]. IEEE Task Force Report, "Load Representation for Dynamic Performance Analysis", *IEEE Trans.*, vol PWRS-8, 1993, pp.472-482
- [31]. IEEE Task Force on load representation for dynamic response, "Standard load models for power flow and dynamic performance simulation", *IEEE Trans. on power systems*, vol.10, no.3, Aug. 1995, pp1302- 1314
- [32]. "Nordic grid code 2007 (Nordic collection of rules)," Nordel, Tech. Rep., Jan. 2004 (Updated 2007).
- [33]. N.W Miller, W.W.Price, J.J. Sanchez-Gasca, "Dynamic modelling of GE1.5 and 3.6 Wind turbine generators" GE- Power systems energy consulting, version 4.1, 2008
- [34]. N. Mithulananthan, C. A. Cañizares, and J. Reeve. "Indices to Detect Hopf Bifurcation in Power systems". In Proc. of NAPS-2000, pp. 15–18–15–23, October 2000
- [35]. P. M. Anderson and A. A. Fouad, *Power System Control and Stability*. IEEE Press, 1994
- [36]. K. Walve, "Nordic32-A CIGRE test system for simulation of transient stability and long term dynamics," Svenska Kraftnät, Sweden, Tech. Rep., 1993
- [37]. CIGRE TF 38.02.08, "Long term dynamics, phase II, final report," CE/SC 38.WG02, Ref. no 102, Tech. Rep., 1995
- [38]. M.S. Calovic, "Modeling and analysis of under-load tap changing transformer control systems", *IEEE Trans. On power apparatus and systems*, vol. PAS-103, no.7, July 1984. pp1909-1915

APPENDIX A: Block diagram of Generators, stabilizers, exciters and governors models

A1: Generators

A simplified block diagram for a typical subtransient machine model used to represent GENROU and GENSAL models is shown in Fig. A1

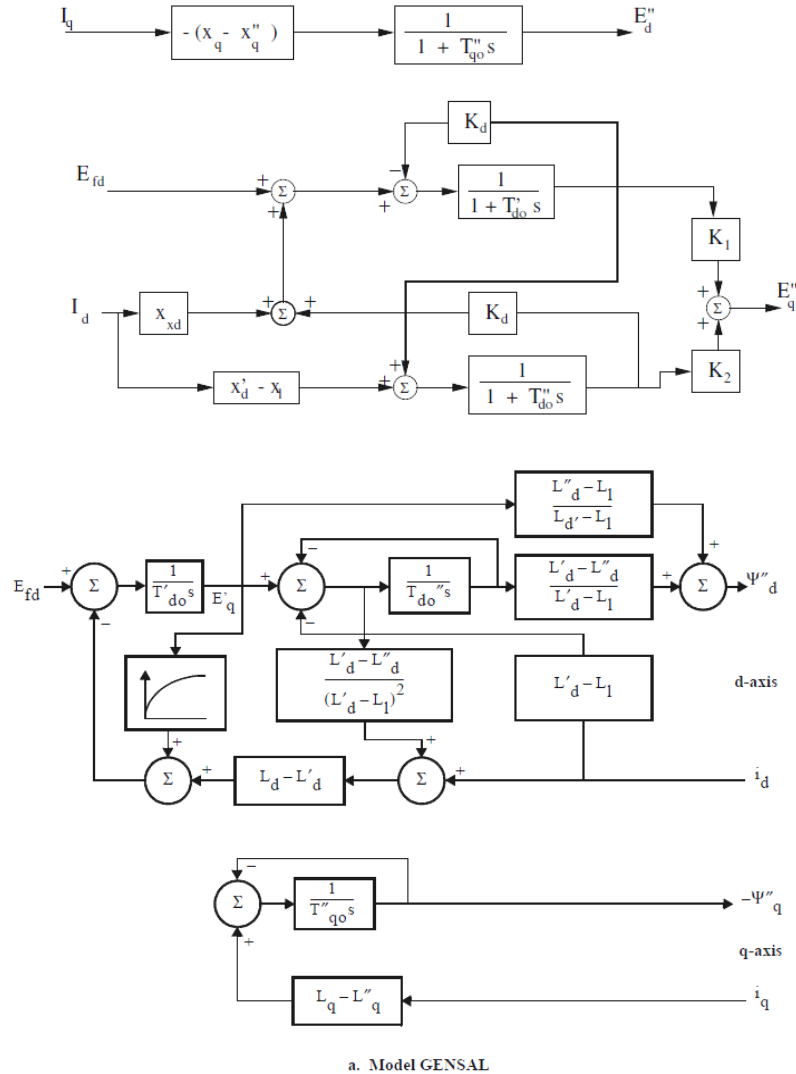


Figure 13-2. Electromagnetic Model of Salient Pole Generator

Figure A1.1 Simplified block diagram for the subtransient machine model in dq

The torque and the speed for the subtransient machine model can be computed according to the Block diagram shown in Fig. A2.

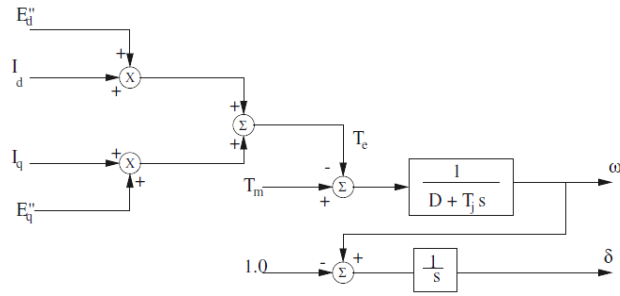


Figure A1.2 Block diagram for computing Torque and speed for the subtransient machine model

A2: AVR and Exciter Model

A simple Automatic Voltage Regulator (AVR) model used in this thesis to represent the excitation control of generators is shown in Fig. A2.1.

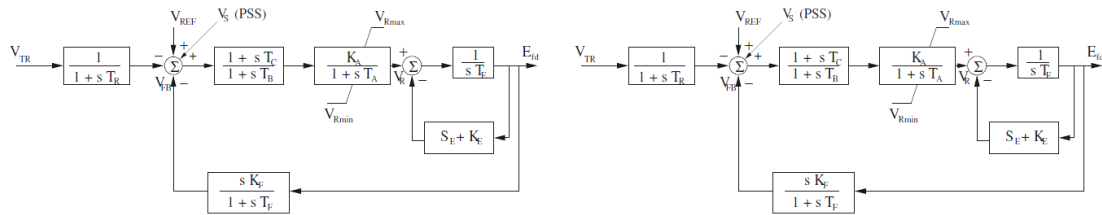
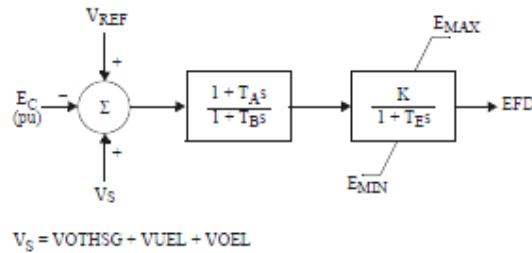


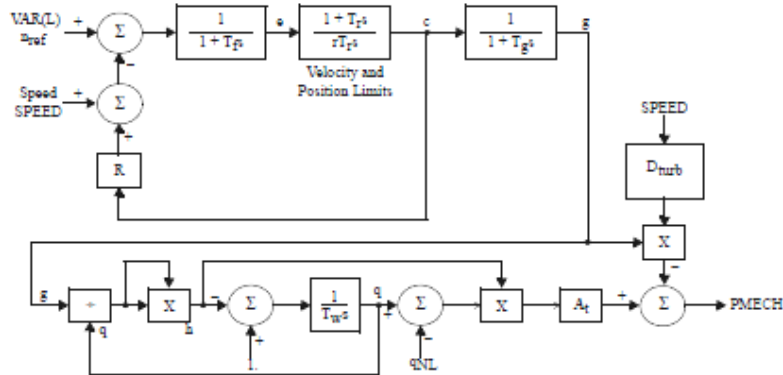
Figure A2.1 AVR and exciter model for synchronous generator

A3: Simplified Excitation System (SEXS) model



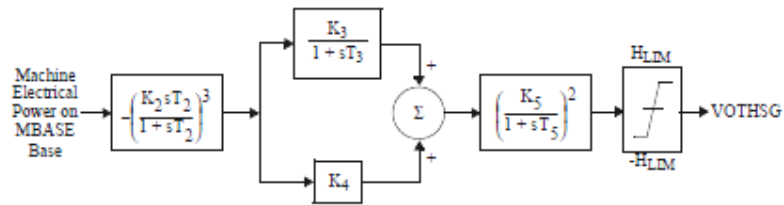
IBUS, 'SEXS', I, TA/TB, TB, K, TE, EMIN, EMAX/

A4: Hydro Turbine-Governor (HYGOV1) model



IBUS, 'HYGOV', I, R, r, Tr, Tf, Tg, VELM, GMAX, GMIN, TW, At, D_turb, qNL/

A5: Power Sensitive Stabilizing Unit (STAB2A) model



IBUS, 'STAB2A', I, K2, T2, K3, T3, K4, K5, T5, HLIM/

APPENDIX B: Distance relay data used in IEEE14-bus and Nordic32-bus test systems

B1: IEEE14-bus test system distance relay data (.dat) file

```
1011-2011-1 RELAY2 0.03876 0.11834
1011-5011-1 RELAY2 0.05403 0.22304
2011-3011-1 RELAY2 0.04699 0.19797
2011-4011-1 RELAY2 0.09811 0.67632
2011-5011-1 RELAY2 0.05695 0.17388
3011-4011-1 RELAY2 0.06701 0.17103
4011-3011-1 RELAY2 0.06701 0.17103
5011-4011-1 RELAY2 0.01335 0.04211
1011-2011-1-1 DISTR1 1 0.0996 71.9 0.04981 0.17027 71.9 0.08515 0.8514 79.6 0.4257
0.0 0.0 0.0 0.0 0.0 0.0 0.0 0.0
1011-5011-1-1 DISTR1 1 0.1836 76.4 0.0918 0.24051 76.2 0.12025 0.3271 75.0 0.1636
0.0 0.0 0.0 0.0 0.0 0.0 0.0 0.0
2011-3011-1-1 DISTR1 1 0.1628 76.64 0.0814 0.249 75.2 0.1245 0.4631 75.75 0.2315
0.0 0.0 0.0 0.0 0.0 0.0 0.0 0.0
2011-4011-1-1 DISTR1 1 0.5467 81.75 0.2734 0.6943 81.6 0.34715 0.91412 78.84 0.4571
0.0 0.0 0.0 0.0 0.0 9.0 0.0 0.0
2011-5011-1-1 DISTR1 1 0.1464 71.86 0.0732 0.194 71.9 0.097 0.4958 79.8 0.2479
0.0 0.0 0.0 0.0 0.0 0.0 0.0 0.0
3011-4011-1-1 DISTR1 1 0.147 68.6 0.0735 0.2806 76.2 0.1171 0.4524 77.4 0.2262
0.0 0.0 0.0 0.0 0.0 0.0 0.0 0.0
1011-2011-2-1 DISTR1 1 0.0996 71.9 0.04981 0.17027 71.9 0.08515 0.8514 79.6 0.4257
0.0 0.0 0.0 0.0 0.0 0.0 0.0 0.0
4011-3011-1-1 DISTR1 1 0.147 68.6 0.0735 0.2341 70.34 0.1171 0.5556 75.56 0.2778
0.0 0.0 0.0 0.0 0.0 0.0 0.0 0.0
5011-4011-1-1 DISTR1 1 0.03534 72.41 0.01767 0.14413 84.69 0.0721 0.4312 83.99 0.2156
0.0 0.0 0.0 0.0 0.0 0.0 0.0 0.0
```

B2: Nordic32-bus test system distance relay data (.dat) file

```
4011-4021-1 RELAY2 0.00600 0.06000
4011-4022-1 RELAY2 0.00400 0.04000
4012-4022-1 RELAY2 0.00400 0.03500
4021-4032-1 RELAY2 0.00400 0.04000
4021-4042-1 RELAY2 0.01000 0.06000
4022-4031-1 RELAY2 0.00400 0.04000
4031-4032-1 RELAY2 0.00100 0.01000
4031-4041-1 RELAY2 0.00600 0.04000
4032-4042-1 RELAY2 0.01000 0.04000
4032-4044-1 RELAY2 0.00600 0.05000
4042-4044-1 RELAY2 0.00200 0.02000
4011-4021-1-1 DISTR1 1 0.04824 84.3 0.02413 0.0703 84.3 0.03515 0.1261 82.5 0.06305 0.0 0.0 0.0 0.0 0.0 0.0 0.0
4011-4022-1-1 DISTR1 1 0.03216 84.3 0.0161 0.0432 84.7 0.0216 0.0905 84.0 0.04525 0.0 0.0 0.0 0.0 0.0 0.0 0.0
4012-4022-1-1 DISTR1 1 0.02818 83.5 0.0141 0.03821 84.0 0.01911 0.0855 83.6 0.04275 0.0 0.0 0.0 0.0 0.0 0.0 0.0
4021-4032-1-1 DISTR1 1 0.03216 84.3 0.01608 0.051 82.6 0.0255 0.09558 83.7 0.04805 0.0 0.0 0.0 0.0 0.0 0.0 0.0
4021-4042-1-1 DISTR1 1 0.04866 80.5 0.025 0.0646 80.7 0.0325 0.081 81.1 0.0405 0.0 0.0 0.0 0.0 0.0 0.0 0.0
4022-4031-1-1 DISTR1 1 0.03216 84.3 0.01608 0.0427 84.3 0.02135 0.09197 82.8 0.04598 0.0 0.0 0.0 0.0 0.0 0.0 0.0
4022-4031-2-1 DISTR1 1 0.03216 84.3 0.01608 0.0427 84.3 0.02135 0.09197 82.8 0.04598 0.0 0.0 0.0 0.0 0.0 0.0 0.0
4031-4032-1-1 DISTR1 1 0.00804 84.3 0.00402 0.0203 80.1 0.01015 0.0779 84.3 0.03895 0.0 0.0 0.0 0.0 0.0 0.0 0.0
4031-4041-1-1 DISTR1 1 0.03236 81.5 0.01618 0.04292 82.0 0.02146 0.05543 77.0 0.02771 0.0 0.0 0.0 0.0 0.0 0.0 0.0
4031-4041-2-1 DISTR1 1 0.03236 81.5 0.01618 0.04292 82.0 0.02146 0.05543 77.0 0.02771 0.0 0.0 0.0 0.0 0.0 0.0 0.0
4032-4044-1-1 DISTR1 1 0.0403 83.2 0.02014 0.0516 83.3 0.0258 0.09185 83.4 0.045930 0.0 0.0 0.0 0.0 0.0 0.0 0.0
4032-4042-1-1 DISTR1 1 0.03298 76.0 0.01649 0.045 76.5 0.0225 0.0662 79.11 0.0331 0.0 0.0 0.0 0.0 0.0 0.0 0.0
4041-4044-1-1 DISTR1 1 0.02412 84.3 0.01206 0.0314 84.5 0.0157 0.04522 84.3 0.02261 0.0 0.0 0.0 0.0 0.0 0.0 0.0
4042-4044-1-1 DISTR1, 1, 0.0161, 84.3, 0.00805, 0.02134, 84.6, 0.01067, 0.06159, 84.9, 0.0308 0.0 0.0 0.0 0.0 0.0 0.0 0.0
```

APPENDIX C: Load characteristics models

C1: Induction motor load

The load connected to bus 41, 51 and 63 are assumed to be purely aggregate of induction motors. Using the IMD auxiliary software of the PSS/E the parameters required in the PSS/E model 'CIM5BL' are tabulated in Table C1. The corresponding induction motor curves are shown in Fig. C.1

Table C1. Induction motor model

Parameters	CIM5BL model-Induction motor		
	Bus 41	Bus 51	Bus63
MVA rating	555	840	640
kV base	130	130	130
E terminal(pu)	0.9855	1.0008	0.9606
Type	1	1	1
Ra	0.01	0.011	0.01
La	0.1013	0.182	0.1163
Lm	3.5	4.2	4.02
R1	0.014	0.011	0.013
L1	0.14	0.018	0.078
R2	0	0	0
L2	0	0	0
Inertia H	1	1	1
Damping D	1	1	1
E1	1	1	1
S(E1)	0.25	0.25	0.25
E2	5	5	5
S(E2)	0.5	0.5	0.5
Pmult	0	0	0
V1	1	1	1
T1	1	1	1
TB	5	5	5
Tnorm	0.5	0.5	0.5

The dynamic data file is modified to include the induction motor parameters. Typical parameters are as follows

```

41 'CIM5BL'      1      1
  0.10000E-01 0.10130   3.5000   0.14000E-01 0.97000E-01
  0.0      0.0      1.0000   0.25000E-01 5.0000
  0.50000   555.00   0.0000   1.0000   1.0000
  1.0000   5.0000   1.0000   0.5000 /

51 'CIM5BL'      1      1
  0.11000E-01 0.182    4.2000   0.110E-01 0.18000E-01
  0.0      0.0      1.0000   0.25000E-01 5.0000
  0.50000   840.00   0.0000   1.0000   1.0000
  1.0000   5.0000   1.0000   0.5000 /

63 'CIM5BL'      1      1
  0.10000E-01 0.11630   4.0200   0.13000E-01 0.78000E-01
  0.0      0.0      1.0000   0.25000E-01 5.0000
  0.50000   644.00   0.0000   1.0000   1.0000
  1.0000   5.0000   1.0000   0.5000 /

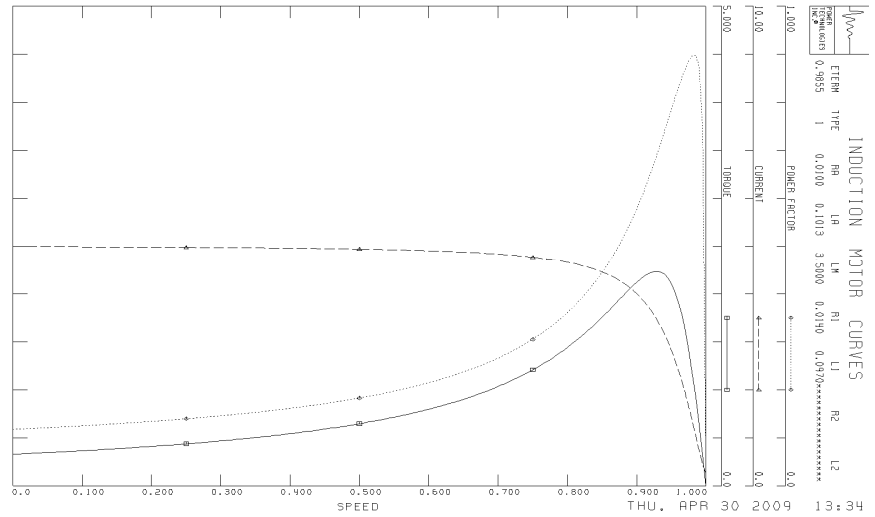
```

C2: Complex load

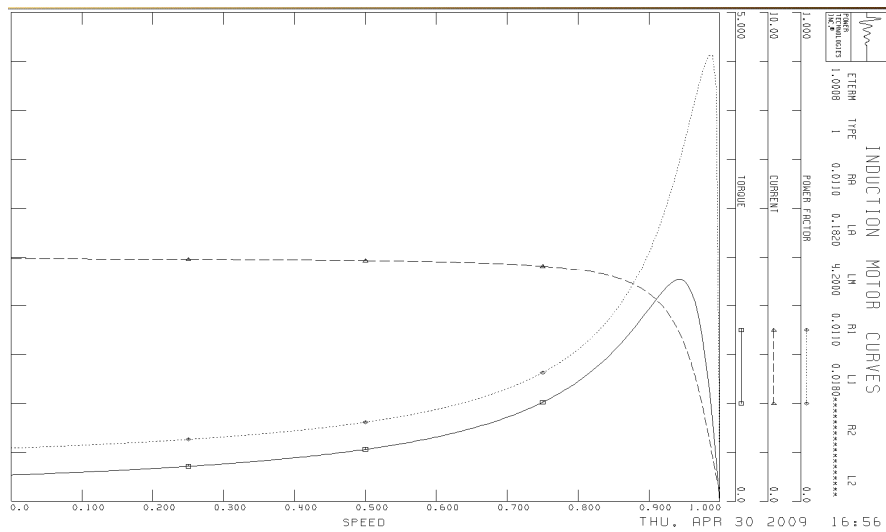
Complex load model is assigned to bus1041, 1044 and 1045. Use is made of an assumption that the load is an aggregate of mixture of motors, distribution transformer excitation, and constant impedance loads. The parameters required for the PSS/E model 'CLODBL' are tabulated in Table C2.

Table C2: Complex load model

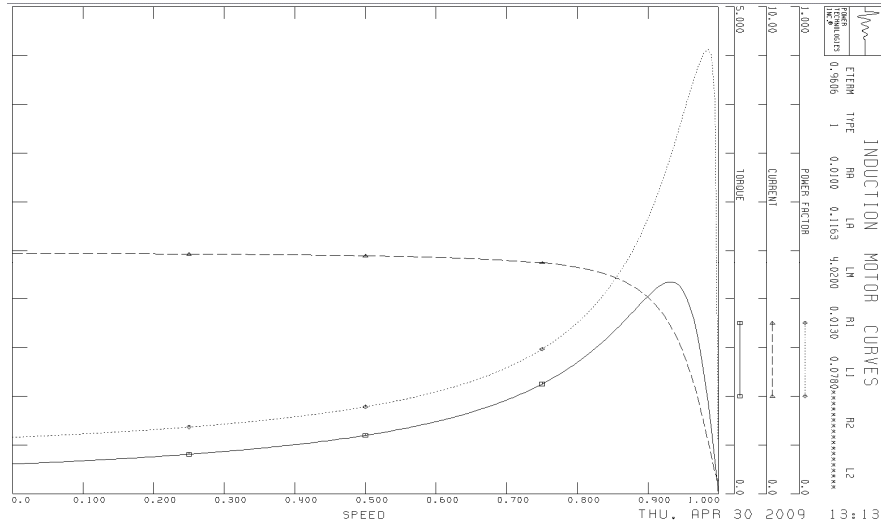
Parameters	CLODBL model-Complex load		
	Bus 1041	Bus 1044	1045
%Large motor	0	90	0
% Small motor	0	0	90
% Transformer excitation current	5	5	5
%Discharge lighting	0	0	0
% Constant power	0	0	0
Kp of remaining load	2	2	2
Branch R(pu Load MW base)	0	0	0
Branch X(pu Load MW base)	0.1	0.1	0.1



(a) Bus 41 induction motor load

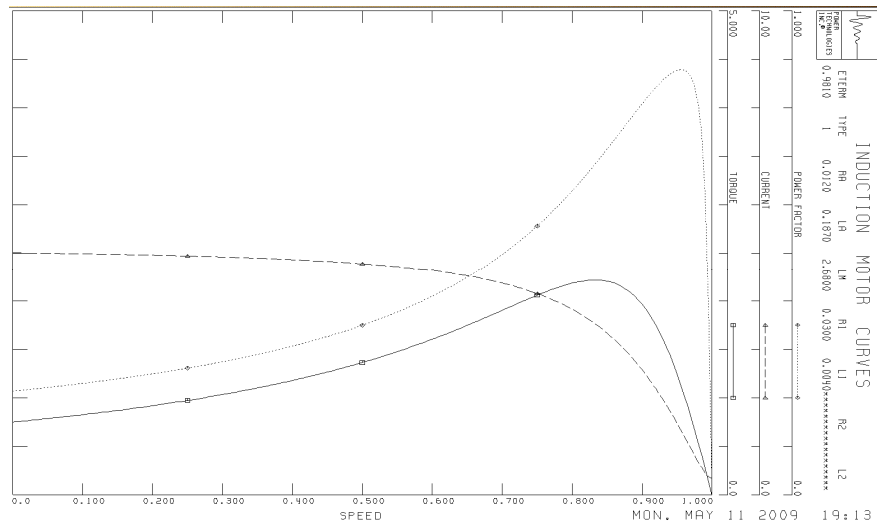


(b) Bus 51 induction motor load



(c) Bus 63 induction motor load

The characteristics of the induction motor load connected to bus 13011 of the IEEE14-bus test system is shown in Fig. C.1 (d).



(d) Induction motor load at IEEE14-bus

Figure C.1 Induction motor curves at Nordic (a) bus 41 (b) bus 51 (c) bus 63 and IEEE14 (d) bus 13011

APPENDIX D: Load Shedding Scheme and OLTC

D1. Underfrequency load shedding

Table D1. Underfrequency load shedding

Parameters	LDSHBL model- Under frequency load shedding												
	Bus 42	Bus 3	Bus 46	Bus 47	Bus 61	Bus 62	Bus 1011	Bus 1012	Bus 1013	Bus 1042	Bus 1043	Bus 4071	Bus 4072
First load shed point (Hz)	48.8	48.8	48.8	48.8	48.8	48.8	48.8	48.8	48.8	48.8	48.8	48.8	48.8
First point pick up time (seconds)	1.2	1.2	1.2	1.2	1.2	1.2	1.5	1.5	1.5	1.5	1.5	1.5	1.5
First fraction of load shed	0.25	0.25	0.25	0.25	0.25	0.25	0.25	0.25	0.25	0.25	0.25	0.25	0.25
Second load shed point (Hz)	48.4	48.4	48.4	48.4	48.4	48.4	48.4	48.4	48.4	48.4	48.4	48.4	48.4
Second point pick up time (seconds)	0.9	0.9	0.9	0.9	0.9	0.9	1.2	1.2	1.2	1.2	1.2	1.2	1.2
Second fraction of load shed	0.25	0.25	0.25	0.25	0.25	0.25	0.25	0.25	0.25	0.25	0.25	0.25	0.25
Third load shed point (Hz)	48	48	48	48	48	48	48	48	48	48	48	48	48
Third point pick up time (seconds)	0.6	0.6	0.6	0.6	0.6	0.6	0.9	0.9	0.9	0.9	0.9	0.9	0.9
Third fraction of load shed	0.5	0.5	0.5	0.5	0.5	0.5	0.5	0.5	0.5	0.5	0.5	0.25	0.25
Breaker time (seconds)	0.3	0.3	0.3	0.3	0.3	0.3	0.3	0.3	0.3	0.3	0.3	0.3	0.3

D2. Undervoltage load shedding

Table D2. Undervoltage load shedding

Parameters	LVSHBL model- Under voltage load shedding						
	Bus 41	Bus 51	Bus 63	Bus 1022	Bus 1041	Bus 1044	Bus 1045
First load shed point (pu Volt)	0.9	0.9	0.9	0.94	0.94	0.94	0.94
First point pick up time (seconds)	0.55	0.52	0.49	1.5	0.55	0.52	0.49
First fraction of load shed	0.25	0.25	0.25	0.25	0.25	0.25	0.25
Second load shed point (pu Volt)	0.85	0.85	0.85	0.9	0.9	0.9	0.9
Second point pick up time (seconds)	0.25	0.22	0.19	1.2	0.25	0.22	0.19
Second fraction of load shed	0.25	0.25	0.25	0.25	0.25	0.25	0.25
Third load shed point (pu Volt)	0.8	0.8	0.8	0.86	0.86	0.86	0.86
Third point pick up time (seconds)	0.22	0.19	0.16	0.9	0.22	0.19	0.16
Third fraction of load shed	0.5	0.5	0.5	0.25	0.5	0.5	0.5
Breaker time (seconds)	0.3	0.3	0.3	0.3	0.3	0.3	0.3

D.2: On-load tap changer models

0 'OLTC1' 1044 4044 1 40 0 7.0/
0 'OLTC1' 1044 4044 2 40 0 7.0/
0 'OLTC1' 1045 4045 1 40 0 8.0/
0 'OLTC1' 1045 4045 2 40 0 8.0/
0 'OLTC1' 41 4041 1 40 0 8.0/
0 'OLTC1' 42 4042 1 40 0 7.9/
0 'OLTC1' 43 4043 1 40 0 6.5/
0 'OLTC1' 46 4046 1 40 0 7.5/
0 'OLTC1' 47 4047 1 40 0 6.1/
0 'OLTC1' 51 4051 1 40 0 7.4/
0 'OLTC1' 61 4061 1 40 0 6.6/
0 'OLTC1' 62 4062 1 40 0 7.1/
0 'OLTC1' 63 4063 1 40 0 6.2/